

LIPID PRODUCTION BY MICROALGAE TREATING MUNICIPAL WASTEWATER

A Thesis

presented to

the Faculty of California Polytechnic State University

San Luis Obispo

In Partial Fulfillment

of the Requirements for the Degree

Master of Science in Biological Sciences

by

James Edward Kelley

June 2013

© 2013

James Edward Kelley

ALL RIGHTS RESERVED

COMMITTEE MEMBERSHIP

TITLE:	Lipid production by microalgae treating municipal wastewater.
AUTHOR:	James Edward Kelley
DATE SUBMITTED:	June 2013
COMMITTEE CHAIR:	Mark Moline, PhD Professor of Biology
COMMITTEE MEMBER:	Trygve Lundquist, PhD Associate Professor of Civil and Environmental Engineering
COMMITTEE MEMBER:	Christopher Kitts, PhD Professor of Biology

ABSTRACT

Lipid production by microalgae treating municipal wastewater

James Edward Kelley

Microalgae hold much promise as a feedstock in liquid biofuel production. Lipid content of microalgae cells range from 30-80% dry weight of biomass. It is projected that microalgae can produce between 1,000-6,500 gallons/acre/year of oil. Currently, production of industrial algae operates in open raceway ponds that use minimal capital and energy inputs to culture algae. Raceway ponds can also be used to grow microalgae from municipal waste streams. Although high biomass productivity can be achieved in these systems, there remains a large production gap between large volumes of biomass cultivation and high lipid content from microalgae cells. Low lipid content has been ameliorated through laboratory manipulations of nitrogen availability and light intensity. This two-part project measured microalgae lipid levels in open raceway ponds located at the San Luis Obispo Water Reclamation Facility (SLO WRF) grown in primary clarifier effluent and then performed nitrogen depletion and light-shift methods on cultures to increase triglyceride (TAG) content. The raceway ponds reached maximum biomass productivity of 24 g/m²-day, but with minimal TAG reserves. Optimization of both biomass productivity and TAG content can be achieved in April and September with 13 g/m²-day productivity and 13% TAG content. Investigation of increased TAG production responses were performed on wastewater microalgae (predominately *Scenedesmus sp.*) through N-depletion and three light treatments: light-shift on day 3 (before N-depletion), light-shift on day 5 (near N-depletion), and a double-illumination treatment. Highest levels of TAG content were observed in the double-illumination treatment and reached a maximum of 49% TAG in 9 days.

Keywords: ammonia, nitrogen depletion, light-shift, light intensity, gas chromatography mass spectrometry, fatty acid methyl esters (FAMES), triglycerides (TAG)

ACKNOWLEDGMENTS

This interdisciplinary project was supported by the California Central Coast Research Partnership (C³RP) along with the College of Civil and Environmental Engineering and the College of Science and Math. Additional financial backing was provided by the Wertman Scholarship, which supports students in Biological Sciences in pursuit of studies in botany.

I want to thank Dr. Tryg Lundquist for his unconditional support, broad vision, and exemplary tireless dedication to the field of bioremediation and biofuels. His vast knowledge and incredible creativity has inspired in me a life-long bridge between a passion for environmental stewardship and feasible problem-solving applications. This experience has not only enriched my knowledge of renewable energy, green engineering, and the microalgae biofuel field, but has also allowed me to mature as a scientist and citizen.

Much gratitude also goes to Dr. Mark Moline for his steadfast support and his committed confidence in me. His courses in marine sciences and phycology are fully responsible for my biological and scientific enlightenment. His knowledge and leadership inspires curiosity and drives ambitiousness in his students for which there is no measurable form of gratitude.

I am also eternally grateful to Ian Woertz and Matt Hutton for being my environmental engineering mentors. Not only did they build the foundation for my project, but their patience and counsel provided invaluable insight. I would also like to thank Dr. John Benemann for the development and structure of the light-shift experiment and to Franco Trabuco as my colleague and friend in preparing and executing experiments with tedious hours. A solid recognition of gratitude goes to Paul Ward, Brant Halfich, Mike Podavin, Giulia Samorì, and Louis Lefbvre for maintaining the field site and their obliging sample collection assistance and data collaboration. Additionally, I want to thank Bryce Swetek, Kyle Fooks, and Ankita Kashyap for saving me in time-sensitive binds; to Doug Brewster for his time and energy for building culturing equipment; and Alice Hamrick for providing the project time saving support and assistance.

This project would not have been possible if it were not for the team of dedicated undergraduates that assisted in sample collection and time-sensitive analysis. A massive and indebted thank you is directed to: Paul Peabody, Antonia Estevez, Seth White, Anthony Bonilla, John Holcombe, Kelsey Thatcher, Kelsey Boulter, Andrew Cortado, Leanne Fogg, Raechel Harnoto, Jack Hutchinson, Melodi Mckay, Mark Perez, Nicole Riordan. The time and accomplishments of these students guaranteed the success of this project.

Appreciations of gratitude also go to Dr. Yarrow Nelson and Dr. Christopher Kitts for their guidance and sincere encouragement; to the Moline lab: Ian Robbins, Anniken Lydon, Johanna Weston, Sam Rankin, with notable mention to Melissa Daugherty and all involved in the Center for Coastal Marine Sciences, for their heartening cheerleading.

And finally, I want to thank my mother and father, Ligaya and Michael Kelley, for their love, support, and words of parental encouragement during challenging times. A very important thank you goes to my partner Hans Otto Thiel, III for his resolute support and limitless encouragement throughout the entirety of the project and forward.

TABLE OF CONTENTS

LIST OF TABLES	ix
LIST OF FIGURES.....	x
LIST OF APPENDICES	xiii
CHAPTER 1: INTRODUCTION.....	1
1.1 THE CURRENT STATE OF ENERGY IN THE UNITED STATES	1
1.2 BIOFUELS	4
1.3 ALGAE	5
1.4 STUDY OBJECTIVES	9
CHAPTER 2: BACKGROUND.....	11
2.1 BATCH GROWTH.....	11
2.2 LIPIDS AND TRIGLYCERIDES	12
2.3 NITROGEN.....	14
2.4 LIGHT-SHIFTS	18
2.5 POND SET UP	19
2.6 EXPERIMENT SET UP.....	20
2.6.1 Agitation and Mixing.....	21
2.6.2 Carbon dioxide supplementation	21
2.6.3 Medium.....	22
2.6.4 Inoculate	22
2.6.5 Light-shifts.....	23
CHAPTER 3: METHODS AND MATERIALS	24
3.1 POND STUDY.....	24
3.1.1 Micrographs.....	24
3.1.2 Solar Irradiance.....	24

3.1.3 Total Suspended Solids and Volatile Suspended Solids	24
3.1.4 Lipid Extraction.....	26
3.1.5 Bligh and Dyer.....	27
3.1.7 Gravimetric Analysis: Total Lipid Concentration	29
3.1.8 Analytical Analysis: Triglyceride Characterization and Quantification	30
3.1.8.1 Transesterification.....	31
3.1.8.2 Fatty Acid Methyl Ester (FAME) Standards.....	32
3.1.8.3 Gas Chromatography Mass Spectrum (GC-MS).....	34
3.1.8.4 FAME and Triglyceride Calculations	35
3.2 LIGHT-SHIFT AND NITROGEN DEPLETION EXPERIMENTS	37
3.2.1 Cell Counts	39
3.2.2 Triglyceride Extraction and Analytical Analysis.....	39
3.2.3 TAG Productivity	40
3.3 SOLIDS AND NITROGEN TESTS	41
3.3.1 Total and Volatile Suspended Solids	41
3.3.2 Daily Growth Rates	41
3.3.3 Nitrogen Analyses	41
3.3.3.1 Total Ammonia as Nitrogen (TAN)	41
3.3.3.2 Nitrate	42
3.3.3.3 Total Kjeldahl Nitrogen (TKN) and Organic Nitrogen (ON).....	43
3.3.4 CHLOROPHYLL-A.....	44
3.3.5 TEMPERATURE AND PH	45
3.3.6 STATISTICAL ANALYSES	45

CHAPTER 4: RESULTS AND DISCUSSION	46
4.1 DISCREPANCIES IN MEASUREMENT METHODS.....	46
4.2 POND STUDY.....	48
4.2.1 Solar Irradiance.....	48
4.2.2 Productivity and Insolation.....	52
4.2.3 Nitrogen	55
4.2.4 Productivity and Nitrogen.....	58
4.2.5 Species Composition	60
4.2.6 Pond Study Discussion	62
4.3 LIGHT-SHIFT AND NITROGEN DEPLETION EXPERIMENT	63
4.3.1 pH and Temperature	64
4.3.2 Growth in the Experimental Cultures	66
4.3.3 Nitrogen	71
4.3.4 Chlorophyll-a.....	74
4.3.5 FAMES and Total Triglycerides.....	76
4.3.6 Light-shift Experiment Discussion	80
CHAPTER 5: CONCLUSION.....	82
BIBLIOGRAPHY	85

LIST OF TABLES

Table 1. Energy sources in the United States in 2011 and their respective share of the total energy consumption. As of 2011, the U.S. consumes about 99 BTU of energy per year. Fossil fuels include petroleum, natural gas, and coal.	4
Table 2. Current oil yields from varying oleaginous feed stocks and theoretical estimates of algae oil yields per year (U.S. DOE, 2010).	7
Table 3. Some of the more common and notable nitrogen experiments. Bracketed days refer to period until the lipid percentage was achieved.	17
Table 4. Influent nitrogen concentrations compiled from Ward (2011) includes total ammonia as nitrogen (TAN), Total Nitrogen (TN), nitrate (NO ₃), and nitrite (NO ₂). Constituent data for each time period are displayed in means with standard deviation of time series data ($\bar{x} \pm SD$). TN analysis was switched to TKN methods on 6/24/2010. Missing values corresponded to data points that were not sampled during the time period.	56
Table 5. Biomass and TAG productivities (dry weight) with corresponding nitrogen concentrations in the influent and the pond.	60
Table 6. pH and temperature of light shift treatments and double illumination control. Shaded boxes represent single-sided illumination and white boxes represent double-sided illumination.	65
Table 7. VSS concentration values, daily specific VSS growth rates (μ), and number of cells per mL for the three types of culture throughout the 9-day experiment. Shaded boxes represent periods of single-sided illumination and white boxes represent periods of double-sided illumination with light-shifts occurring on day 3 and day 5 of the experiment.	67
Table 8. Consumption rates of TAN were calculated from the beginning of the experiment (day 0) until the first day TAN levels fell below 1 mg/L. %ON decline rates day ⁻¹ were determined from the peak %ON of each culture to the final day of the experiment (day 9). Light-shift 2 experienced the only increase in %ON at the start of the experiment until day 5.	71
Table 9. Rates of chlorophyll-a production were calculated from day 2 until the peak in chlorophyll-a concentration for each treatment. Consumption rates were calculated from respective concentration peaks to the final day (9) of the experiment.	74
Table 10. TAG content as a percentage of VSS on each day for all three treatments. Single-sided illumination is represented with grayed boxes and double-sided illumination is represented by the white boxes.	77
Table 11. Maximum TAG concentrations were for all three cultures on the final day of the experiment. Maximum TAG productivity was achieved on day 8 for Light-shift 1 and Double Illumination, and day 5 for Light-shift 2.	78

LIST OF FIGURES

Figure 1. Keeling curve tracking carbon dioxide (CO ₂) concentrations observed at the Mauna Loa summit on the Big Island of Hawai'i beginning in the late 1950s. The sinuous oscillations (red line) depict seasonal CO ₂ increases during northern hemisphere spring (high) and autumn (low). Low CO ₂ concentrations in the autumn are a result of massive carbon fixation during the summer by terrestrial plants. The highlighted box on the right shows a 4-year trend with a fitted average (black line). < http://www.ncdc.noaa.gov/paleo/pubs/mann2008/mann2008.html >	2
Figure 2. Schematic of relationships between bacteria and microalgae in an open raceway pond (Oswald et.al, 1953; U.S. DOE, 2010)	8
Figure 3. Microalgae biomass curve including five growth phases.....	11
Figure 4. A triacylglycerol molecule with a saturated fatty acid, monosaturated fatty acid and polysaturated fatty acid. (http://pbsg.npolar.no/en/methods/fatacid.html)	13
Figure 5. Light-rack treatments with six 1-L Pyrex® Roux bottles, air-1%CO ₂ manifold, and stir plates.	21
Figure 6. Layers separated by centrifugation at 7,000 rpm. The clear top layer (a) consisted of methanol and DI-water, the middle layer (b) is cellular debris from the cell wall, and the bottom layer (c) consists of the lipophilic compounds in chloroform.....	28
Figure 7. Aluminum weighing dishes with lipid extracts for gravimetric analysis.	29
Figure 8. Transesterification pathway of a triglyceride molecule into three fatty acid methyl esters (FAMES) and one glycerol compound (Scott et al., 2010).	32
Figure 9. FAME sample in hexane from transesterified lipid extract in a 12-mL glass vial.	32
Figure 10. A gas chromatograph of sample FAMES bracketed by internal standards.....	35
Figure 11. Daily sample processing of light-shift experiments depicting treatment culturing, solids determination, and analytical analysis of TAG and nitrogen compounds.	38
Figure 12. Bland-Altman plot for %TAG and %Total lipids from samples collected from microalgae polycultures in raceway ponds. Data for %TAG was collected through analytical methods and data for %Total lipids was collected through gravimetric methods.	47
Figure 13. (Top) VSS (■) in raceway ponds and mean weekly solar irradiance from August 2009 to December 2010. (Bottom) %TAG (●) in raceway ponds and mean weekly solar irradiance from August 2009 to December 2010.....	49
Figure 14. Correlations of microalgae VSS concentrations and TAG content in VSS to mean weekly solar irradiance (W/m ²). TAG content may decrease with increased VSS due to shading in the water column and as a result of potential increases in TAG consumption for respiration.....	50
Figure 15. VSS concentration and TAG content for raceway pond microalgae, separated by season. Shown are means with standard deviation and sample size distribution (contour). The dates were chosen based on solstices and equinoxes from September 2009 to December 2010.....	51
Figure 16. VSS concentrations and %TAG values do not have any conspicuous relationships.....	51

Figure 17. Control pond biomass productivity (■) and % TAG content (●) with respect to mean weekly solar irradiance. The intersection between the two factors is 231 W/m ² , at which point the highest TAG productivity would be expected.	53
Figure 18. Biomass productivity (■) and TAG Productivity (●) of raceways ponds from March 2010-October 2010. Spring to autumn provides ample solar irradiance for biomass productivity with optimal lipid productivity in April and September.	54
Figure 19. Organic nitrogen content in algal biomass grown in raceway ponds with respective TAG content in the biomass. The smoothed line shows possible optimum of organic nitrogen and TAG contents.....	58
Figure 20. Biomass productivity (■) and TAG productivity (●) in relation to ammonia concentration in the pond influent (clarifier effluent) and effluent. Both biomass productivity and TAG productivity increase with higher influent ammonia concentrations. Absence of ammonia in the ponds is a result of assimilation of nitrogen which increases productivities of both biomass and TAG.	59
Figure 21. Examples of organisms found in the raceway ponds. Clockwise, specimens include: (a) <i>Actinastrum sp.</i> and <i>Closterium sp.</i> (L-R), (b) <i>Micractinium sp.</i> , (c) rotifer, (d) Euglenid, (e) <i>Scenedesmus sp.</i> , (f) ostracod, and (g) <i>Cyclotella sp.</i> Microscope magnification show in parentheses.	61
Figure 22. Mean VSS concentration (triplicates) and standard error values for Light-shift 1, Light-shift 2, and Double Illumination treatments throughout the 9-day experiment. Day of light-shift is indicated with an arrow.	68
Figure 23. Daily growth rates based on VSS (■) for Light-shift 1, Light-shift 2, and Double Illumination treatments throughout the 9-day experiment. The day of the light-shift is indicated with an arrow.....	69
Figure 24. Correlation of VSS (■) concentration and culture density (number of microalgae cells mL ⁻¹). Cultures were 99% <i>Scenedesmus sp.</i> Light-shift 1 ended the experiment with the highest VSS concentration and highest cell density of all three cultures. Light-shift 2 had a lowest cell density and lowest VSS concentration. Double Illumination had nearly the same VSS concentration as Light-shift 1 with a lower cell density.....	70
Figure 25. Total Kjeldahl nitrogen (TKN) and the nitrogen constituents (ammonia, nitrate, organic nitrogen) in the culture media for (a) Light-shift 1, (b) Light-shift 2, and (c) Double Illumination. Organic nitrogen (ON) (▲) was compared to daily VSS values to determine a percentage of biomass that was nitrogen within the microalgae cells. ON was not measured for the first two sample days in order to conserve culture volume.	73
Figure 26. Ammonia (TAN) (▲) consumption displayed in (a) Light-shift 1 (b) Light-shift 2, and (c) Double Illumination treatments. Chlorophyll-a (◆) production stops at the onset of nitrogen depletion (<1 mg/L) and is thereafter consumed (broken down) in the cells.....	75

Figure 27. Daily total TAG content with respective fatty acid profiles for three treatments: (a) light shifted on day 3, (b) light shifted on day 6, and (c) double-side illumination. Cellular starvation occurs when the %ON (Δ) reaches below 3-5% (dashed horizontal line).79

LIST OF APPENDICES

Appendix A	91
Appendix B	93
Appendix C	95
Appendix D	97
Appendix E	99
Appendix F	101

Chapter 1: Introduction

1.1 The Current State of Energy in the United States

The infrastructure supporting the modern comforts of society relies heavily on liquid fossil fuels to meet and perpetuate growing energy demands (U.S. EIA, 2012a). In 2010, the United States consumed 20% of the world's total energy, yet comprised approximately 4.5% of the global population (U.S. EIA, 2012b). Fossil fuels provide the energy and power to support transportation, heat generation, and electricity (U.S. EIA, 2012a). U.S. petroleum consumption trends are set to increase by 0.4% in 2014 and, although imported crude oil and petroleum products have declined since 2005, these imports comprised 36% of total U.S. fuel consumption in 2011 (U.S. EIA, 2012a). In 2011, the EPA concluded that fossil fuel combustion accounted for 94.6% of carbon dioxide released into the atmosphere in the U.S. (U.S. EPA, 2013 draft). Fossil fuels are derived from ancient plant and animal matter that has—over eons—been transformed into crude oil, natural gas, and coal. Since the dawn of the Industrial Revolution in the early 19th century, carbon dioxide concentrations in the atmosphere of the northern hemisphere have steadily increased from roughly 280 ppm to nearly 400 ppm as of May 2013 (Figure 1). The heat trapping properties, or global warming potential, of carbon dioxide places it in a category along with methane, nitrous oxide, and hydrofluorocarbons which are collectively named greenhouse gases (GHGs). Carbon dioxide is the standard compound in which to compare global warming potential to other GHGs. When compared over a 100-year time frame, carbon dioxide molecule has a GWP of 1, methane

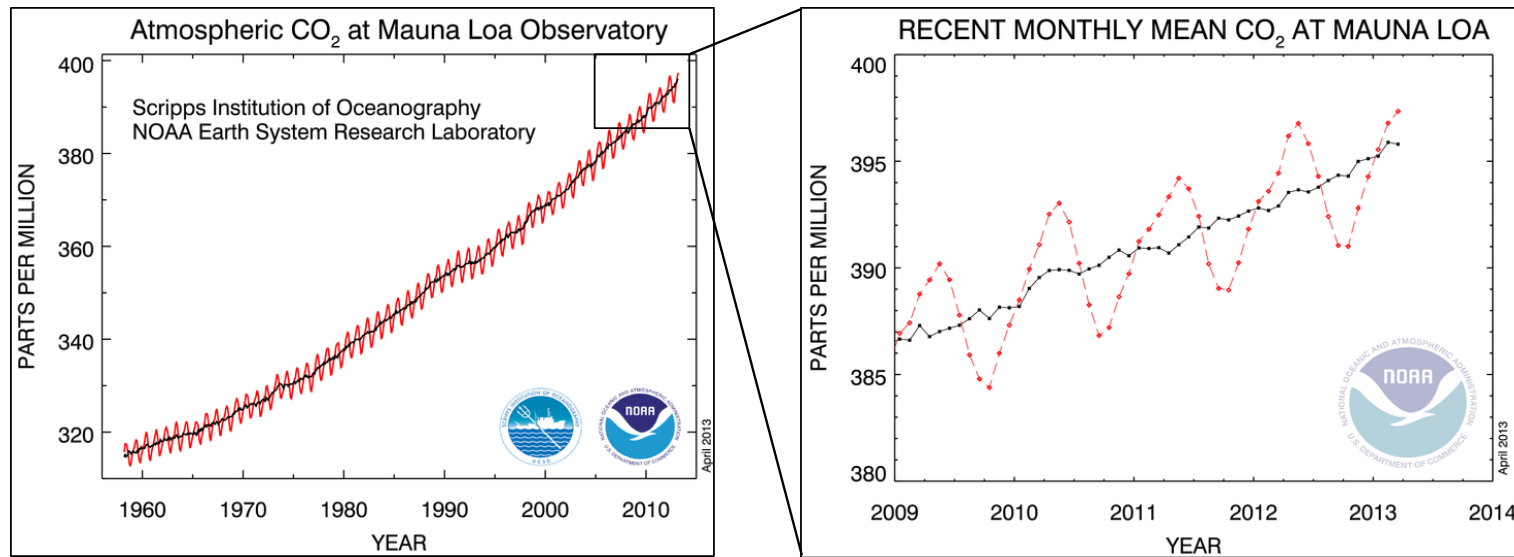


Figure 1. Keeling curve tracking carbon dioxide (CO₂) concentrations observed at the Mauna Loa summit on the Big Island of Hawai'i beginning in the late 1950s. The sinuous oscillations (red line) depict seasonal CO₂ increases during northern hemisphere spring (high) and autumn (low). Low CO₂ concentrations in the autumn are a result of massive carbon fixation during the summer by terrestrial plants. The highlighted box on the right shows a 4-year trend with a fitted average (black line).

<<http://www.ncdc.noaa.gov/paleo/pubs/mann2008/mann2008.html>>

a GWP of 20 and Sulfur hexafluoride (SF₆) a GWP of 23,900 (IPCC, 2012). Overall, GHGs are beneficial and solely responsible for the temperate climate observed on earth, but ever-increasing concentrations of these compounds in the atmosphere have been linked to global consequences such as elevated average global temperatures, climate change, ocean acidification, stronger storm systems, and rising sea levels (Wigley & Raper, 1987; Orr et al., 2005, IPCC, 2012). Unlike other GHGs, carbon dioxide can be recaptured by autotrophic organisms and fixed to form organic compounds like sugars (U.S. EPA, 2013; Wang, Li, Wu, & Lan, 2008; Schenk et al., 2008). When appropriate, photosynthates can be converted into complex carbohydrates (starch) or used to signal the production of lipids and accumulate storage reserves at the onset of stress (Ratledge, 2002).

U.S. citizens' intense demand for fossil fuels inextricably links national energy dependence to foreign sources and creates an obligatory policy to minimize trade instabilities (Sheehan et al., 2000). Continual accumulation of carbon dioxide in the atmosphere and heavy reliance on imported energy has many American innovators looking for solutions in domestic renewable energy. Renewable energies are derived from naturally regenerating resources like solar, wind, tidal, hydro, geothermal, biomass, and biofuels and have the capability to mitigate our current energy quandaries. These alternative energy resources can be established in the U.S. to expand the domestic economy and can theoretically function in perpetuity unlike their finite fossil fuel counterparts (Sheehan et al., 2000). However, the U.S. renewable energy market has much progress to make considering it only comprises 9% of the energy consumption (99 Quad BTU) while fossil fuels comprise 82% of the total (Table 1).

Table 1. Energy sources in the United States in 2011 and their respective share of the total energy consumption. As of 2011, the U.S. consumes about 99 BTU of energy per year. Fossil fuels include petroleum, natural gas, and coal.

Source	Consumption in the U.S. (2011) (Quad BTU)
Petroleum	36
Natural Gas	26
Coal	20
Renewable Energy	9
Nuclear Electric Power	8
Total	99

Due to its easily substitutable liquid properties, biofuel consumption in the U.S. increased 680% from 0.25 QBtu in 2011 to 1.95 QBtu in 2011 (Balat & Balat, 2010, U.S. EIA, 2012). These invaluable renewables are derived from plant matter in the form of either biomass or carefully extracted organic compounds. Since the cultivation of these resources requires the bio-fixation of atmospheric carbon dioxide, they do not contribute additional GHGs into the atmosphere and are nearly carbon neutral (Sheehan et al., 2000).

1.2 Biofuels

The large U.S. transportation sector necessitates the production of liquid renewable energy not only for automobiles, but also airplanes and ships (Sims, Mabee, Saddler, & Taylor, 2010). While current liquid fuels, like gasoline, diesel, and kerosene are derived from fossilized organic matter, biofuels like biodiesel and ethanol are created from contemporary plant matter. Biodiesel derived from plant oils can be mixed with or substituted for petroleum diesel and reduces tailpipe emission of CO₂ by 78%, CO by 35%, SO_x by 8%, particulate matter by 32%, and

sometimes NO_x depending on the engine (Sheehan et al., 2000; Balat & Balat, 2010). Biodiesel is currently processed from a variety of oleaginous plants that include soybean (*Glycine max*), oil palm (*Elaeis guineensis*), jatropha (*Jatropha curcas*), and rapeseed (*Brassica napus*) (Balat & Balat, 2010; U.S. DOE, 2010). Aiding in the development and implementation of a domestic biofuel industry, the Energy Independence and Security Act (EISA) of 2007 requires federal fleets to increase supplementation of biofuels in gasoline from 4.7B gallons in 2007 to 36B gallons in 2022 and reduce petroleum consumption by 20% in 2015 (U.S. DOE, 2010; US EIA, 2011). While providing many political and environmental benefits, the push for increased biofuel production has also created unintended repercussions including intense land-use change, inflation of food crop prices, and extensive habitat destruction (Fargione et al., 2008; Singh, Nigam, & Murphy, 2011). Even if the United States had dedicated the entire 2005 crop-year of corn and soybean to biofuel production, it would have only offset energy demands by 12% and 6%, respectively (Hill et al., 2006). These concerns have spurred a resurgence of attention toward microalgae—a biofuel feedstock that contains between 30-80% lipid (oil) content of dry-weight mass (Enssani et al., 1982; Sheehan et al., 1998; Chisti, 2007; Brennan & Owende, 2010).

1.3 Algae

The taxonomic group of algae is a mélange of diverse organisms belonging to many biological kingdoms. One of the simplest ways to categorize an alga is by size of the individual. Macroalgae are large, multicellular organisms with specialized organs that predominately include marine kelp. Microalgae are inconspicuous, microscopic phytoplankton and can survive as solitary cells or form colonies. Microalgae species include prokaryotic cyanobacteria and eukaryotic protists. As the ancient ancestor to terrestrial plants, microalgae developed the blueprint for harvesting solar energy and transforming carbon dioxide into high-energy organic compounds

(Lewis & McCourt, 2004). Although solitary algae cells may be small, as a whole, microalgae are responsible for 40% of the world's carbon dioxide bio-fixation—making them one of the largest and most efficient carbon sinks (Falkowski, 1994). The ability of large microalgal populations to continually fix carbon dioxide and convert it into biomass or lipids makes it an ideal candidate for a renewable energy resource (Nigam & Singh, 2011). Studies have shown that even conservative estimates of microalgae lipid yields are greater than agricultural crops used in conventional biodiesel production (Table 2). There are also hosts of other benefits for cultivating microalgae over other crops destined for biofuel production. Unlike corn and soybean, microalgae are not a substantial food crop and can be grown on non-arable land without contributing to food price inflation (Dismukes et al., 2008). The required land to grow rapeseed or soybean requires up to 49 or 132 times more space than microalgae with 30% w/w oil content (Balat & Balat, 2010). Also, carbon dioxide recapture from industrial flue gas or digester biogas combustion can be used to increase the biomass productivity 100% in laboratory settings and >30% in the field (New Zealand pilot-scale high rate algal pond in the summer) (Park, Craggs, & Shilton, 2011). Due to the high productivity rate of microalgae, if placed in prime climate locations, harvest could continue through the year rather than annually like conventional crops (Weyer et al., 2009; Balat & Balat, 2010).

Table 2. Current oil yields from varying oleaginous feed stocks and theoretical estimates of algae oil yields per year (U.S. DOE, 2010).

CROP	OIL YIELD (GALLONS/ACRE/YR)
Soybean	48
Camelina	62
Sunflower	102
Jatropha	202
Oil palm	635
Algae	1,000-6,500 ^b

^a Adapted from Chisti (2007)

^b Estimated yields, this report

One promising sector of this industry—first proposed by Oswald and Golueke (1959) for anaerobic digestion—focuses on open raceway ponds for culturing microalgae in municipal wastewater. Open raceway ponds maximize oxygen production for bacterial breakdown of organic compounds and optimize nutrient and solar irradiance availability for microalgae productivity (Oswald et al., 1953). Since the beginning of life on earth microalgae have thrived off waste streams. By metabolizing dissolved nutrients to fuel growth and reproduction, microalgae decrease nitrogen, carbon, and phosphorous concentrations in the water (Thompson Jr., 1996).

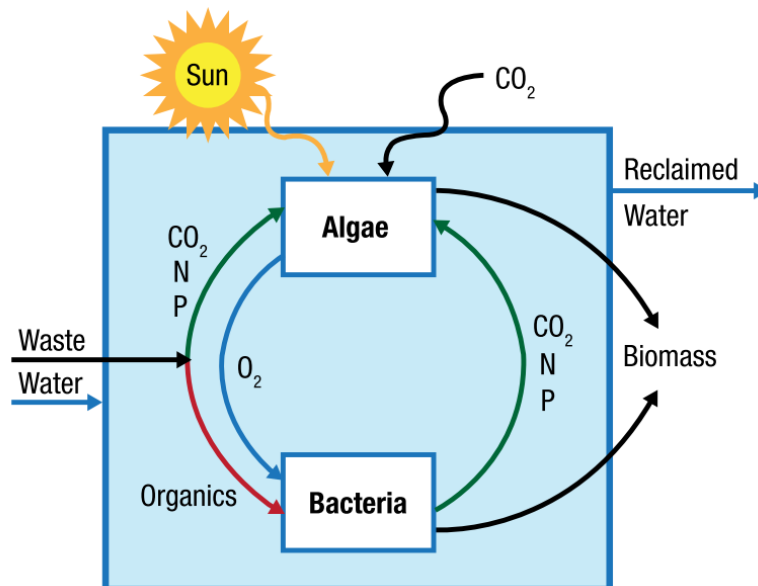


Figure 2. Schematic of relationships between bacteria and microalgae in an open raceway pond (Oswald et.al, 1953; U.S. DOE, 2010)

If fed with municipal wastewater from primary clarifier effluent, the nutrient load can be significantly reduced in discharged water without the need for chemical treatment (Golueke & Oswald, 1959; Enssani, 1982; Ward, 2011). Studies have shown that pairing wastewater treatment with microalgae aquaculture, not only has the highest environmental rescue, but is perhaps the only way the biofuel industry can become energy neutral and cost effective (Benemann et al., 1982; Enssani, 1982; Sheehan, 1998). While a raceway pond system produces large volumes of biomass, this outcome is consistently at the expense of cellular lipid content within the microalgae (Scott et al., 2010). Research into lipid production in microalgae is typically performed in closed systems reactors that are diligently and expensively controlled.

Cultivation in transparent closed system reactors, called photobioreactors (PBRs), allows for complete control of the media, temperature, pH, nutrient load, and microalgae species composition—typically a monoculture. These reactors are responsible for reporting the higher-end

lipid concentrations found in microalgae (Christi, 2007). Though PBRs require high initial capital and maintenance cost, the biomass productivity is much greater when compared to raceway ponds (Christi, 2007). Since fatty acid composition is affected by temperature, light, and nutrient quality, one benefit of PBR cultivation is the target production of specific fatty acid chains which is crucial to nutraceuticals and biodiesel refining (Enssani, 1982; Tedesco et al., 1989; Solovchenko et al., 2008; Balat & Balat, 2010).

Both raceway ponds and PBRs provide measurable costs and benefits to algae aquaculture. Decades of research have described the great potential of developing a biofuel feedstock from microalgae, but there remains a large gap between industrial biomass production and high lipid content—two inherently antagonistic processes. Past studies have investigated this challenge by inducing lipid production in microalgae through increasing photosynthetic efficiencies of chloroplasts or manipulating nutrient availability in the media.

1.4 Study Objectives

The goal of this project aims to investigate natural triglyceride production in the open raceway ponds at the San Luis Obispo Wastewater Reclamation Facility (SLO WRF) and how to improve their lipid content through nitrogen depletion and increased light intensity. Included in this thesis is a two-part study involving: (1) tracking lipid content of wastewater microalgae in open ponds over the course of one year (2009-2010) then (2) manipulating microalgae cells in a controlled laboratory setting to produce elevated triglyceride content.

Presented here are observations from the open raceway ponds at the SLO WRF including a comparison between gravimetric and analytical analyses and observed seasonal variation of triglyceride content in the microalgae. These findings built the foundation to explore the combined

effects of nitrogen deficiency and light intensity shifts on microalgae in laboratory cultures with the purpose of producing increased triglyceride content.

Objectives of the pond study:

1. Compare total lipids and triglycerides analytes.
2. Measure TAG content in open raceway ponds.
3. Investigate effects of water nitrogen concentration on lipid production or disappearance.

Hypotheses:

- I. High solar irradiances lead to high wastewater microalgae biomass productivity with high lipid content. .
- II. TAG content in wastewater microalgae is inversely related to influent ammonia concentrations from the primary clarifier.

Objectives of light-shift experiment:

- I. Increase triglyceride content wastewater microalgae during nitrogen depletion and increasing sequential light intensities.

Hypotheses:

- I. During nitrogen depletion, wastewater microalgae with high concentrations of chlorophyll-a will increase cellular TAG content when exposed to high light intensity.
- II. Increased light intensity at the onset of nitrogen depletion improves TAG content in wastewater microalgae.

Chapter 2: Background

2.1 Batch Growth

In batch cultures, microalgae exhibit a growth curve pattern including a lag-phase, exponential growth (log-phase), linear phase, stationary phase, and death phase (Figure 3).

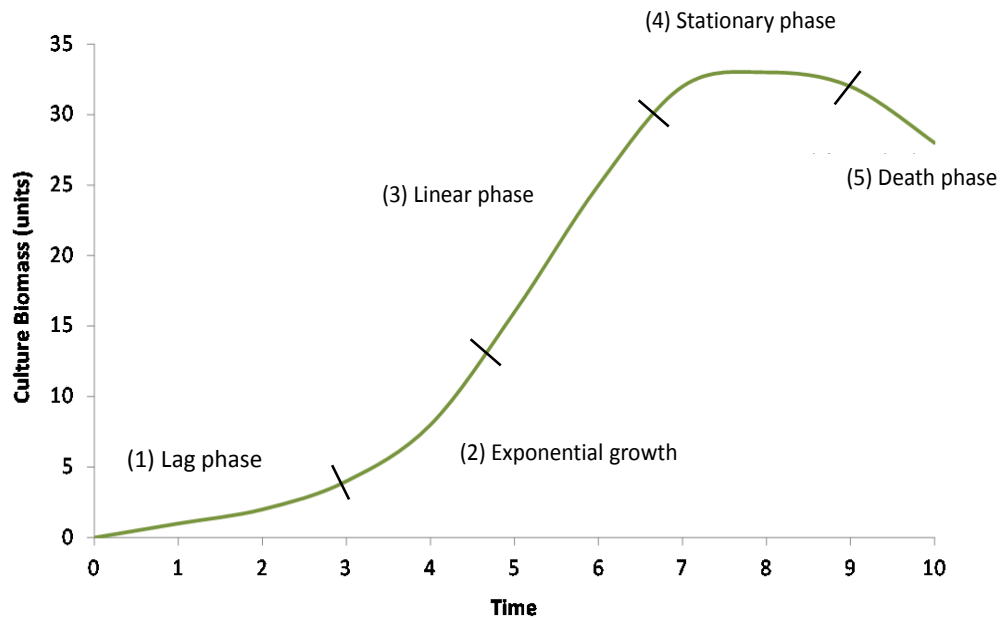


Figure 3. Microalgae biomass curve including five growth phases.

Initially, when single-celled organisms, like microalgae or bacteria, are placed in a new medium they are forced to acclimate to the new environment which manifests via delayed growth. This period is described as lag-phase in which the population of the organism lags for a short time before growing rapidly. After this stage, the population enters exponential growth, in which the cells in the culture grow, reproduce, and divide at a compounding rate. Eventually exponential growth leads into the linear phase which is a steadier rate of continual growth. In continuous cultures, this phase is maintained as best as possible by adding extra nutrients and either increasing space or removing a portion of the population. Once the cells have exhausted certain

limiting nutrients in the media—such as nitrogen or phosphorous—the cells no longer undergo cellular division and the population remains static. At this point, in stationary phase, the cells respond to the physiological stress by shifting their metabolism to accumulate energy storage compounds. Shortly after, the cells begin to senesce and the population of the microalgae cells decline into death-phase. The growth curve of any culture can be inversely correlated with the decline and consumption of a limiting nutrient (or nutrients) in the media.

2.2 Lipids and Triglycerides

When referring to oil, research in the literature is vague on discerning between lipids and its many constituents. This nebulous term can lead to the misrepresentation of actual energy availability in the extract. Many oil studies report on lipid content in microalgae, but, depending on the method of extraction, the lipid quantity in a lipophilic extract may include a variety of compounds such as fatty acids and their derivatives, carotenoids, terpenes, and steroids (Christie, 2003). Isolating these molecules involves extractions with organic solvents such as chloroform, benzene, ethers, and alcohols (Christie, 2003).

Of particular interest to the biofuel industry are triacylglycerides (TAGs or triglycerides). One TAG molecule is composed of three fatty acid hydrocarbon chains attached via ester bonds to a singular glycerol backbone (Figure 4). In IUPAC (International Union of Pure and Applied Chemistry) nomenclature, free fatty acids are denoted as “C16:0”, where the number before the colon refers to the number of carbons in the chain and the number after the colon denotes the level of hydrogen saturation of the chain (Christie, 2003).

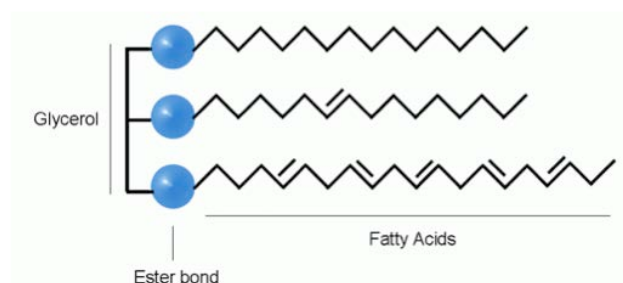


Figure 4. A triacylglycerol molecule with a saturated fatty acid, monosaturated fatty acid and polysaturated fatty acid. (<http://pbsg.npolar.no/en/methods/fatacid.html>)

In microalgae, fatty acid chains are predominantly saturated or monosaturated which allows for more efficient packaging by the cells, provides more energy upon oxidation than polyunsaturated fatty acids (PUFAs), and contains nine times more energy than carbohydrates (Roessler, 1990; J. Benemann & Oswald, 1996)). However, there are notable PUFAs in microalgae like omega fatty acids which can be cultivated for nutraceuticals (Guschine et al., 2006; Solovchenko et al., 2008; U.S. DOE, 2010). TAGs are readily oxidized to fulfill energy requirements during periods of reproduction or a limitation of crucial nutrients (Thompson Jr., 1996). Triglyceride production begins in the chloroplast by means of fatty acid synthesis which occurs via the addition of carbon-pairs by acetyl-coenzyme (acyl-coA) (Ohlrogge & Jaworski, 1997). Free fatty acids are transported to the endoplasmic reticulum where, through a series of enzymatic reactions, they are assembled into triglyceride compounds (Chrisite, 2003). TAGs can be harvested from microalgae and separated from other cellular components through organic solvent extractions then processed into biodiesel through transesterification.

Goals of increasing lipid content in microalgae to levels above 40% of dry-weight have been explored by the National Renewable Energy Laboratory (NREL) and the Department of Energy (DOE) since 1978 (Sheehan et al., 1998). The most common lipid induction triggers explored involved stress factors like nutrient deprivation, salinity changes, and light intensity alterations, which has been observed to increase energy storage compounds. Many studies,

including NREL's Algae Species program (1978-1996) have investigated successful culture manipulations that show increases microalgal lipid content up to 80% (Sheehan et al., 1998). The research goals of this project explore simple measures to induce lipid production in microalgae involving nutrient depletion and varying light intensities.

2.3 Nitrogen

Induction of increased lipid content through nutrient limitations in microalgae has been studied in *Chlorella vulgaris* since the 1940s (Spoehr & Milner, 1949). The most common and well-studied methods for increasing lipid concentrations in microalgae include nitrogen and phosphorous manipulations in green microalgae and silicate manipulations for diatoms (Sheehan, 1998). The three main avenues to study nutrient manipulation in microalgae include: starvation, limitation, and depletion. Starvation involves growing microalgae in nutrient replete media then transferring the cells into an environment that is void of a particular nutrient. The absence of the nutrient creates an acute biological shock and signals the production of high-energy compounds (Mandal & Mallick, 2009; Shifrin & Chisholm, 1981; Y. Singh & Kumar, 1992). This process can be done in a laboratory using filters, centrifuges, and washes, but is more difficult to recreate out in the field with a high cost potential (Tedesco et al., 1989; Chisti, 2007). Nutrient limited growth is commonly grown in continuous cultures. This process involves growing cells in an environment with sufficient nutrients save one nutrient which is administered at a continuous low rate. This method is typically automated with a chemostat which is an instrument capable of controlling various nutrients in the media. Physiological responses are observed in reaction to the limiting nutrient (Benemann & Oswald, 1996). Nutrient deficiency methods involve growing organisms in batch cultures with an environment replete with necessary nutrients. Growth rate of the organisms increase along with cell density until the nutrients in the media are exhausted. Once nutrient

depletion has been achieved, future growth results in metabolic consequences involving alterations in metabolic processes like growth rate reduction, decreased photosynthesis potential, and increase in high energy storage compounds (Benemann & Oswald, 1996).

Nitrogen deficiency tests are one of the most common and simplest ways to induce lipid production in microalgae. Under limited nitrogen condition, the flow of fixed carbon in photosynthesis is diverted from protein synthesis to either lipid or carbohydrate synthesis (Richardson et al., 1969; Scott et al., 2010). In the transition from nitrogen replete to nitrogen deplete cells, the microalgae undergo a physiological shift from producing polar lipids to creating neutral TAG lipids (Thompson Jr., 1996). Since lipid content and cellular nitrogen are inversely related, measuring organic nitrogen can be used as a proxy for nitrogen starvation and the onset of lipid induction (Benemann & Tillett, 1987). Organic nitrogen starvation is typically calculated at <3% organic nitrogen per biomass (Richardson et al., 1969).

Many studies and entire programs have aimed to find the critical nitrogen deficient levels that induce lipid production in microalgae (Sheehan, 1998). It has been well observed that many microalgae reach high concentration of lipids well into 7-20 days of deficient nitrogen growth and variety of microalgae species have the potential to reach 30-80% lipid production during this timeframe (Table 3) (Lien & Spencer, 1983; Benemann & Tillett, 1987; Suen, Hubbard, Holzer, & Tornabene, 1987; Mandal & Mallick, 2009). The microalgae *Botryococcus braunii* has been able to achieve 61% lipid content in the laboratory, but this strain is fickle and difficult to maintain (Y. Singh & Kumar, 1992). Other fresh water algae genera, like *Scenedesmus* and *Chlorella* are able to reach 43% and 50% lipid content within 7 and 12 days; respectively (Lien and Spencer, 1983; Mandal & Mallick, 2009).

Nitrate is the most common nitrogen compound used in nitrogen depletion studies with little research performed on ammonia. Microalgae grown in wastewater would first metabolize

ammonia before nitrate (Ahmad & Hellebust, 1990; Dortch, 1990) and studies combining the reclamation of water along with ammonia depletion would be invaluable to future research and the growing biofuel industry.

Table 3. Some of the more common and notable nitrogen experiments. Bracketed days refer to period until the lipid percentage was achieved.

Author (Year)	Nitrogen Source	N-Free or N-deficiency	Algal Species	Lipid Percent [Day achieved]
Mandal et al (2009)	KNO ₃	Stationary phase to N-deficient media	<i>Scenedesmus obliquus</i>	43% [7]
			<i>Chlorella</i> sp.	18.7% [7]
			F&M-M48	
Rodolfi et al (2008)	NaNO ₃	N-Deficiency	<i>Scenedesmus</i> sp. DM	21.1% [7]
			<i>Tetraselmis suecica</i> F&M-M33	8.5% [9]
			<i>Nannochloropsis</i> sp. F&M-M24	35.7% [9]
Singh et al (1992)	KNO ₃	N-deficiency ^a to N-Free	<i>Botryococcus braunii</i>	61.4% [10]
		for 10 days	<i>Botryococcus protuberans</i>	52.2% [10]
Benemann & Tillet (1987)	mg as N	N-deficiency	Nanno Q	~41-48% [8]
Suen et al (1987)	KNO ₃	N-deficiency	<i>Nannochloropsis</i> sp. Q II	55% [10]
Lien & Spencer (1983)	NO ₃	N-deficiency	CHLS01	30-50%
			(<i>Chlorella</i> sp.)	[7-12]
Shifrin & Chisholm (1981)	NO ₃	N-deficiency ^b to N-Free for 10 days	Green Alga and Diatoms	30-50% [4-9]

^aMid-growth phase (23-24 days)

^bUntil late log-phase (1-2 days before light limitation)

2.4 Light-Shifts

Another simple tool for manipulating lipid content in microalgae involves altering light availability and intensity. Chlorophytes (green algae) and diatoms prefer high light regimes, but are able to optimally photosynthesize at conditions below full sunlight ($17,000 \mu\text{E}/\text{m}^2/\text{s}$) (Richardson, Beardall, & Raven, 1983). Light preference and optimization in microalgae are two different physiological factors that must be reconciled in order to maximize productivity and TAG production. The light harvesting efficiency of pigments greatly suppresses productivity potential in most algae. Since eight photons of light are required to fix CO_2 into carbohydrates, the maximum photosynthetic efficiency is about 12% (Scott et al., 2010). When respiration and suboptimal conditions are accounted for, the efficiencies are reduced to about 4.5-7% which translates to an open pond yield of 30-40 $\text{g}/\text{m}^2\text{-day}$ (Scott et al., 2010). Manipulating this metabolic deficiency with increased light levels would greatly increase biomass productivity in open ponds or could induce physiological changes in microalgae cells to produce TAGs. Increasing biomass productivity carries another challenge of managing dense cultures with decreased light penetration into the pond. One way to ameliorate decreasing light availability in dense cultures is to provide light intensity shifts (Benemann & Tillett, 1987; Wahal & Viamajala, 2010). By perpetuating the positive growth rate of the culture with sequential increases in intensity, cultures are able to produce more biomass than possible at a steady intensity or initial high light (Wahal & Viamajala, 2010).

Due to the phototropic nature of algae, elevated levels of irradiance result in higher growth rates and biomass production, but it also creates a metabolic cascade that affects nitrogen consumption, chlorophyll-a concentrations, and lipid content (Tedesco et al., 1989; Thompson Jr., 1996). High light intensities are known to increase the lipid content in green algae and diatoms (Tedesco et al., 1989) and even induce *de novo* TAG synthesis (Suknik & Carmeli, 1989). When

nitrogen is depleted and light energy exceeds the cellular capacity for growth and reproduction, photosynthates in the cells are diverted toward TAG synthesis (Roessler, 1990; Geider, 1987). Microalgae cultures growing in low light intensities compensate by producing high levels of chlorophyll-a in order to maximize the harvest of light (Benemann & Tillett, 1987). When a culture has an overdeveloped concentration of chlorophyll-a, the cells can be exposed to a bombardment of photons in which case they are unable to process and results in shuttling the energy into storage reserves (Benemann & Tillett, 1987, Thompson Jr., 1996). Interestingly, it is important to note that microalgae algae respond more favorably (higher TAG content) with double-sided illumination compared to single-sided illumination despite the same number of photons impacting the cultures (Rodolfi et al., 2009). This is an important consideration when cultivating microalgae in open ponds which are exposed to light on one surface. Increased turbidity due to cellular density will also need to be taken into account.

2.5 Pond Set Up

A pond study of microalgae lipid content was conducted at the San Luis Obispo Water Reclamation Facility (SLO WRF) Algae Ponds from October 2009 to December 2010. During this time ENVE graduate student Paul Ward operated four raceway ponds (Ponds 1-4) with dimensions of 2.5 m x 1 m x 0.5 m with, a volume of 920 L, and water depth of 30 cm. Effluent from the primary clarifiers at SLO WRF was used as influent to feed the ponds. Weekly samples from raceway ponds were analyzed for total suspended solids (TSS), volatile suspended Solids (VSS), total ammonia nitrogen (TAN), and oil content (lipids and triglycerides).

During the course of the study, Ponds 1 and 2 were used for experimental tests and Ponds 3 and 4 were left as controls. Data from control ponds 3 and 4 were used for the lipid analysis. In May and June of 2010, Ponds 3 were supplemented with CO₂ to set the pH at 8.3. The findings

from the experiment found the addition of CO₂ provided no significant difference between experimental and control ponds and were therefore were not removed in analysis of lipid content.

2.6 Experiment Set Up

Light-shift experiments on microalgae were conducted in concert with nitrogen depletion for the purpose of increasing triglyceride content. Batch cultures were grown in a set of six 1-L Pyrex® Roux bottles (120.1 mm x 55 mm x 175 mm) placed inside light racks flanked 1.5 inches on both sides from a pair of 40-W Vita-Lite full spectrum light bulbs (Duro-Test Lighting Corp.) (Figure 5). At the start of the experiment, treatments receiving one-sided illumination had only one pair of light bulbs on one side while the double-sided illumination had all four light bulbs in place. A light-dark cycle of 16:8 was automated with an Intermatic digital timer. A Gossen Panlux electronic Lux Meter measured the illumination of the lights to the surface of the roux bottles at 7000 lux for single-sided illumination and 14000 lux for double-sided illumination. This is equivalent to an overcast day to full daylight with indirect sun (Schlyter, 2010).

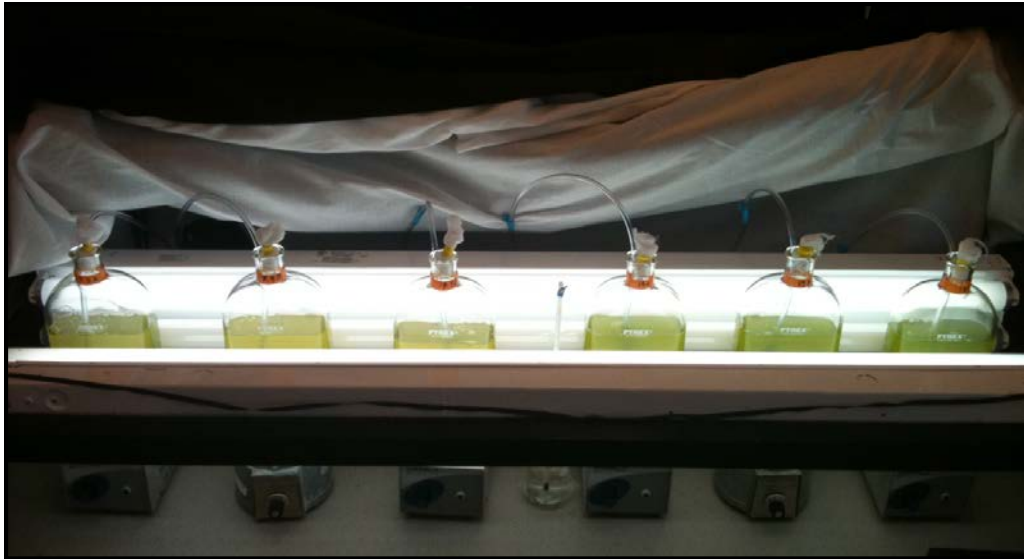


Figure 5. Light-rack treatments with six 1-L Pyrex® Roux bottles, air-1%CO₂ manifold, and stir plates.

Light-hampering covers were placed over the light racks to eliminate the ambient light from the laboratory and windows. As a result, the temperatures of the treatments were slightly elevated compared to room temperature. Fans were placed on one side of the racks to circulate in room temperature air. Bottles were also rearranged each day to minimize the effect of local hot spots within the light racks.

2.6.1 Agitation and Mixing

The cultures were agitated on a magnetic stir plate (Hanna Instruments HI 190M) with stir bars at approximately 300 rpm to prevent settling.

2.6.2 Carbon dioxide supplementation

A gas mixing rotameter (Matheson Model 603/610A) sparged all Roux bottles with a combination of 99% air and 1% carbon dioxide (CO₂) at a steady flow rate of 2.5 L/min. The air was sourced from laboratory spigots pumped from facility fans and CO₂ was supplied from a 50-lb

tank with 99.97% CO₂. Nylon tubing in a gang-type manifold was set up with air stones to administer the gas mixture to each Roux bottle. Air stones were submerged approximately $\frac{3}{4}$ into each roux bottle and individual valve regulators were used to standardize the flow rate across all Roux bottles. Cotton balls wrapped in cheese cloth were used to plug the Roux bottles to avoid evaporation.

2.6.3 Medium

An initial mother batch of wastewater microalgae was set up to in the lab to create a wastewater media with approximately 35 mg/L TAN to match previous experiments. Effluent from the primary clarifier at the SLO WRF was collected, brought to the lab, and placed in a 20-L fish tank. The wastewater was inoculated with microalgae from a continuous culture grown in 20-L outdoor fish tanks on a south facing patio by ENVE graduate student Louis Lefebvre. Originally, the outdoor fish tank culture had been inoculated with a diverse community of microalgae species from the SLO WRF raceway pond, but overtime the community of species shifted predominantly to a monoculture of *Scenedesmus* sp.

Ammonia was tracked (described in the TAN analysis in section 3.3.3.1) on the laboratory mother batch culture until the ammonia concentration reached 37.12 mg/L. On the third day of growth, the 20-L mother batch wastewater media was separated from the microalgae using a continuous centrifuge (US Centrifuge Model M212). Nitrogen reduction in the media was performed to match previous experiments with defined media containing nitrogen concentrations of 30 mg/L. A nitrogen concentration of 35 mg/L was also appropriate in maximizing results for the experimental time allotment of nine days.

2.6.4 Inoculate

Microalgae inoculate for the experiment was harvested from the laboratory mother batch during centrifugation of the wastewater media. The purpose for separating the microalgae from the

media was to reduce the effect of cellular shading at the beginning of the experiment. The centrifuged wastewater from the previous section was placed back into the 20-L fish tank, inoculated with microalgae, and a solids test was performed for an initial VSS value (35.53 ± 2.23 mg/L VSS). The culture was mixed with an aquarium fan and measured in 1-L graduated cylinders to be placed in 1-L Roux bottles. Treatment delegation of the Roux bottles was randomized to reduce measuring variances from the 20-L fish tank.

2.6.5 Light-shifts

The two experimental light-shift treatments differed in timing of increased light intensity and therefore their respective TAN levels were not similar at the time of the manipulation. Light-shift 1 changed from single-sided illumination to double-sided illumination two days prior to limiting TAN levels (<1 mg/L) and Light-shift 2 changed from single-sided illumination to double-sided illumination one day prior to TAN limitation. The double-illumination treatment experienced no light-shift.

Illumination on both sides of the cultures is also an important distinction. Flanked light exposure from both sides of the culture increases light availability to all cells in the medium. In fact, when the amount of photons is controlled, double-sided illumination increases storage lipids over single-sided illumination (Rodolfi et al., 2009).

Chapter 3: Methods and Materials

Presented in this chapter are the materials and methods for the pond study lipid assessment of raceway pond at the SLO WRF and the nitrogen depletion, light-shift experiment.

3.1 Pond Study

3.1.1 Micrographs

Pond biodiversity was assessed by identifying microalgae genera and general zooplankton taxa. Micrographs were captured with an Olympus CX41 optical microscope and an attached Infinity 2 digital camera at 40x and 400x magnification.

3.1.2 Solar Irradiance

Since evaluating the light history of microalgae cells in the pond is difficult, measures were taken to accurately describe the solar irradiance effect on microalgae in the raceway ponds (Richardson, 1983). Daily means of solar irradiance were collected from the Cal Poly CIMIS (California Irrigation Management Information System) station. Weekly means for each sample were calculated using daily means from seven days prior to the sample day. This better represents the solar energy input into the raceway ponds for photosynthesis rather than using day-of sample values.

3.1.3 Total Suspended Solids and Volatile Suspended Solids

The solids content in the ponds were assessed through total suspended solids (TSS) and volatile suspended solids (VSS) tests on pond water grab samples (See Paul Ward's thesis (2011) for sampling details). Solids testing was executed according to the APHA 2540-D Solids protocol in Standard Methods 19th Edition (Eaton et al., 1995).

Prior to the biomass test, glass fiber filters with a 1.2- μm pore size and 47-mm diameter were washed to remove any loose fibers or dust on the filters. Each filter was held with tweezers over a sink and washed for about 3 seconds with DI water from a squeeze bottle with a snipped tip to give higher flow. Next, the rinsed filter was placed on a filter holder attached to a vacuum pump, and 30 mL of deionized water was poured through with the vacuum pump running with approximately 20-25 psi of vacuum. The dewatered filter was then stacked with other washed filters on a 20-mL fluted aluminum weighing dish. This stack was placed in a 550°C muffle furnace for 15 minutes to ash any volatile material present from manufacturing. Due to the tendency of the bookend filters to burn or melt, two extra filters were rinsed and placed in the stack and discarded after ashing.

After 15 minutes, the stack was removed from the furnace and placed in a desiccator until it cooled to room temperature. Single filters were placed in assigned weighing dishes and tared to the nearest 10^{-4} gram on an electronic balance (Mettler Toledo).

Prior to pouring samples into a graduated cylinder for solids testing, sample bottles with pond water were vigorously shaken to suspend any settled material. One at a time, filters were placed on the vacuum apparatus and 30 mL of pond water was suctioned through leaving the particulate material on the filter. The filters were returned to their respective aluminum weighing dishes and placed in a 105°C oven between 2 to 24 hours. Typically, samples were left in the oven overnight to dry. This process evaporates any water on the filter leaving all total suspended solids on the filter. Once dried, the weighing dishes with filters were transferred to a desiccator to cool to room temperature. The samples were weighed, and this value was used to calculate total suspended solids (TSS).

$$TSS = \frac{(\text{filter and weighing dish at } 105^{\circ}\text{C}) - (\text{tare of filter and weighing dish})}{\text{sample volume}}$$

The samples were then placed in the 550°C muffle furnace for 15 minutes to incinerate any organic particulates on the filter. Afterwards, the weighing dishes were returned to the desiccator and once they had reached room temperature they were weighed to calculate volatile suspended solids (VSS).

$$VSS = \frac{(\text{filter and weighing dish at } 105^{\circ}\text{C}) - (\text{filter and weighing dish at } 525^{\circ}\text{C})}{\text{sample volume}}$$

TSS and VSS assessment of the raceways ponds was conducted by Paul Ward from July 2009 - December 2010. The solids data was used to calculate the dry weight of the algae pellet for lipid analyses.

Areal biomass productivity values was also calculated using VSS concentration, hydraulic residence time (HRT), and water depth of the pond (30 cm). HRT changed from 4 days to 3 days on July 7th, 2010.

$$\text{Biomass productivity} = \frac{VSS \times \text{pond depth}}{HRT}$$

3.1.4 Lipid Extraction

Extraction of lipids from the microalgae was performed with the Bligh and Dyer method (Bligh & Dyer, 1959). Pond samples were split to measure lipid concentrations via two methods—gravimetric and analytical analyses. The former method quantified the total lipids and the latter method characterized and quantified specific fatty acid methyl esters (FAMES).

The bottles of pond water grab samples were shaken vigorously and a graduated cylinder was used to collect 200 mL of sample. The sample was then placed in Erlenmeyer flasks prior to being pelletized. The microalgae in the grab samples were pelletized using a centrifuge for four minutes at approximately 7,000 rpm. Due to the destructive properties of organic solvents used in the Bligh and Dyer lipid extraction procedure, a 50-mL solvent safe PTFE (Teflon) centrifuge tube was used to capture the algae pellet. As a result of the limited centrifuge tube volume, the 200 mL pond samples were centrifuged in batches in which the supernatant was repeatedly decanted and saved. The centrifuge tube was refilled with more sample from the Erlenmeyer flask and centrifuged again. The process took about five to six rounds of centrifugation to fully pelletize the 200 mL sample. Once centrifugation was completed, microalgae pellets were preserved by flushing the headspace of the centrifuge tube with nitrogen gas and placed in a 0° C freezer until lipid analysis. The pellet supernatant was analyzed for TSS and VSS in order to calculate the estimated dry weight of the microalgae pellet.

$$\text{Pellet mass} = (\text{pond VSS} - \text{sample supernatant VSS}) \times \text{sample volume}$$

3.1.5 Bligh and Dyer

Lipid extractions were performed using the Enssani amended Bligh and Dyer protocol (Bligh & Dyer, 1959; Enssani, 1987). Centrifuge tubes with microalgae pellets were removed from the freezer and administered 4 mL of DI water and allowed to reach to room temperature. Methanol and chloroform were added to the samples in a 2:1 ratio (10 mL MeOH and 5 mL CCl₄) then sonicated with a probe descended into the sample using a Branson Sonifier 250 (102). The sonicator was set at a duty cycle of eight for 1 minute at a constant pulse. This process aided in the disruption of microalgae cell walls and released the internal components of the cells. After each sample had been sonicated, the centrifuge tube was tightly capped and the sonicator probe rinsed

with DI water and blotted dry for the next sample. After all samples had been sonicated, they were placed in a horizontal shake table for six to eight hours and agitated with 6 cm oscillations at 2 cycles per second. This ensured that all disrupted microalgae cells were continuously bathed in organic solvents and the lipids were completely extracted from the cells. After six to eight hours, the samples were removed from the shake table, administered another 5 mL of chloroform, and vortexed for 30 seconds. Once thoroughly vortexed, the samples were centrifuged at 7,000 rpm for four minutes. As a result, three distinct layers formed within the PTFE tube. The top layer contained water and methanol, the middle layer consisted of insoluble cell debris including remnants of cell walls, and the bottom layer contained chloroform along with lipophilic molecules like chlorophyll, triglycerides, and membranous phospholipids (Figure 6).

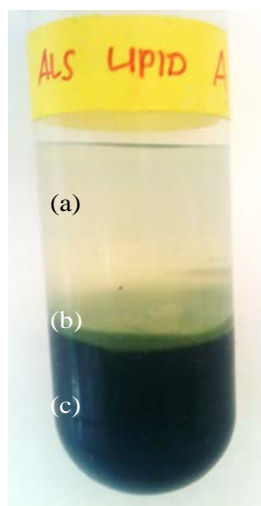


Figure 6. Layers separated by centrifugation at 7,000 rpm. The clear top layer (a) consisted of methanol and DI-water, the middle layer (b) is cellular debris from the cell wall, and the bottom layer (c) consists of the lipophilic compounds in chloroform.

The bottom lipophilic layer was extracted under a fume hood using a disposable 1-mL glass Pasteur pipette. To ensure the exclusion of impurities and cell debris, the extract was filtered using a 25-mL glass syringe, PTFE solvent safe plunger, and a disposable 0.2- μ m pore size nylon

filter. The disposable filter was pre-rinsed with 2-3 mL of chloroform prior to lipid extraction. Approximately 10% of the bottom lipophilic layer was left in the centrifuge tube to reduce cellular debris contamination in the extract. The extraction process was repeated in order to maximize the lipid extraction from the sample.

3.1.7 Gravimetric Analysis: Total Lipid Concentration

The lipophilic-chloroform layer from the samples was filtered into tared 40-mL aluminum weighing dishes. The second round of extractions from a single sample was placed in separate tared weighing dish due to limited volume capacity. These dishes were transferred to a desiccator sparged with nitrogen gas and left to evaporate the chloroform overnight. The next day, the weighing dishes were placed in a nitrogen gas sparged oven at 105°C for one hour. This ensured the vaporization of all the chloroform leaving the concentrated total lipids. The weighing dishes were cooled in a desiccator sparged with nitrogen and weighed on an electronic balance for the nearest 10^{-4} of a gram (Figure 7).



Figure 7. Aluminum weighing dishes with lipid extracts for gravimetric analysis.

Masses from each set of extractions were combined and compared to the mass of the algae pellet resulting in a percentage of total lipids from the sample. Due to the extensive processing time, one gravimetric sample was measured for each pond.

$$\text{Total lipid mass} = (\text{weighing dish}_1 + \text{weighing dish}_2)$$

$$\text{Total lipid percentage} = \left(\frac{\text{Total lipid mass}}{\text{Pellet mass}} \right) \times 100$$

3.1.8 Analytical Analysis: Triglyceride Characterization and Quantification

Lipid-chloroform extractions were filtered into 30-mL glass vials with sealable lids. Rather than place the second round of lipid extractions in new vials, they were added to the same vial. The glass vials were placed in a Caliper Life Science TurboVap II desiccator to actively vaporize the chloroform solvent and concentrate the lipid compounds. The vials were opened and quickly placed in a large 200-mL glass tubes submerged in a 30°C water bath. The samples were continuously sparged with nitrogen gas at 10 psi to prevent lipid oxidation during the drying process. After three hours, samples were periodically checked and weighed until they reached consistent mass. Due to the large mass of the glass vial relative to the lipids, this value was considered inaccurate in determining weight via gravimetric methods. Instead, these samples were further processed to select and determine triglyceride mass through transesterification and Gas Chromatography-Mass Spectrometry.

Gas Chromatography and Mass Spectrometry (GC-MS) allows us to separate, characterize, and quantify a heterogeneous solution comprised of many lipid types. Triglycerides are large compounds and are difficult to process through the GCMS—therefore they must be transformed into their smaller, non-polar fatty acid methyl ester (FAME) counterparts through transesterification.

3.1.8.1 Transesterification

After the chloroform had been actively vaporized, the remaining lipophilic compounds were given a 5 mL volume of toluene to re-suspend the concentrated lipids. A 1 mL aliquot was retrieved for analysis and the remainder was capped and saved in the freezer. A 2 mL volume of anhydrous sodium methoxide in 0.5 M methanol solution was added to the vial and placed in a 50° C water bath for 10 minutes. This base-catalyzed reaction separates triglycerides into its glyceroxide and FAME constituents. Fatty acid chains are severed from the larger triglyceride compound via transmethylation by the methoxide molecule creating FAMES and the strong base glyceroxide (Figure 8). This reaction transforms methoxide ion into methanol. Subsequently, the glyceroxide is protonated by the methanol which regenerates the methoxide ion. This regeneration maximizes the transmethylation of all the fatty acids in the sample. After 10 minutes, 10 µL of glacial acetic acid was added to neutralize the reaction. The solution was washed with 5 ml of hexane and 5 ml of deionized water and vigorously shaken for 20 seconds. The mixed solution quickly separated in two layers: the top layer containing hexane with FAMES and the bottom layer containing water, residual methanol, acetic acid, and other impurities. The top layer was transferred to a separate glass vial using a 1 ml glass pipette. Approximately 90% of this layer was recovered due to the narrow hexane-water barrier. Anhydrous sodium sulfate was added to dry the sample and remove excess water—as water in the GC-MS may damage the instrument. This solution was vigorously shaken for 20 seconds and filtered into a 12-mL glass vial (Figure 9) using a funnel created from a coarse pore Fisher Scientific F8 filter. The samples were stored in a freezer until further analysis.

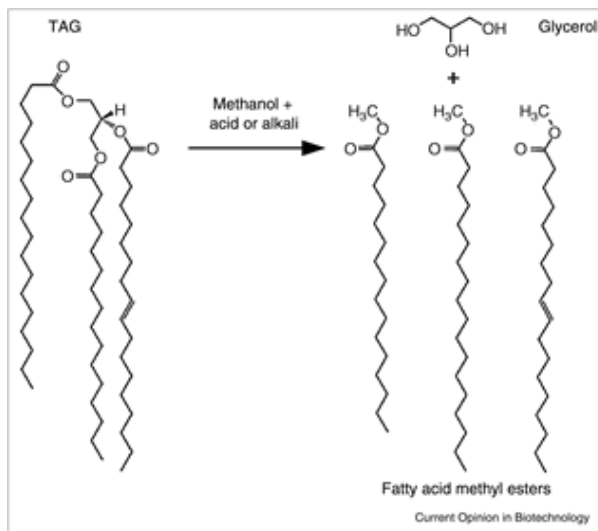


Figure 8. Transesterification pathway of a triglyceride molecule into three fatty acid methyl esters (FAMEs) and one glycerol compound (Scott et al., 2010).



Figure 9. FAME sample in hexane from transesterified lipid extract in a 12-mL glass vial.

3.1.8.2 Fatty Acid Methyl Ester (FAME) Standards

Proper analytical analysis of the FAME compounds via GC-MS requires the addition of known internal standards to the sample. Pentadecanoic acid methyl ester (C15:0) and nonadecanoic acid methyl ester (C19:0) were purchased from Grace Davison Discovery Sciences in 100-mg standard vials. These odd-carbon FAMEs were most desirable because they bracketed

the target compounds—hexadecanoic acid methyl ester (C16) and octadecanoic acid methyl ester (C18)—and were not present in the sample. Odd-carbon FAMES are typically foreign compounds because fatty acid synthesis in plants and microalgae involves the extension of a carbon chains via the addition of carbon pairs and therefore seldom produces odd-chain FAMES (Ohlrogge and Jaworski, 1997; Christie, 2003). The concentration of FAME constituents from each lipid extract were quantified using the Volmer, Meiborg and, Muskiet bracket method described in Hutton (2009).

FAME standards were poured into separate 10-mL vials and the standard vials were cleaned with hexane to capture any remaining standard. The 10-mL glass vial was then filled with hexane and weighed. The original glass vial tare and standard mass was subtracted from this value to give the mass of the hexane in the vial.

$$\text{Hexane mass} = \text{vial}_{\text{hexane} + \text{std}} - (100 \text{ mg std} + \text{vial tare})$$

From this value the FAME concentration standard solution (g/g) was calculated.

$$[FAME] = \frac{100 \text{ mg std}}{\text{hexane mass}}$$

These FAME standard concentrations were used to make a range of dilutions using the $C_1M_1=C_2M_2$ equation. Dilution concentrations were confirmed through QA/QC calibration curves then appropriately matched to gas chromatographs from the preliminary sample runs. This ensured relatively equal composition of standards and target FAMES.

3.1.8.3 Gas Chromatography Mass Spectrum (GC-MS)

Once the samples had been transesterified, a 100 μL aliquot was placed in a GC crimp top vial and diluted with 400 μL of hexane. A preliminary run was used to determine the appropriate standards to place in each sample. Once the initial abundance of the sample had been determined via the chromatograph, the closest diluted standards were selected and placed in a GC vial with a 100 μL aliquot of sample, 100 μL aliquot from each standard, and 200 μL of hexane for total volume of 500 μL .

A method for targeting medium carbon chain length FAMES had been previously programmed in Chemstation by graduate student, Matt Hutton, and Cal Poly professor Dr. Corinne Lehr (Hutton, 2009). An Agilent gas chromatograph (6890) was used along with 50 m by 0.25 mm fused silica column (Agilent #190915-433). The GC was programmed to run a 10:1 split with a sample size of 5 μL for a total column flow of 13.7 mL/min during a 10.20 minute run. The inlet was heated to 250°C and the initial temperature of the column was heated to 120°C. Once the sample had been injected, the chromatograph oven increased 50°C every minute to 280°C and held at this temperature for 2 minutes until the run was completed. The quadrupole and mass spectrometer source were heated to 250°C and 230°C, respectively.

The process was automated with an autosampler that would flush and discard the injection needle five times with hexane and three times with the sample prior to injection. The final sample was drawn using four fill-discharge cycles to minimize air bubbles in the syringe. The injection needle was also programmed to clean itself after the sample with two flushes of hexane. Each sample was analyzed in duplicate. A gas chromatograph described the concentrations of the standards and sample FAME constituents (Figure 10). Each peak was characterized using the MS Search 2.0 database from the United States National Institute of Standards and Technology (NIST) (National Institute of Standards and Technology, 2006).

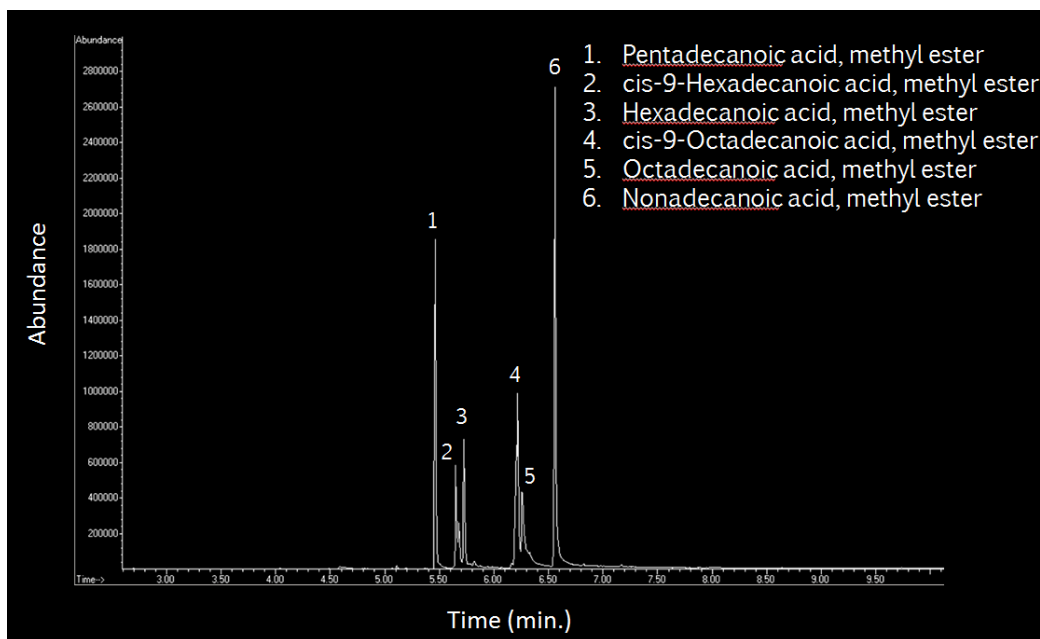


Figure 10. A gas chromatograph of sample FAMES bracketed by internal standards.

3.1.8.4 FAME and Triglyceride Calculations

The following steps were used to determine individual FAME concentrations based on the known internal standards. Triglyceride concentrations were calculated based on the FAME concentrations obtained through integrated chromatograph abundance peaks for each standard based at the time point they eluted from the sample.

$$area = \int_{Time_1}^{Time_2} Abundance$$

This gave us a ratio of standard FAME concentration to chromatograph abundance.

$$P_x = \frac{[STD]}{Area_{std}}$$

A slope was obtained from the difference of the two internal standards divided by the difference in elution time.

$$Slope = \frac{P_{19} - P_{15}}{Time_{19} - Time_{15}}$$

This linear relationship between internal standards allowed us to calculate sample FAME concentrations (g/g).

$$[FAME_A] = Area_A \times P_{15} + [Slope \times (Time_A - Time_{15})]$$

The total mass of each FAME (g) was calculated for the whole sample.

$$FAME_A = \left[\frac{[FAME_A] \times Total\ GC\ Sample\ Volume}{FAME\ GC\ Sample\ Volume} \right] \times [Volume\ of\ hexane\ in\ transmethylation \times density\ of\ hexane]$$

Since natural triglycerides may have an array of fatty acid combinations, hypothetical uniform triglycerides were calculated to determine specific carbon-chain triglyceride mass (mg).

$$TAG_A = \frac{FAME_A \times MW_{TAG}}{3(MW_{FAME})} \times 1000$$

These values were summed and compared to the dry-weight of the algae pellet (mg).

$$\%TAG = \frac{TAG_{C16} + TAG_{C16:1} + TAG_{C18} + TAG_{C18:1} + TAG_{C18:3}}{pellet\ mass} \times 100$$

The consolidation of calculated TAG values resulted in total triglycerides as a percentage of the VSS for each sample (%TAG).

3.2 Light-shift and Nitrogen Depletion Experiments

After the completion of the daily light period at 2:00 pm, each experimental Roux bottle was shaken vigorously for 15 seconds to dislodge growth along the bottle walls and consolidated in a large vessel respective of treatment. The treatment cultures were homogenized with a stir plate and stir bar spinning at 300 rpm for 5 minutes. Once homogenized, various sample volumes were pulled from the large vessel using a 1-L or 50-mL graduated cylinder for: solids tests, nitrogen tests, and TAG analysis (Figure 11). After the sample pull, the culture was poured back into 1-L Roux bottles to either full capacity (1 L) or a standardized volume across an appropriate number of bottles. The time the cultures spent out of the treatments was minimized by performing swift sample collections and quickly returning the Roux bottles to the light racks.

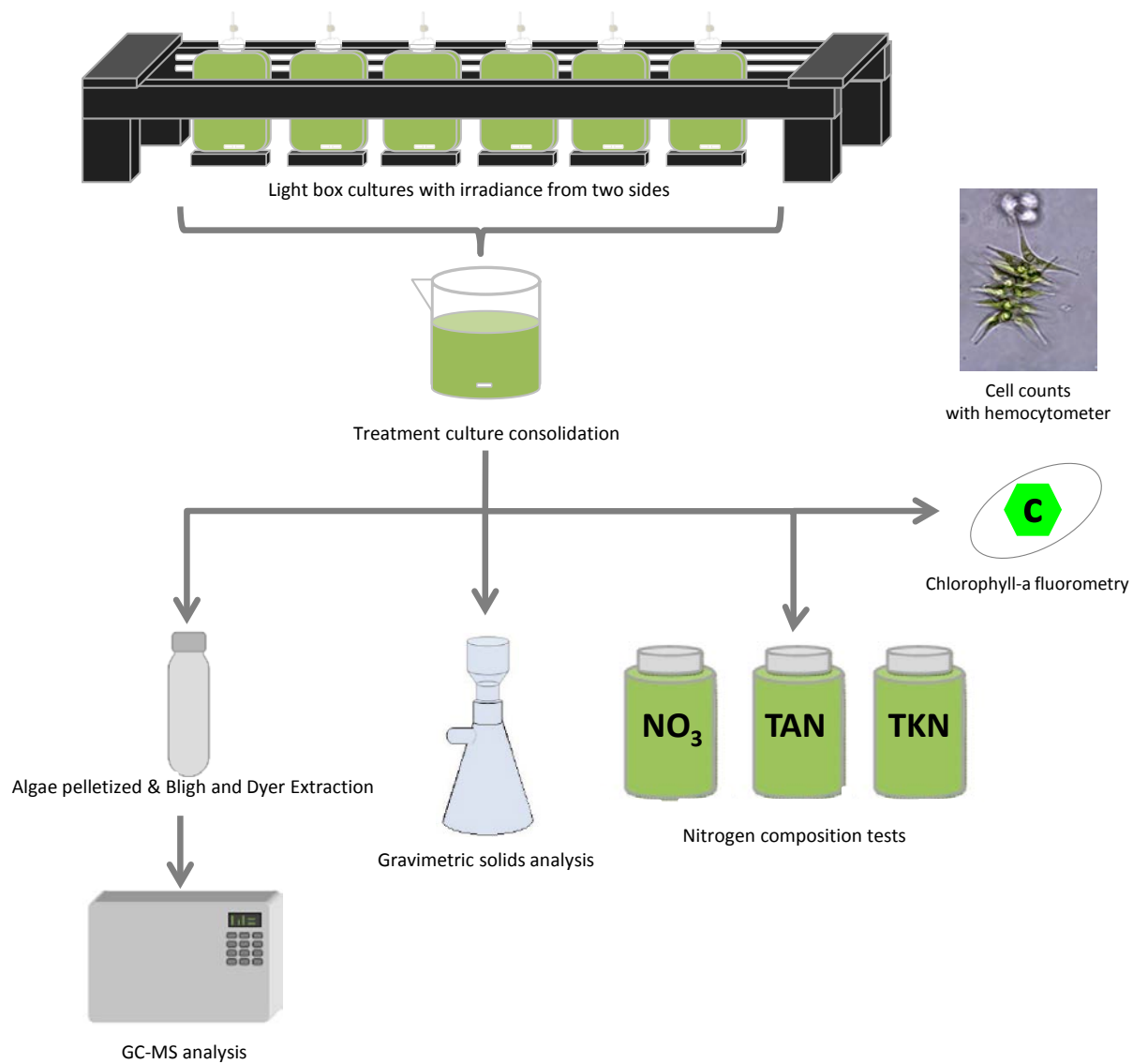


Figure 11. Daily sample processing of light-shift experiments depicting treatment culturing, solids determination, and analytical analysis of TAG and nitrogen compounds.

3.2.1 Cell Counts

Cell counts were made on a hemocytometer. A 1-mm thick cover slip was placed on top of the hemocytometer and a small aliquot of sample was added to the capillary end and pulled the water into the chamber. Cell numbers were collected by counting the large 1 cm x 1 cm grid at 40x. Samples were performed in triplicate and averaged to determine daily population size.

3.2.2 Triglyceride Extraction and Analytical Analysis

Sample volumes needed for a 50 mg pellet were calculated with VSS from the previous day in an effort to conserve the volume of the culture to span the entire duration of the experiment. As a result, various sample volumes were pulled throughout the experiment for pelletizing. A two-step centrifugation process was developed which included batch centrifugation and smaller individual centrifugation.

The first step involved centrifuging samples in batches using 400-mL Teflon bottles and a DuPont Instruments RC-5 Superspeed Refrigerated Centrifuge with a Sorvall rotor at 11,000 RPM for 5 minutes. As the experiment progressed, the sample volume required for a 50 mg pellet decreased from 690 mL to 300 mL due to the overall increase in microalgae VSS. The pellets from the centrifuge bottles were dislodged with small amounts of supernatant and recombined into one 400-mL Teflon bottle. The sample was centrifuged again and the supernatant was collected and saved. The last pellet was dislodged with supernatant and transferred to a 30-mL PTFE centrifuge tube.

For the second step, the sample was spun in the centrifuge tube at 8850 RPM for 5 minutes in a Thermo Electron Corporation IEC Multi RF (cat #: 75004521). The supernatant was re-combined with the original supernatant and the headspace of the final pellet was flushed with N₂ gas and stored in a 0°C freezer. The dry-weight of the pellet was determined through a 30 mL volume of the supernatant, TSS and VSS analyses, and calculations from section 3.1.3.

The Bligh and Dyer Enssani amended method was used for lipid extractions on the microalgae pellets in the same manner as section 3.1.5. Transesterification, FAME characterization, and FAME quantification was completed in the same method as section 3.1.8.

3.2.3 TAG Productivity

Productivity was calculated used methods from Griffiths (2011). Concentrations of TAG (mg/L) for each day were calculated using the VSS and TAG content values for each day.

$$[TAG] = Culture\ VSS \times \%TAG$$

The maximum concentration of each culture was determined from a review of the values from the 9 day experiment.

Productivity (mg/L-day) was calculated by taking the daily rate increase in TAG concentrations from each day.

$$TAG\ Productivity = \frac{[TAG]_2 - [TAG]_1}{time_2 - time_1}$$

A rolling average was determined by averaging values from three days (one day before, the day of sample, and the day after). The maximum productivity value was determined after reviewing all values from the experiment.

3.3 Solids and Nitrogen Tests

3.3.1 Total and Volatile Suspended Solids

De-ashing and initial tare of the filter and weighing dishes were performed in the same manner as the pond study in section 3.1.3. Triplicate 30 mL samples were taken from the homogenized cultures and processed for TSS and VSS values in accordance to the APHA 2540 Solids-D protocol in Standard Methods 19th Edition.

3.3.2 Daily Growth Rates

Daily growth rates were calculated each day for all three treatments.

$$\mu = \frac{\ln(N_2 - N_1)}{(t_2 - t_1)}$$

Where N_n was the VSS and t_n was the sample day in the experiment.

3.3.3 Nitrogen Analyses

Nitrogen was analyzed through various methods to distinguish between the content of ammonia, nitrate, and organic nitrogen. Ammonia tests were performed each day during the experiment and—due to timing constraints and the ease of sample preservation—nitrate and total Kjeldahl nitrogen tests were performed after the experiment had ended.

3.3.3.1 Total Ammonia as Nitrogen (TAN)

Samples of 30 mL were taken from the homogenized culture and analyzed for total ammonia nitrogen (TAN). The test followed the TAN analysis protocol in Standard Methods and used a Thermo Scientific NH_3 Selective Electrode (ORION 9512HPBNWP). The membrane on the electrode is sensitive and must be stored in 1000 ppm NH_3 solution. Prior to testing, the electrode was calibrated by creating a 5-point logarithmic calibration curve with 100-mL volumetric flasks and Fisher Scientific ammonia standard (2500 ppm as NH_3). The standard

calibration curve exceeded the maximum and minimum concentration limits of potential TAN values found in the sample in order to ensure all data collected would fall within the calibration range. Since temperature can affect the volatilization rate—and therefore detection—of ammonia, samples were tested within $\pm 1^\circ\text{C}$ of each other. QA/QC tests were also performed on selected samples using a spike of 2500 ppm ammonia standard at 1.5-2 times the recorded TAN value. A recovery between 85% and 115% of the original sample value was concluded as a successful test.

Daily rates of consumption were calculated using the equation:

$$\text{Rate of Consumption} = \frac{(TAN_2 - TAN_1)}{(t_2 - t_1)}$$

Averages of the rate of consumption for each treatment were calculated from day 2 to the first day of nitrogen depletion determined to be when the culture fell below 1 mg/L TAN.

3.3.3.2 Nitrate

During the solids analysis, a 30-mL flat bottom test tube was placed under the filter in the filtration apparatus in order to recapture the VSS filtrate. The filtrate was transferred to 40-mL sample bottles and stored in the freezer until nitrate testing. A nitrate electrode (Thermo Scientific Nitrate Ion Selective Electrode, cat # ORION 9707BNWP) was calibrated using a 5-point logarithmic calibration curve with 100-mL volumetric flasks and 1000 ppm NaNO_3 standard. Both the nitrate standard and samples were raised to room temperature prior to testing. The test followed the protocol in the Thermo Scientific Nitrate Ion Selective Electrode User Guide. For small volumes, Nitrate Interference Suppressor Solution (NISS; ORION 930710) solution was used in accordance with the manual.

3.3.3.3 Total Kjeldahl Nitrogen (TKN) and Organic Nitrogen (ON)

Total Kjeldahl Nitrogen (TKN) tests were performed with an open Kjeldahl apparatus (cat # 2117803) using the APHA 4500-N_{org} Macro-Kjeldahl protocol from Standard Methods 19th Edition. A 250 mL sample was retrieved from a homogenized culture and preserved by reducing the pH to less than 2 with 2-8 drops of 18M H₂SO₄ solution from a disposable glass Pasteur pipette. Lowering the pH suppressed ammonia volatilization in the sample and aided in preventing the reporting of erroneous TKN values.

Due to the extensive time and limited available space for testing, one TKN test involved running many items at once. One test including running the experimental samples, two standards (20 mg/L as N and 50 mg/L as N) created from 2500 ppm ammonia standard solution, a blank with DI water, and a spike of 2500 ppm ammonia standard on selected samples. The blank and spike were used for QA/QC testing. For the spike, a recovery between 85% and 115% of the original sample value was concluded as a successful test.

TKN values were used to calculate the organic nitrogen (ON) concentration by deducting TAN and nitrate concentrations from the respective sample.

$$\text{Organic nitrogen} = \text{TKN} - \text{TAN}$$

Organic nitrogen concentration was then compared with the respective sample's VSS to describe the percent of organic nitrogen (%ON) as VSS. Nitrogen starvation in microalgae cells is determined through %ON and the threshold for starvation in this experiment was <5% ON (Richardson et al., 1969; Becker, 1994).

$$\%ON = \frac{ON}{VSS} \times 100$$

3.3.4 Chlorophyll-a

Sampling for chlorophyll-a began on day 2 and continued until the end of the experiment.

A volume of 5 mL was collected from a homogenized culture and filtered through 1.2-μm pore size and 47-mm diameter glass fiber filter. The sample was folded and preserved in aluminum foil and stored in a -80° C freezer until further testing at the end of the experiment.

Chlorophyll-a extractions were prepared by dimming the ambient lighting, removing the filters from the aluminum wrapping, and placing them in clean separate 15 mL test tubes. Each sample was administered 10 mL of 90% acetone, covered with parafilm, and placed in an aluminum foil covered test tube rack in a 4°C refrigerator overnight. The following day, the samples were removed from the refrigerator and allowed to come to room temperature. During this time, the fluorometer (Turner Designs 10-AU Fluorometer) was warmed up for 10 minutes and regular maintenance parameters were checked to assess any temporal drift in the instrument. A 40X dilution of each sample was made by combining a 125 μL aliquot of chlorophyll-a extract (inverted 5 times before extraction) and 4875 mL of 90% acetone in 10 mL (13 mm diameter) borosilicate test tubes. The dilution samples were covered with parafilm and mixed by inversion five times prior to the fluorescence reading. Next, the dilution samples were administered a volume of 150 μL 0.1N HCL, inverted 5 times, and allowed to acidify for 90 seconds. After acidification, fluorescence readings were collected again. Chlorophyll-a concentrations were calculated using the following formula:

$$Corrected [chl\ a] \left(\frac{\mu g}{L} \right) = F_s \times \left(\frac{Acid\ ratio}{Acid\ ratio - 1} \right) \times (R_b - R_a) \times \left(\frac{extract\ volume}{volume\ filtered} \right) \times dilution\ factor$$

where F_s is 1 (sensitivity of the fluorometer), the acid ratio is 1.96, R_b is the fluorescence value before the acid, R_a is the fluorescence value after the acid, the extract volume is 125 μL, the

volume filtered is 5 mL, and the dilution factor is 40X. Samples were run in triplicate and combined to calculate mean corrected chlorophyll-a concentration value for each day.

Daily rates of production and consumption were calculated similar to TAN consumption rates. Positive chlorophyll-a rates were noted as periods of production and negative chlorophyll-a rates were noted as periods of consumption. Although an increase in VSS could account for the drop in chlorophyll-a concentration, consumption was assumed because microalgae are known to break down chlorophyll-a at the onset of nitrogen depletion (Lien and Spencer, 1983).

3.3.5 Temperature and pH

The temperature of the homogenized culture was checked with a spirit thermometer and pH was tested with a SevenEasy pH meter (Mettler Toledo) and Orion electrode. Once all samples for the day had been pulled for testing, the pH of the culture was brought back to a pH of 8 with 2-3 drops of 18M H₂SO₄ or 2 N NaOH depending on the pH reading.

3.3.6 Statistical Analyses

Statistical analyses were performed with JMP Pro 10. ANOVAs and t-tests were performed within a 95% confidence interval ($\alpha = 0.05$).

Chapter 4: Results and Discussion

This chapter presents observations from the pond study and light-shift experiments along with discussions of results. Before discussing the main results, a comparison between the gravimetric and analytical methods for lipid measurement is discussed. The discrepancy between results from both analyses is explored in the following section.

4.1 Discrepancies in Measurement Methods

A continual pattern of bias towards TAG content was observed, which is improbable because TAGs are constituents of the total lipids analysis. As described in a later section, algae biomass sampled from the raceway ponds over the year contained a wide range of total lipids (1%-30%) and TAGs (2%-50%). Initially, a slight bias in the data was expected due to the gravimetric method's indiscriminate extraction of lipophilic compounds, which was apparent by the dark green color of the extract due to chlorophyll. A matched pair t-test showed a significant difference between means of total lipid content and TAG content with a significant bias towards TAG values ($p = 0.0002$) (Figure 12). If the data from the analytes were more equal, the respective differences of the split samples would be centered along a 1:1 ratio along $y = 0$. This revealed that the discrepancy must be a result of one of the two method extractions.

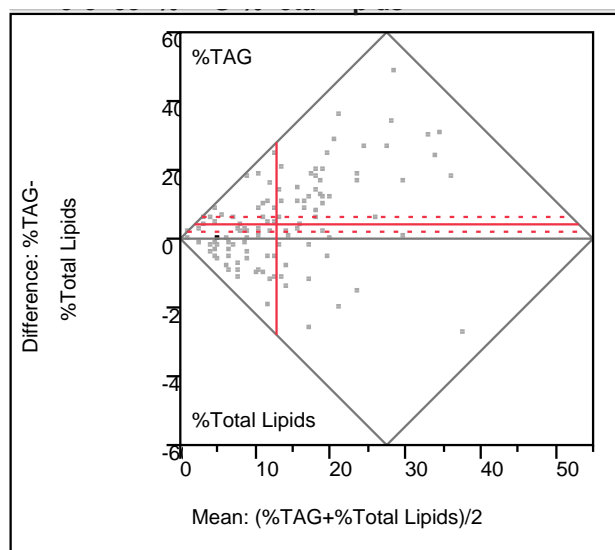


Figure 12. Bland-Altman plot for %TAG and %Total lipids from samples collected from microalgae polycultures in raceway ponds. Data for %TAG was collected through analytical methods and data for %Total lipids was collected through gravimetric methods.

Further investigation into the literature confirmed the observed TAG bias was likely due to high vaporization temperatures from the gravimetric analysis (105°C) compared to the lower vaporization temperature of the analytical analysis (30°C) (Widjaja, Chien, & Ju, 2009). At elevated temperatures, lipid compounds readily oxidize and reduce the mass of extract (Oehrl, et al., 2001). Because gravimetric analyses resulted in suppressed values of total lipids, TAG content via analytical methods were used in further oil content analyses.

A QA/QC test was performed on the drying temperatures of the gravimetric method. A comparison between 105°C and 30°C was investigated through gravimetric analysis in triplicate. The samples were dried for one hour and allowed to reach room temperature before weighing. The mass from both drying temperatures were not significantly different, but the 105°C samples were conspicuously depressed compared to the 30°C drying temperature (Appendix A).

4.2 Pond Study

Samples were collected and analyzed weekly from two 3-m² raceway ponds operated with primary effluent wastewater. The ponds reported in this thesis were acting as control ponds (Pond 3 and Pond 4) for multiple consecutive experiments by environmental engineering graduate student Paul Ward. The content of the ponds were not manipulated in any way throughout the study with the exception of a decrease in hydraulic residence time (HRT) from 4 days to 3 days which is accounted for from July 7, 2010 and forward. The following sections describe the chemical and biological characteristics of the samples collected from these ponds.

4.2.1 Solar Irradiance

Plotted along a time-series graph, the mean weekly solar irradiance depicts a typical sinuous seasonal pattern expected in San Luis Obispo, Calif. (latitude 35°N) (Figure 13). Maximum solar irradiances occurred from May to July, and minimum irradiances from December to February. Seasonal effects on VSS and TAG content of were also examined and based on the 2009 and 2010 solstices and equinoxes.

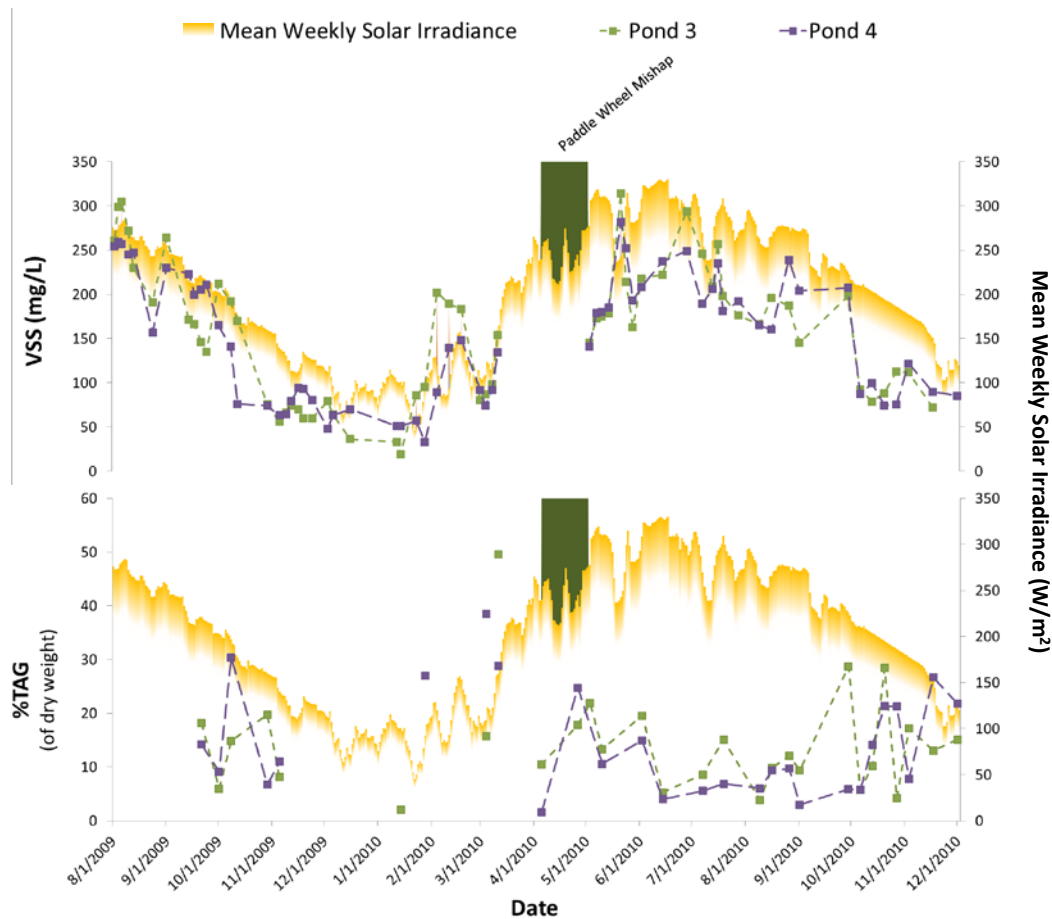


Figure 13. (Top) VSS (■) in raceway ponds and mean weekly solar irradiance from August 2009 to December 2010. (Bottom) %TAG (●) in raceway ponds and mean weekly solar irradiance from August 2009 to December 2010.

In ponds 3 and 4, VSS concentration was directly correlated with mean weekly solar irradiance ($R^2 = 0.59$, $p < 0.001$) (Figure 14). Divided into seasons, VSS concentrations had the following averages: spring ($\bar{x} = 222$ mg/L), summer ($\bar{x} = 185$ mg/L), autumn ($\bar{x} = 118$ mg/L), and winter ($\bar{x} = 89.7$ mg/L) (Figure 15). Using a one-way ANOVA test and Tukey HSD post hoc analysis, VSS content was significantly different between spring-summer and autumn-winter means ($p < 0.0001$) (Figure 15).

TAG content of the microalgae displayed an inverse relationship with mean weekly solar irradiance ($R^2 = 0.16$, $p = 0.0039$) (Figure 14). Using a one-way ANOVA and Tukey HSD post hoc analysis, a conspicuous difference was observed between TAG content means in winter ($\bar{x} = 23\%$) and summer ($\bar{x} = 8.3\%$) ($p = 0.0136$) (Figure 15). Both spring ($\bar{x} = 13.4\%$) and autumn ($\bar{x} = 15.0\%$) means did not show a significant difference in TAG content.

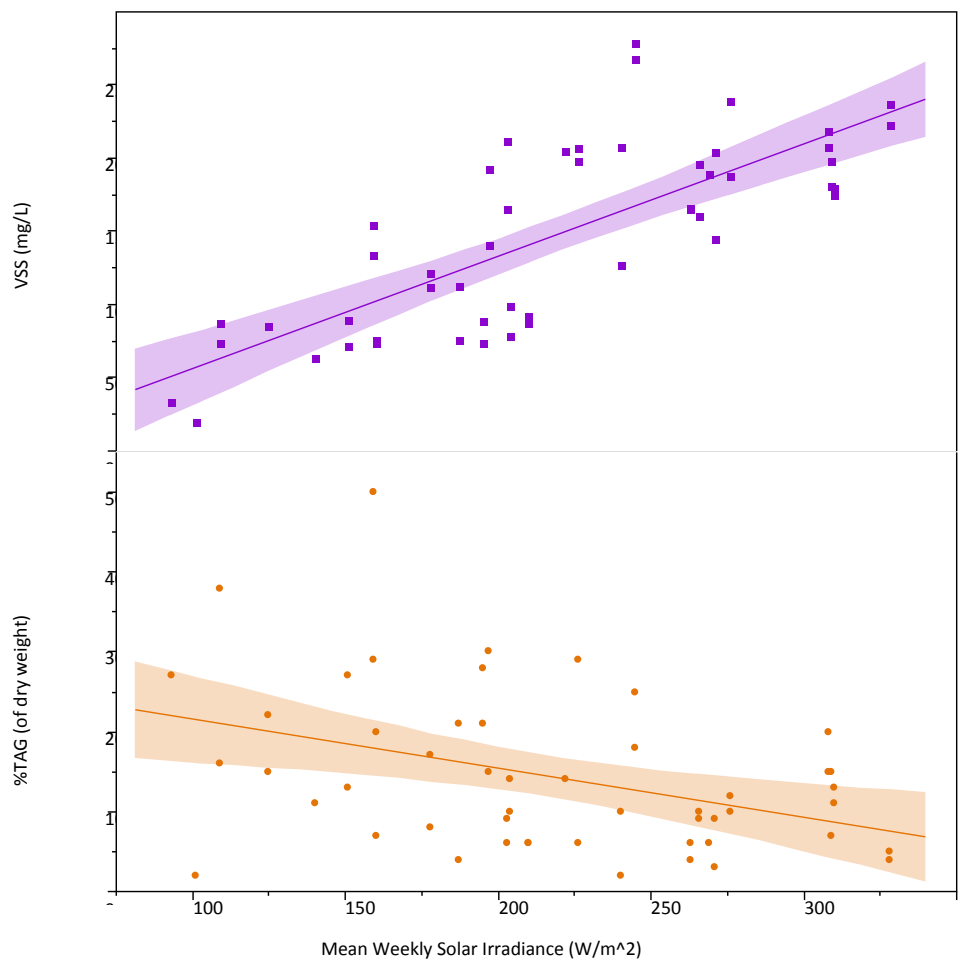


Figure 14. Correlations of microalgae VSS concentrations and TAG content in VSS to mean weekly solar irradiance (W/m^2). TAG content may decrease with increased VSS due to shading in the water column and as a result of potential increases in TAG consumption for respiration.

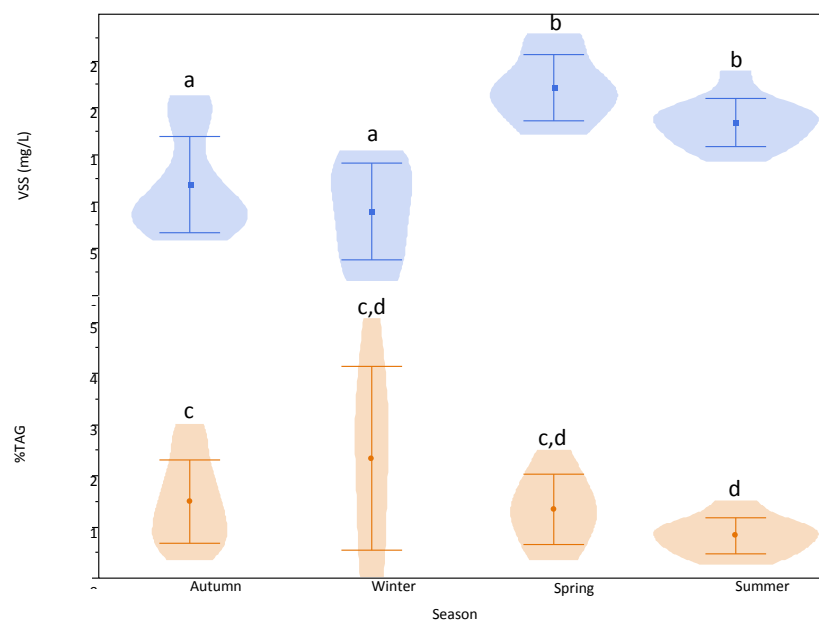


Figure 15. VSS concentration and TAG content for raceway pond microalgae, separated by season. Shown are means with standard deviation and sample size distribution (contour). The dates were chosen based on solstices and equinoxes from September 2009 to December 2010.

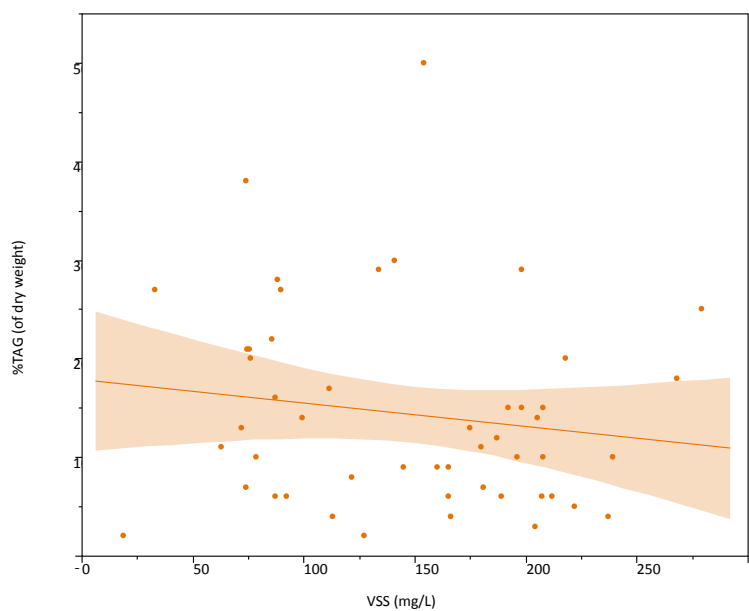


Figure 16. VSS concentrations and %TAG values do not have any conspicuous relationships.

Interestingly, when comparing VSS and TAG content data together, no immediate relationship is discerned ($R^2 = 0.023$, $p = 0.2985$) (Figure 16). VSS concentration is linked with mean weekly solar irradiance and TAG content may be affected by reduced light availability due to mutual shading. Otsuka and Morimura (1966) claim this decreases the photosynthesis-respiration ratio during the light cycle and contributes to the consumption of TAG reserves during the dark cycle (Thompson, 1996).

Biomass productivity is used in the following section to clarify the inverse TAG concentration response.

4.2.2 Productivity and Insolation

Algae productivity can only be estimated when organic wastewaters are used as media, due to bacterial growth and wastewater detritus. However, biomass productivity was calculated for the period of the present study (Ward, 2011). These estimates are used in the following analysis of data stemming from the present thesis.

In order to produce enough lipids to maintain a feasible biofuel operation, harvest must occur at least 8-10 months through the year (Lundquist et al., 2010). Biomass productivity ranged between 6 g/m²-day to 24 g/m²-day from March 2010 to October 2010. Biomass productivity was correlated with an increase of mean weekly solar irradiance ($R^2 = 0.63$, $p < 0.0001$), while TAG content displayed an inverse relationship ($R^2 = 0.16$, $p = 0.0039$) (Figure 17). Again, lower TAG content values were not necessarily due to high solar irradiance, but rather, depressed concentrations of TAGs may be a result of shading from an increase in VSS concentration.

When comparing biomass productivity (g/m²-day) and TAG content as responses to mean weekly irradiance, a conspicuous intersection emerges at 231 W/m². At this irradiance level, biomass productivity was 13.5 g/m²-day and contained 13.5% TAG content. Calculated lipid

productivity at this time would be $1.76 \text{ g/m}^2\text{-day}$. Irradiance values of 231 W/m^2 occurred in April and September and matched optimal TAG productivities of $2.65 \text{ g/m}^2\text{-day}$ and $2.22 \text{ g/m}^2\text{-day}$; respectively (Figure 18).

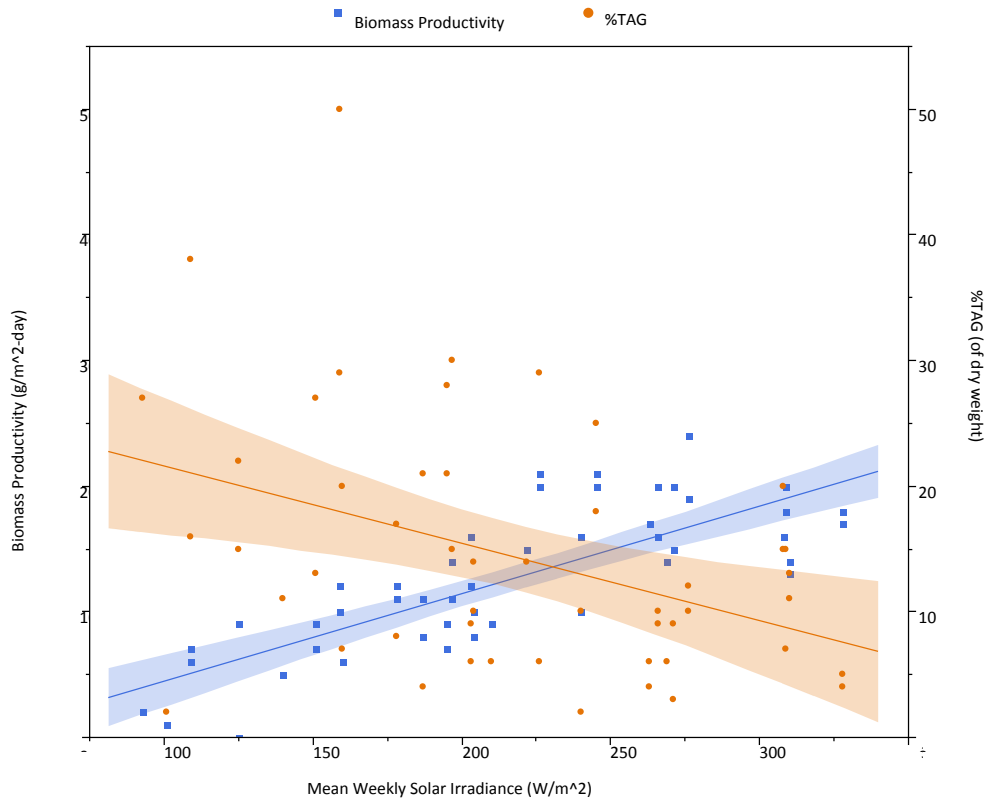


Figure 17. Control pond biomass productivity (■) and % TAG content (●) with respect to mean weekly solar irradiance. The intersection between the two factors is 231 W/m^2 , at which point the highest TAG productivity would be expected.

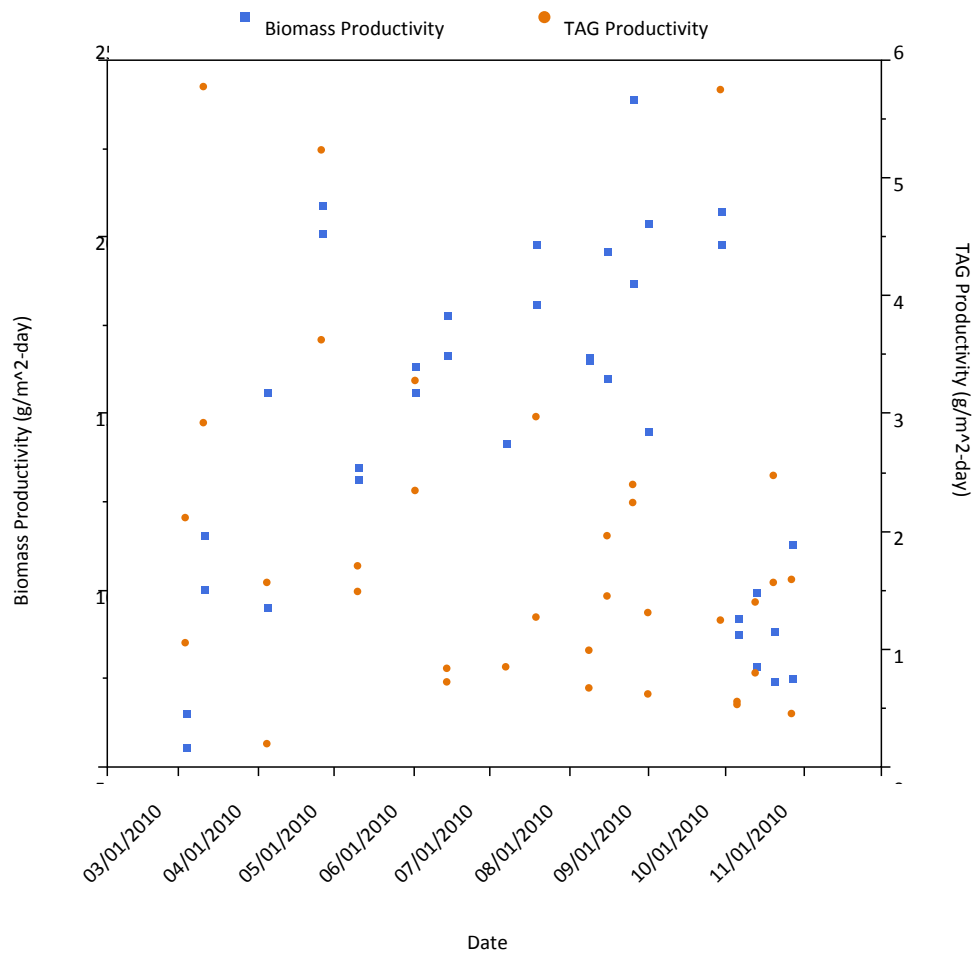


Figure 18. Biomass productivity (■) and TAG Productivity (●) of raceways ponds from March 2010-October 2010. Spring to autumn provides ample solar irradiance for biomass productivity with optimal lipid productivity in April and September.

4.2.3 Nitrogen

Nitrogen is an important nutrient for microalgae metabolism and the amount of nitrogen present in the ponds can affect biomass production (VSS) and triglyceride (TAG) concentrations. Decreases in available nitrogen can result in an increase of TAG production. Three nitrogen parameters explored in the pond study include: (1) influent total ammonia nitrogen (TAN) which measures the amount of ammonia entering the raceway ponds that is readily available for use by the microalgae, (2) pond TAN which measures the amount of ammonia in the pond water at the time of sampling that has not been assimilated into microalgae biomass, and (3) organic nitrogen which measures the nitrogen concentration in cellular tissue and can be used to determine starvation thresholds. Nitrite (NO_2) and nitrates (NO_3) are not discussed because of limited data due to inoperable instruments at the time of sample processing (Table 4).

Primary clarifier effluent from the SLO WRF was used as pond influent and continuously fed the open raceway ponds during the study period. Water quality tests were performed on the influent from July 2009 to September 2010 by Paul Ward (2011) and influent flow was not compromised during the study period (Appendix B). Rain events were examined with regards to TAN due to its instantaneous effect on nitrogen concentration via dilution. Low concentrations of nitrogen can signal a stress response in microalgae and increase TAG production. Precipitation data was documented by the Cal Poly CIMIS station and

Table 4. Influent nitrogen concentrations compiled from Ward (2011) includes total ammonia as nitrogen (TAN), Total Nitrogen (TN), nitrate (NO₃), and nitrite (NO₂). Constituent data for each time period are displayed in means with standard deviation of time series data ($\bar{x} \pm SD$). TN analysis was switched to TKN methods on 6/24/2010. Missing values corresponded to data points that were not sampled during the time period.

Constituent	Influent Water Quality				
	2009 Autumn 9/22-12/21	2010 Winter 12/21/09-3/20/10	2010 Spring 3/20-6/21	2010 Summer 6/21-9/22	2010 Autumn 9/22-12-21
TAN, NH _x -N (mg/L)	39.6±7.85 (n=3)	28.2±6.76 (n=9)	41.9±10.4 (n=17)	32.5±7.43 (n=13)	32.0±5.91 (n=9)
TN* (mg/L)	77.5±12.1 (n=9)	--	40.3±7.50 (n=5)	38.9±2.35 (n=4)	37.8±5.66 (n=7)
NO ₃ -N (mg/L)	--	1.18±1.10 (n=5)	1.65±0.00 (n=3)	0.006±0.012 (n=5)	--
NO ₂ -N (mg/L)	--	0.456±0.213 (n=4)	0.575±0.855 (n=1)	--	--

transformed to weekly averages similar to the treatment of solar irradiance in the previous section. Weekly precipitation data was used to account for dilution effects on the influent and pond cultures. Over the course of the study, influent TAN fluctuated between a maximum and minimum of 17.2 mg/L on July 28, 2010 and 55.9 mg/L on May 11, 2010 (Appendix C). The mean influent TAN concentration for the study was 36 mg/L.

In the late-autumn and winter months of 2009, influent TAN and rain events displayed a significant relationship ($R^2 = 0.14$, $p = 0.002$). Dilution seems like the likely cause of the decrease because TAN concentrations appear to recover shortly after each successive rain event. Interestingly, the influent also decreased in mid to late-summer of 2010. This could be due to ammonia volatilization, metabolism by microbes already present in the wastewater, or by a large portion of the San Luis Obispo population leaving the local area for the summer (Valero & Camargo, 2007). With regards influent TAN concentrations, biomass production (VSS) displayed an expected direct relationship ($R^2 = 0.22$, $p = 0.0015$) while TAG content in the microalgae displayed no discernible pattern ($R^2 = 0.01$, $p = 0.5616$).

Increased TAG production can also result from low organic nitrogen concentrations in the cellular tissue. Organic nitrogen concentrations for the pond data set were determined as total nitrogen (or total Kjeldahl nitrogen) minus ammonia (Ward, 2011). Organic nitrogen content of 8-10% are considered typical for microalgae grown in nitrogen replete media (Fulton, 2009). Nitrogen depletion in the media can lead to decreased nitrogen concentrations in the cell tissue and <3% organic nitrogen is conventionally considered a lipid accumulation trigger. However, in the present study, the highest TAG contents were found in cells that would not be considered nitrogen starved, with about 8% N content. At the lowest observed nitrogen tissue contents (<4%), which could be considered stressfully low, the TAG content was lower (Figure 19). Also, no seasonality was observed for organic nitrogen content or TAG content.

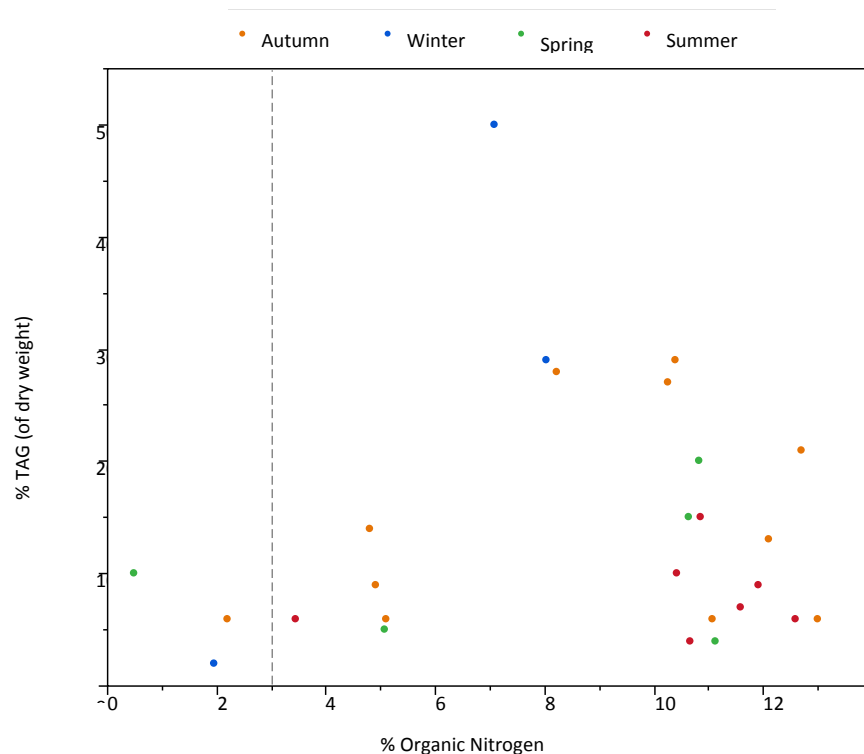


Figure 19. Organic nitrogen content in algal biomass grown in raceway ponds with respective TAG content in the biomass. The smoothed line shows possible optimum of organic nitrogen and TAG contents.

4.2.4 Productivity and Nitrogen

As noted in the irradiance section above, biomass productivity ranged between 6 g/m²-day to 24 g/m²-day from March 2010 to October 2010. Biomass productivity showed a direct correlation to increases of influent TAN ($R^2 = 0.24$, $p = 0.0026$) and an inverse correlation with pond TAN ($R^2 = 0.13$, $p = 0.0340$) (Figure 20). Understandably, high growth rates of microalgae within the ponds are in part fueled by ammonia consumption. TAG productivity during the 8 month period from March to October 2010 ranged from 0.191-5.74 g/m²-day. There appears to be

no conspicuous relationship with influent TAN ($R^2 = 0.03$, $p = 0.3471$) nor pond TAN ($R^2 = 0.04$, $p = 0.2398$) with regards to TAG productivity (Figure 20).

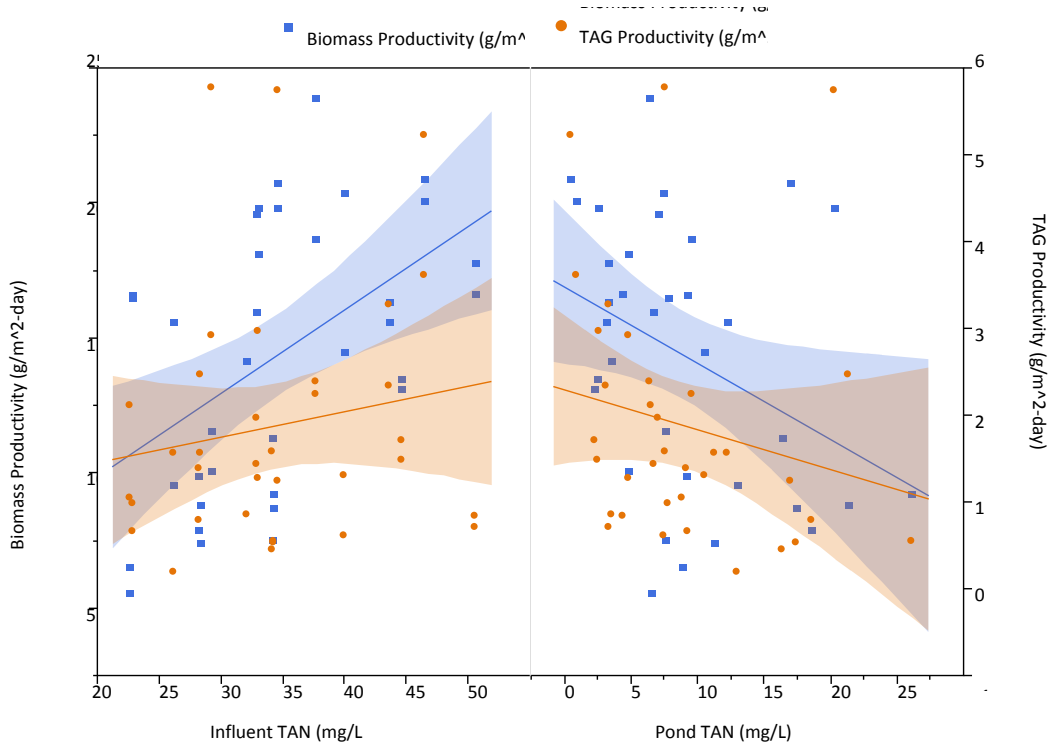


Figure 20. Biomass productivity (■) and TAG productivity (●) in relation to ammonia concentration in the pond influent (clarifier effluent) and effluent. Both biomass productivity and TAG productivity increase with higher influent ammonia concentrations. Absence of ammonia in the ponds is a result of assimilation of nitrogen which increases productivities of both biomass and TAG.

Tracking variations in TAG productivity with regards to ammonia concentrations is difficult in the raceway ponds because the microalgae are essentially growing in a continuous culture. The maximum value of TAG production ($5.74 \text{ g/m}^2\text{-day}$) co-occurs with high biomass productivity and high TAN concentrations (Table 5). From these observations, TAG productivity

in the raceway ponds does not increase with low concentrations of TAN, but is perhaps more closely dependent on elevated biomass productivity.

Table 5. Biomass and TAG productivities (dry weight) with corresponding nitrogen concentrations in the influent and the pond.

	Biomass Productivity (g/m ² -day)		TAG Productivity (g/m ² -day)	
Date	3/4/2010	8/26/2010	4/5/2010	9/29/2010
Range	6	24	0.191	5.74
Biomass Prod.	--	--	9.53	19.8
TAG Prod.	2.11	2.39	--	--
Inf. TAN (mg/L)	22.6	37.7	26.2	34.6
Pond TAN (mg/L)	6.5	6.4	13	20.3

4.2.5 Species Composition

The ponds harbored a large variety of organisms such as microalgae, rotifers, and ostracods. Microalgae genera that were often dominant included *Akinodesmus*, *Actinastrum*, *Micractinium*, *Scenedesmus*, *Euglena*, *Closterium* and *Cyclotella* (Figure 21). Major shifts in genera abundance occurred over the course of the study, but no correlation with elevated TAG values were discerned.

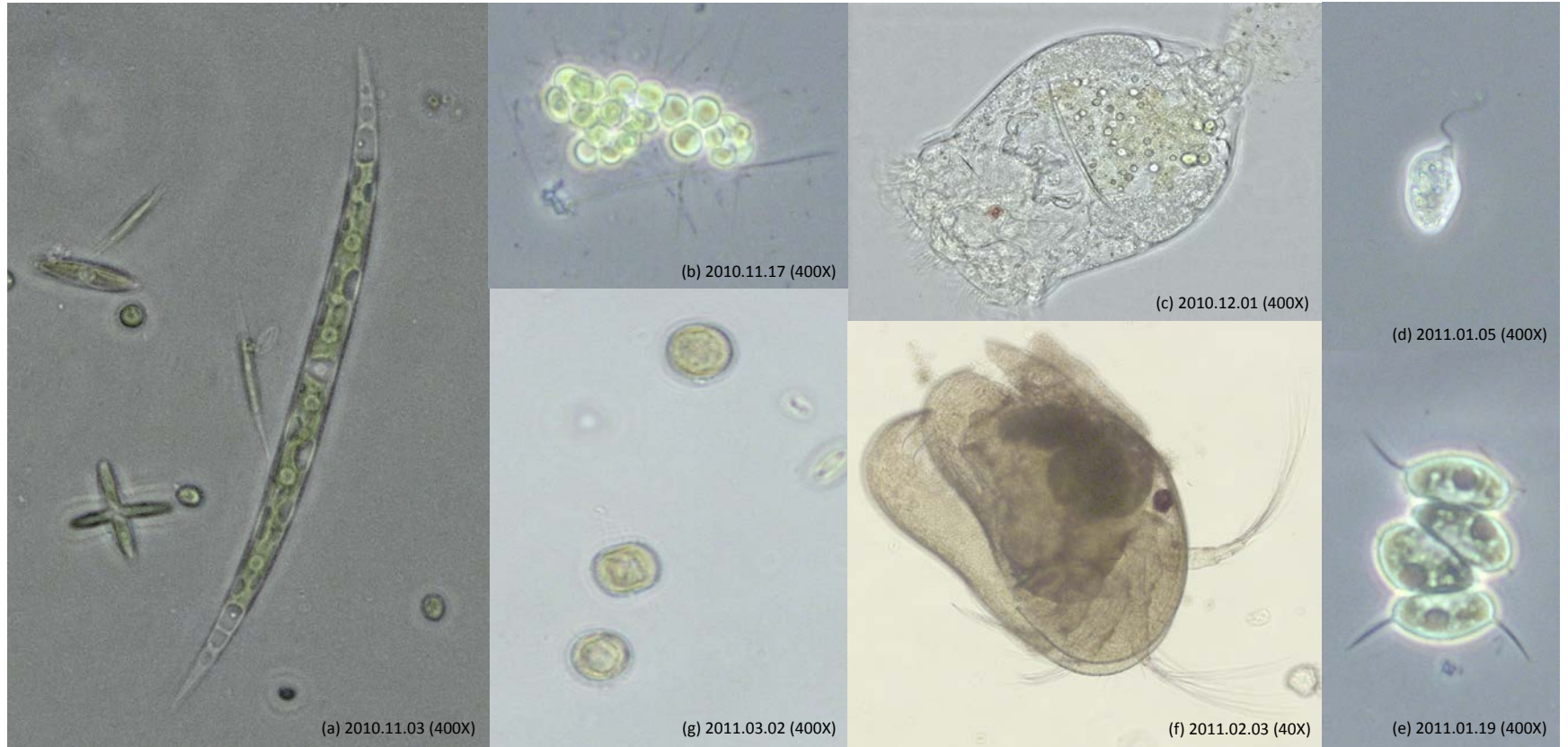


Figure 21. Examples of organisms found in the raceway ponds. Clockwise, specimens include: (a) *Actinastrum sp.* and *Closterium sp.* (L-R), (b) *Micractinum sp.*, (c) rotifer, (d) Euglenid, (e) *Scenedesmus sp.*, (f) ostracod, and (g) *Cyclotella sp.* Microscope magnification show in parentheses.

4.2.6 Pond Study Discussion

Triglyceride content of microalgae in the raceway ponds appears to be dependent on biomass production (VSS) rather than solar irradiance or nitrogen concentrations. More so, due raceway pond cultivation methods being similar to that of continuous cultures, the microalgae were not subjected to limiting concentration of nitrogen and therefore were mostly dependent on solar irradiance availability in determining productivity rates. This was evident in the rise of biomass productivity from 6 to 24 g/m²-day (80 mg/L-day) from March to October 2010 with maximum peaks during high solar irradiances in the summer. This maximum productivity value is similar to observations in the literature of 50-100 mg/L-day of biomass for 15-20-cm deep raceway ponds (Griffiths et al., 2011). These months were examined because during winter, productivity is probably too low to justify operation for biofuels production (Lundquist et al., 2010). Optimization of TAG content and biomass productivity corresponded irradiance levels of 230 W/m² which occurred in April and September 2010 (Figure 17). During these two months observed TAG productivity was 2.6 and 2.2 g/m²-day; respectively. In the summer months, between April and September, biomass productivity increased, but was never maintained beyond ~20 g/m²-day (with the exception of the observed maximum of 24 g/m²-day) (Figure 18). This corresponded to some of the lowest observed TAG content values (<10%) and TAG productivity values (< 1.5 g/m²-day) (Figure 18)

The lower TAG productivity during summer may be due to mutual shading of the microalgae thereby increasing the critical cell density and restricting biomass productivity (Park & Craggs, 2010). Mutual shading also leads to photorespiration which is energetically costly in the cell. Mutual shading can be illustrated by the fact that light is only able to penetrate to a depth of 15 cm in a 30-cm deep pond with 300 TSS/m³ (Park, Craggs, & Shilton, 2011). Due to solar irradiance limitation in the ponds, productivity was most likely maximized at 250 W/m² (Figure 17).

The pond study highlights the need to increase TAG production if microalgae are going to be used as a viable feedstock for biodiesel. While open raceway pond research has focused its efforts on increasing microalgae TAG production through optimal latitudinal solar irradiances (Weyer et al., 2010), laboratory TAG research has focused on inducing a physiological stress responses in microalgae monocultures through media with insufficient nutrient composition (Sheehan et al., 1998). When confined to a particular location like San Luis Obispo, California (35° N), nutrient manipulations would be the next feasible step in increasing TAG production. Interestingly, although nitrogen stress responses have been widely studied with various forms of nitrates, little research has been performed with ammonia as the predominant nitrogen source. Using wastewater not only provides abundant media, but it is also high in ammonia which is the preferred nitrogen source of microalgae (Park & Craggs., 2010; Ahmad & Hellebust, 1990). Investigation into the effects of ammonia depletion and increased light availability in wastewater microalgae are explored in the following sections.

4.3 Light-Shift and Nitrogen Depletion Experiment

The goal of the following experiment was to compare three cultivation techniques for their ability to generate microalgae with high triglyceride content. As described in the Methods chapter, the algae were grown on recycled municipal wastewater media in 1-L Pyrex[®] Roux bottles. Illumination was provided from one side or two sides, so the terms single-sided and double-sided illumination are used hereafter.

Two sets of duplicates had their illumination doubled prior to nitrogen depletion. The first treatment (Light-shift 1) experienced an increase in light from single-sided to double-sided on day 3 of the experiment and the second treatment (Light-shift 2) experienced an increase in light

form single-sided to double-sided on day 5 of the experiment. A third set (Double Illumination) was the control, with consistent double-sided illumination for the entirety of the experiment.

4.3.1 pH and Temperature

Temperature and pH throughout the experiment were kept as stationary as possible to reduce confounding observations related to increases in TAG content. pH was controlled with air supplemented with 1% CO₂ which helped to keep the cultures from rising above 8.3 (Table 6) A pH above 8.3 can inhibit cellular division (Guckert & Cooksey, 1990). Each day the treatments and the control were measured for pH values and returned to a pH of 7.8 with the addition of 1N NaOH or 18M H₂SO₄.

The temperature was measured each day immediately after the consolidation of all Roux bottles. The temperature of the treatments and control was maintained with 10-in portable circulation fans. This was a necessary precaution due to the heat from the light racks and heat-trapping effect of the light hampering blankets. The temperature goal for the experiment was 25°C which was achieved in the light shift treatments, but showed to be difficult to maintain in the control (Table 6).

Table 6. pH and temperature of light shift treatments and double illumination control. Shaded boxes represent single-sided illumination and white boxes represent double-sided illumination.

	Day								
	1	2	3	4	5	6	7	8	9
Light-shift 1									
pH		7.4	7.47	7.33	7.29	7.42	7.33	7.43	7.71
Temperature (°C)		26	28	28	21	26	24	24	25
Light-shift 2									
pH		7.30	7.48	7.57	7.18	7.34	7.47	7.40	7.40
Temperature (°C)		22	23	25	23	23	25	26	25
Double Illumination									
pH		7.80	8.24	7.68	8.06	7.25	7.25	7.28	7.20
Temperature (°C)		35	28	29	26	30	31	28	25

4.3.2 Growth in the Experimental Cultures

Solids testing and cell counts were performed daily on all three cultures to measure growth throughout the experiment. Light-shift 1 achieved the highest VSS concentrations of the three treatments ($x=1,693$ mg/L) at 9 days, followed by Double Illumination (1,596 mg/L) at 9 days and Light-shift 2 (1,502 mg/L) at 9 days (Table 7) (Figure 22). Based on solids data, the growth rate for Light-shift 1 averaged 0.81 day^{-1} during single-sided illumination and 0.37 day^{-1} during double-sided illumination (Table 7). Light-shift 2 averaged 0.57 day^{-1} during single-sided illumination and 0.37 day^{-1} during double-sided illumination while the Double Illumination control averaged a growth rate of 0.48 day^{-1} throughout the 9 day experiment (Figure 23).

Cell counts were performed in addition to VSS measurements. Light-shift 1 reached a maximum of $1.31 \times 10^7 \text{ cell mL}^{-1}$ on day 7 and ended the experiment with $1.11 \times 10^7 \text{ cell mL}^{-1}$ on day 9 (Table 7). Light-shift 1 had the highest number of cells per mL as well as the highest VSS observed throughout the experiment (Figure 24). Light-shift 2 reached a maximum of $9.11 \times 10^6 \text{ cell mL}^{-1}$ on day 7 and ended the experiment with $8.86 \times 10^6 \text{ cell mL}^{-1}$ on day 9 (Table 7). Light-shift 2 had the lowest number of cells per mL as well as the lowest VSS observed throughout the experiment (Figure 24). The Double Illumination control reached a maximum of $1.03 \times 10^7 \text{ cell mL}^{-1}$ on day 8 and ended the experiment with $9.00 \times 10^6 \text{ cells/mL}$ on day 9 (Table 7). The Double Illumination control experienced the similar high VSS concentrations as Light-shift 1, but also low cell density similar to Light-shift 2 (Figure 24).

Table 7. VSS concentration values, daily specific VSS growth rates (μ), and number of cells per mL for the three types of culture throughout the 9-day experiment. Shaded boxes represent periods of single-sided illumination and white boxes represent periods of double-sided illumination with light-shifts occurring on day 3 and day 5 of the experiment.

	Day								
	1	2	3	4	5	6	7	8	9
Light-shift 1									
VSS (mg/L, Mean \pm SE)	36 \pm 2.23	89 \pm 4.43	178 \pm 9.68	331 \pm 7.20	540 \pm 4.74	809 \pm 14.40	1180 \pm 4.74	1453 \pm 9.44	1693 \pm 4.70
μ (1/d)		0.92	0.69	0.62	0.49	0.40	0.37	0.21	0.15
Cell density (cell mL ⁻¹)		1.44E+06	1.63E+06	2.94E+06	8.34E+06	1.09E+07	1.31E+07	1.11E+07	1.11E+07
Light-shift 2									
VSS (mg/L, Mean \pm SE)	36 \pm 2.23	73 \pm 3.84	151 \pm 8.00	267 \pm 8.16	349 \pm 14.4	502 \pm 11.9	889 \pm 2.69	1273 \pm 0.00	1502 \pm 7.20
μ (1/d)		0.73	0.72	0.57	0.27	0.36	0.57	0.36	0.17
Cell density (cell mL ⁻¹)		1.10E+06	8.80E+05	1.96E+06	3.92E+06	8.04E+06	9.11E+06	7.87E+06	8.86E+06
Double Illumination									
VSS (mg/L, Mean \pm SE)	36 \pm 2.23	142 \pm 4.47	336 \pm 4.43	620 \pm 24.5	802 \pm 23.5	1111 \pm 13.6	1244 \pm 35.35	14670 \pm 0.00	1596 \pm 30.3
μ (1/d)		1.39	0.86	0.61	0.26	0.33	0.11	0.16	0.08
Cell density (cell mL ⁻¹)		1.44E+06	4.34E+06	6.80E+06	8.93E+06	7.90E+06	8.95E+06	1.03E+07	9.00E+06

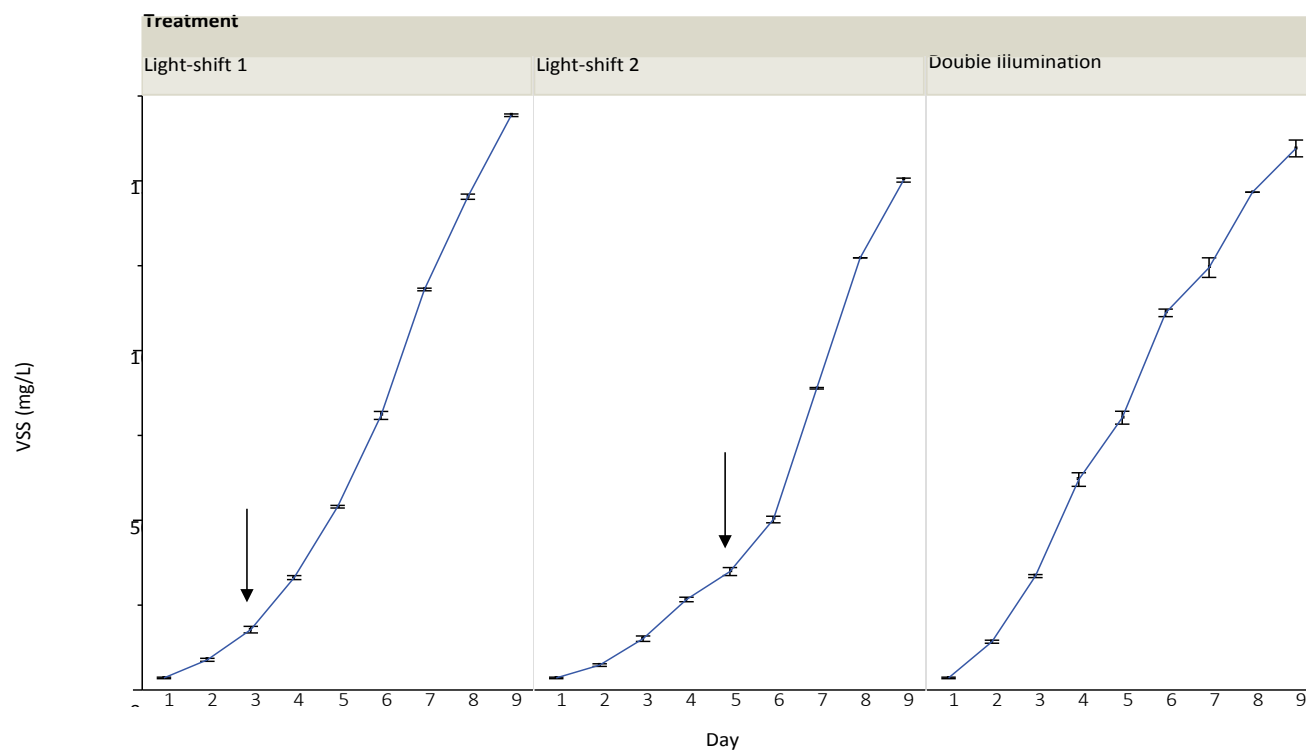


Figure 22. Mean VSS concentration (triplicates) and standard error values for Light-shift 1, Light-shift 2, and Double Illumination treatments throughout the 9-day experiment. Day of light-shift is indicated with an arrow.

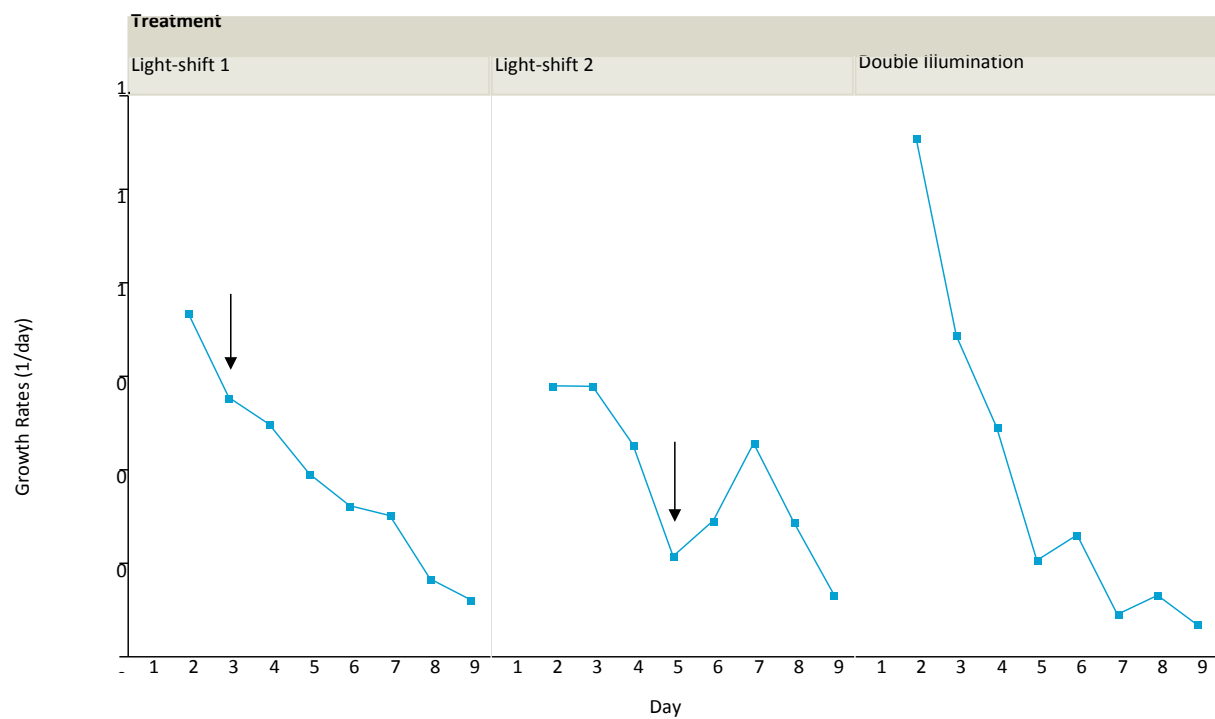


Figure 23. Daily growth rates based on VSS (■) for Light-shift 1, Light-shift 2, and Double Illumination treatments throughout the 9-day experiment. The day of the light-shift is indicated with an arrow.

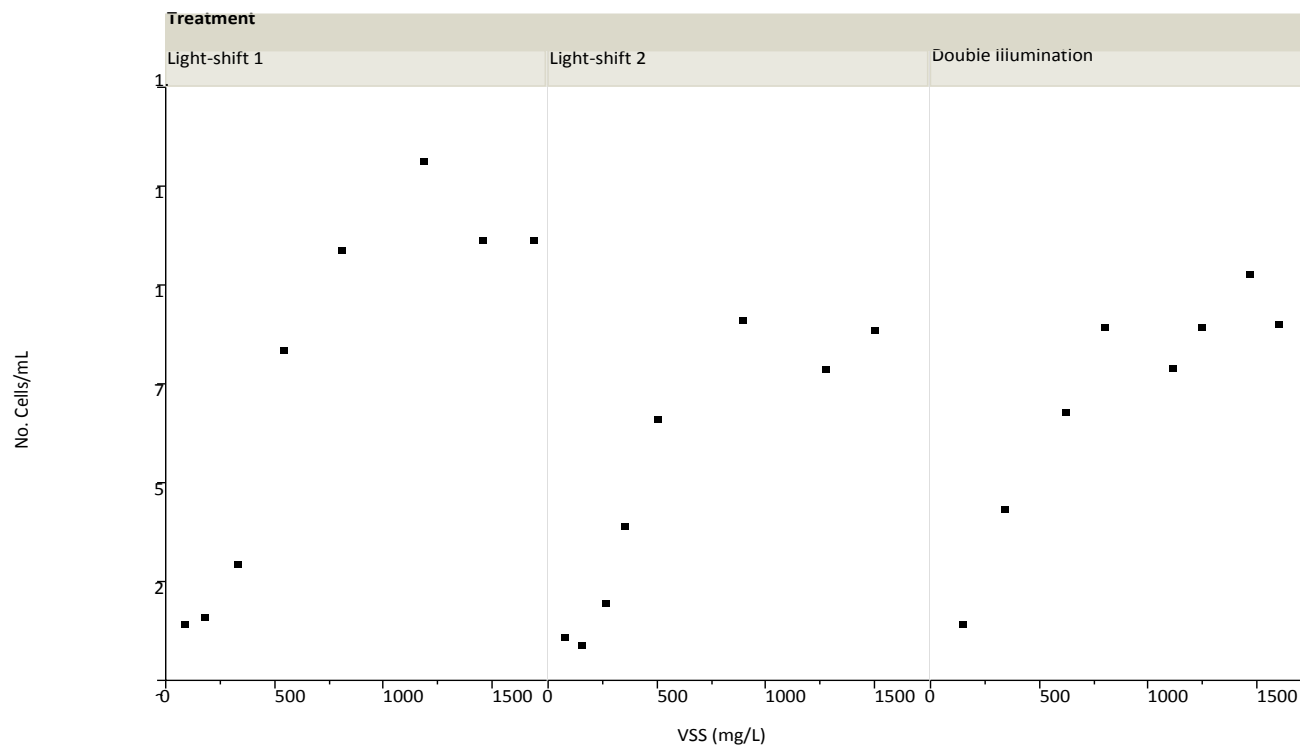


Figure 24. Correlation of VSS (■) concentration and culture density (number of microalgae cells mL^{-1}). Cultures were 99% *Scenedesmus* sp. Light-shift 1 ended the experiment with the highest VSS concentration and highest cell density of all three cultures. Light-shift 2 had a lowest cell density and lowest VSS concentration. Double Illumination had nearly the same VSS concentration as Light-shift 1 with a lower cell density.

4.3.3 Nitrogen

Nitrogen stress was measured in this experiment by tracking three main nitrogen constituents in wastewater and microalgae: ammonia (total ammonia nitrogen or TAN), nitrate (NO_3), and organic nitrogen (via total Kjeldahl nitrogen analysis). As stated before, ammonia is the preferable nitrogen source of microalgae in wastewater (Ahmad & Hellenbust, 1990). The initial concentration of TAN in the recycled wastewater medium for all three treatments was 37.1 mg/L. Nitrogen depletion was determined by the exhaustion of ammonia in the media which marks a physiological change in microalgae metabolic processes and can be qualified by low chlorophyll content and the chlorosis, or yellowing, of the culture (Richardson, 1969; Ahmad & Hellenbust, 1990). The Double Illumination culture consumed TAN at the fastest rate (-12.4 mg/L-day) (Table 8) reaching N-depletion day 4 (Figure 25). Light-shift 2 consumed TAN at the slowest rate (-7.4 mg/L-day), reaching N-depletion by day 6.

Table 8. Consumption rates of TAN were calculated from the beginning of the experiment (day 0) until the first day TAN levels fell below 1 mg/L. %ON decline rates day^{-1} were determined from the peak %ON of each culture to the final day of the experiment (day 9). Light-shift 2 experienced the only increase in %ON at the start of the experiment until day 5.

	TAN	%ON	
	Consumption Rate (mg/L-day)	Production Rate (% ON day^{-1})	Decline Rate (% ON day^{-1})
Light-shift 1	-9.27	--	-1.43
Light-shift 2	-7.42	+1.25	-1.95
Double Illumination	-12.36	--	-0.98

Evidence that ammonia was fully consumed by the microalgae and not volatilized is supported by total Kjeldahl nitrogen (TKN) tests performed on the samples. TKN values from each treatment remained relatively consistent between 37.5-46.8 mg/L TKN, with no significant

difference between treatments ($p = 0.1131$) (Figure 25). Sparging the cultures with CO_2 may have also discouraged ammonia volatilization by maintaining a reduced pH below 8 (Park & Craggs, 2010).

Sampling for organic nitrogen began on day 3 of the experiment due to the large volume needed for total Kjeldahl nitrogen analysis. Organic nitrogen as a component of biomass (%ON) was calculated for all three cultures using VSS concentrations. The %ON in Light-shift 1 and Double Illumination cultures steadily decreased from day 3 to the end of the experiment (Figure 25). During this time period both cultures experienced double-sided illumination and because sampling for organic nitrogen began on day 3 of the experiment there are no measurements for Light-shift 1 with single-sided illumination. Interestingly, %ON increased in Light-shift 2 during 5 days of single-sided illumination and began to decrease once exposed to double-sided illumination (Table 8) (Figure 25).

The average nitrogen for green microalgae is between 6-12% dry weight, and a level $\leq 3\%$ ON is considered cellular starvation in microalgae (Richardson et al., 1969; Becker, 1994). Light-shift 2 achieved a maximum of 10.3% ON on day 5, experienced the fastest rate of %ON decline ($-1.95\% \text{ ON day}^{-1}$) reaching starvation on day 9. Double Illumination reached a maximum of 8.56% ON on day 3, had the slowest rate of %ON decline ($-0.98\% \text{ ON day}^{-1}$), and reached starvation by day 8 (Figure 25). Chlorosis, a symptom of etiolation where photoautotrophs lack nutrients to produce chlorophyll, was visually apparent in Double Illumination by day 6 of the experiment when the culture experienced 3.37% ON (Appendix D, Appendix E).

The relationship between nitrogen and chlorophyll is explored in the following section.

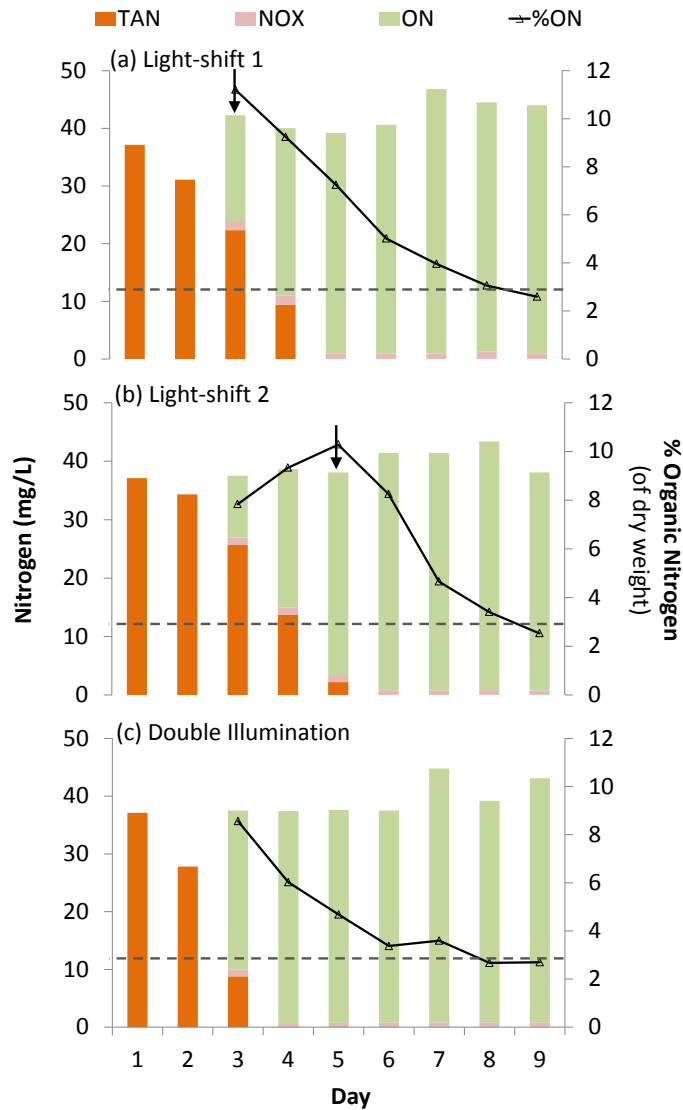


Figure 25. Total Kjeldahl nitrogen (TKN) and the nitrogen constituents (ammonia, nitrate, organic nitrogen) in the culture media for (a) Light-shift 1, (b) Light-shift 2, and (c) Double Illumination. Organic nitrogen (ON) (\triangle) was compared to daily VSS values to determine a percentage of biomass that was nitrogen within the microalgae cells. ON was not measured for the first two sample days in order to conserve culture volume.

4.3.4 Chlorophyll-a

Chlorophyll-a sampling began on day 2 of the experiment and initial concentrations of chlorophyll-a for the cultures were 297 µg/L for Light-shift 1, 125 µg/L for Light-shift 2, and 404 µg/L for Double Illumination (Figure 26). Maximum chlorophyll-a concentrations were achieved on day 4 for Double Illumination (2,790 µg/L), day 5 for Light-shift 1 (3,600 µg/L), and day 6 for Light-shift 2 (3,750 µg/L). Interestingly, both light-shift treatments achieved chlorophyll-a concentrations approximately 20% higher than the Double Illumination which was similar to reports in Benemann (1987) involving single-sided illumination.

High chlorophyll-a productivity (1193 µg/L-day) in the Double Illumination treatment is most likely attributed to abundant light and rapid consumption of TAN by the microalgae. Light-shift 2 experienced the longest accumulation of chlorophyll-a at a production rate of 846 µg/L-day, due to longer period of single-sided illumination. During single-sided illumination, the relatively abundant available nitrogen allows microalgae cells to produce elevated concentrations of chlorophyll-a in order to optimize photosynthesis (Solovchenko et al., 2008), but once nitrogen is exhausted, chlorophyll-a production ceases (Ahmad & Hellebust, 1990).

Table 9. Rates of chlorophyll-a production were calculated from day 2 until the peak in chlorophyll-a concentration for each treatment. Consumption rates were calculated from respective concentration peaks to the final day (9) of the experiment.

	Chlorophyll-a	
	Production Rate (µg/L-day)	Consumption Rate (µg/L-day)
Light-shift 1	1070	-660
Light-shift 2	846	-764
Double Illumination	1193	-483

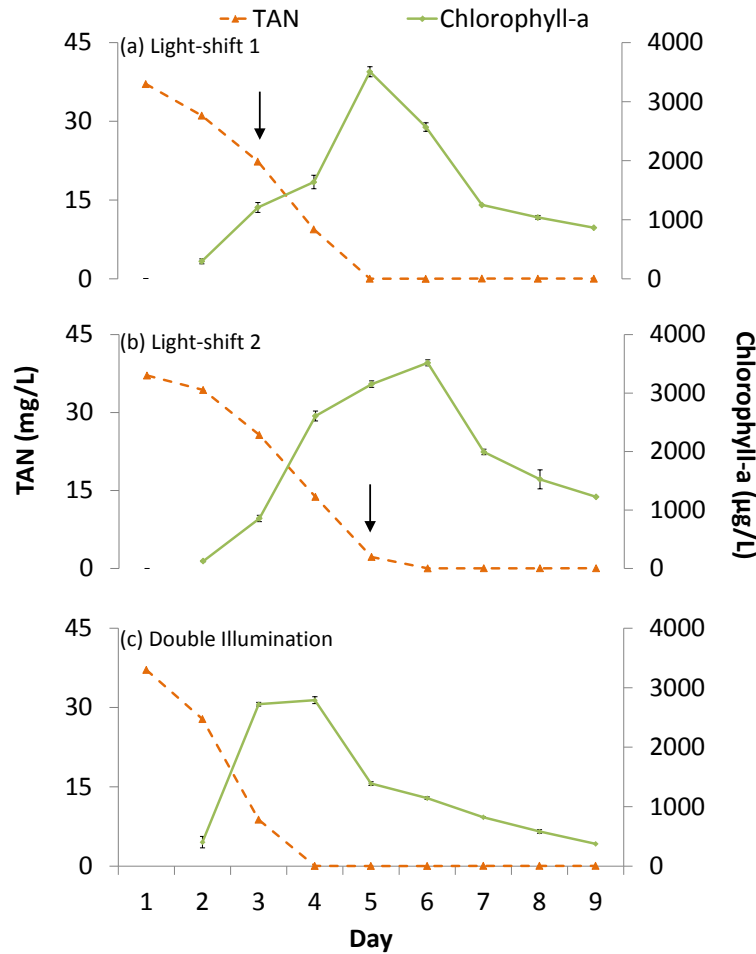


Figure 26. Ammonia (TAN) (▲) consumption displayed in (a) Light-shift 1 (b) Light-shift 2, and (c) Double Illumination treatments. Chlorophyll-a (◆) production stops at the onset of nitrogen depletion (<1 mg/L) and is thereafter consumed (broken down) in the cells.

Evidently, one day of nitrogen depletion (≤ 1 mg/L TAN) resulted in the subsequent decline of chlorophyll-a concentrations in all cultures even as cellular division progressed (Figure 26). This suggests that the absence of ammonia either restrained the production of chlorophyll-a in newly developed microalgae cells or chlorophyll-a was metabolized (Lien & Spencer, 1983). The breakdown of chlorophyll-a was visually apparent through chlorosis in the cultures (Appendix D).

Although visually striking, the qualitative method of tracking N-depletion through chlorophyll-a breakdown was not as accurate as quantitative analysis through TAN and ON measurements.

The Double Illumination treatment had the slowest chlorophyll-a consumption rate (-483 µg/L-day) and ended the experiment with the lowest chlorophyll-a concentration (375 µg/L) (Table 9). Light-shift 1 and Light-shift 2 rapidly depleted the large quantities of chlorophyll-a they had produced from earlier in the experiment (-660 µg/L-day and -764 µg/L-day; respectively) suggesting N-depletion created a physiological stress that established a competition between chloroplast development and other cellular processes (Table 9) (Ahmad & Hellebust, 1990).

Because of the tight relationship between chlorophyll-a and ON, %chlorophyll-a as biomass could be used as a proxy for nitrogen starvation (Appendix E). This would provide faster analysis of cellular starvation than determining organic nitrogen through the time consuming TKN analysis.

4.3.5 FAMES and Total Triglycerides

Due to the large volume of sample required to create a 50 mg microalgae pellet for lipid extraction, sampling for TAG content began on day 3 of the experiment after the cultures completed lag-phase.

Light-shift 1 switched from single-sided to double-sided illumination on day 3 with ample nitrogen remaining in the media (22.4 mg/L TAN) and Light-shift 2 switched from single-sided to double-sided illumination one day prior to N-depletion (2.21 mg/L TAN) on day 5. As stated previously, nitrogen starvation (measured through %ON) was achieved on day 9 for the light-shift treatments and day 8 for the Double Illumination control. Though the TAG content of the treatment cultures increased one day after the increase in light, overall, the TAG content displayed no maintained response to increases in light intensity (Figure 27). Maximum TAG content was

achieved directly after the illumination increase for Light-shift 1 on day 4 at 10.3% TAG of dry weight and for Light-shift 2 at 12.1% TAG of dry weight on day 6 (Table 10). More promising, the TAG content in the Double Illumination treatment increased from 7.9% to 42% TAG content on day 7 of the experiment.

Table 10. TAG content as a percentage of VSS on each day for all three treatments. Single-sided illumination is represented with grayed boxes and double-sided illumination is represented by the white boxes.

	Day								
	1	2	3	4	5	6	7	8	9
Light-shift 1	18.5		5.66	10.9	8.80	4.17	5.09	8.15	6.23
Light-shift 2	18.5		9.14	8.92	8.41	12.1	7.20	4.95	5.46
Double Illumination	18.5		9.21	9.84	7.18	7.94	42.3	41.6	49.4

All TAGs observed in the samples are similar to hydrocarbons found in plant-based biodiesel (Durrett, Benning, & Ohlrogge, 2008). The composition of fatty acids also changed towards the later part of the experiment suggesting a metabolic evolution of the fatty acid profile (Figure 27). Days 3 to 5 displayed similar fatty acid composition in all three cultures with *cis,cis,cis*-9,12,15-Octadecatrienoic acid (C18:3) and Hexadecanoic acid (C16:0) being dominant. The end of the experiment saw the emergence of Octadecanoic acid (C18:0) in all culture fatty acid profiles and *cis*-9-Octadecanoic acid (C18:1) in Light-shift 2 and Double Illumination. The dominance of C18:1 and C16:0 in the fatty acid profile of Light-shift 2 and Double Illumination at the conclusion of the experiment is similar to observations of *Scenedesmus sp.* grown in a 14-day nitrogen limiting batch culture (Griffiths, 2012).

Of particular interest is the TAG spike that occurred on day 7 in the Double Illumination experiment predominately from *cis*-9-Octadecanoic acid (C18:1) and Hexadecanoic acid C16:0 fatty acids (Figure 27). The TAG content increased from 7% to 43% and elevated levels of TAG were maintained for three days. The Double Illumination culture concluded the experiment with 49% TAG of dry weight at day 9. Interestingly, this spike has been observed in *Chlorella vulgaris* grown in artificial wastewater where the batch cultures increased from <10% to 34% (Feng, Li, & Zhang, 2011).

Maximum TAG volumes were all achieved on the final day of the experiment for all three cultures (Table 11). TAG productivities were calculated using a three-day rolling average with maximum TAG productivity occurring on day 8 for Light-shift 1, day 5 for Light-shift 2, and day 8 for Double Illumination. These production and productivity values are similar to finding from Griffiths (2012) for nitrogen limited *Scenedesmus sp.* batch cultures.

Table 11. Maximum TAG concentrations were for all three cultures on the final day of the experiment. Maximum TAG productivity was achieved on day 8 for Light-shift 1 and Double Illumination, and day 5 for Light-shift 2.

	Triglycerides (TAGs)	
	Concentration _{max} (mg/L)	Productivity _{max} (mg/L-day)
Light-shift 1	122	24
Light-shift 2	72.5	15.7
Double Illumination	699	233

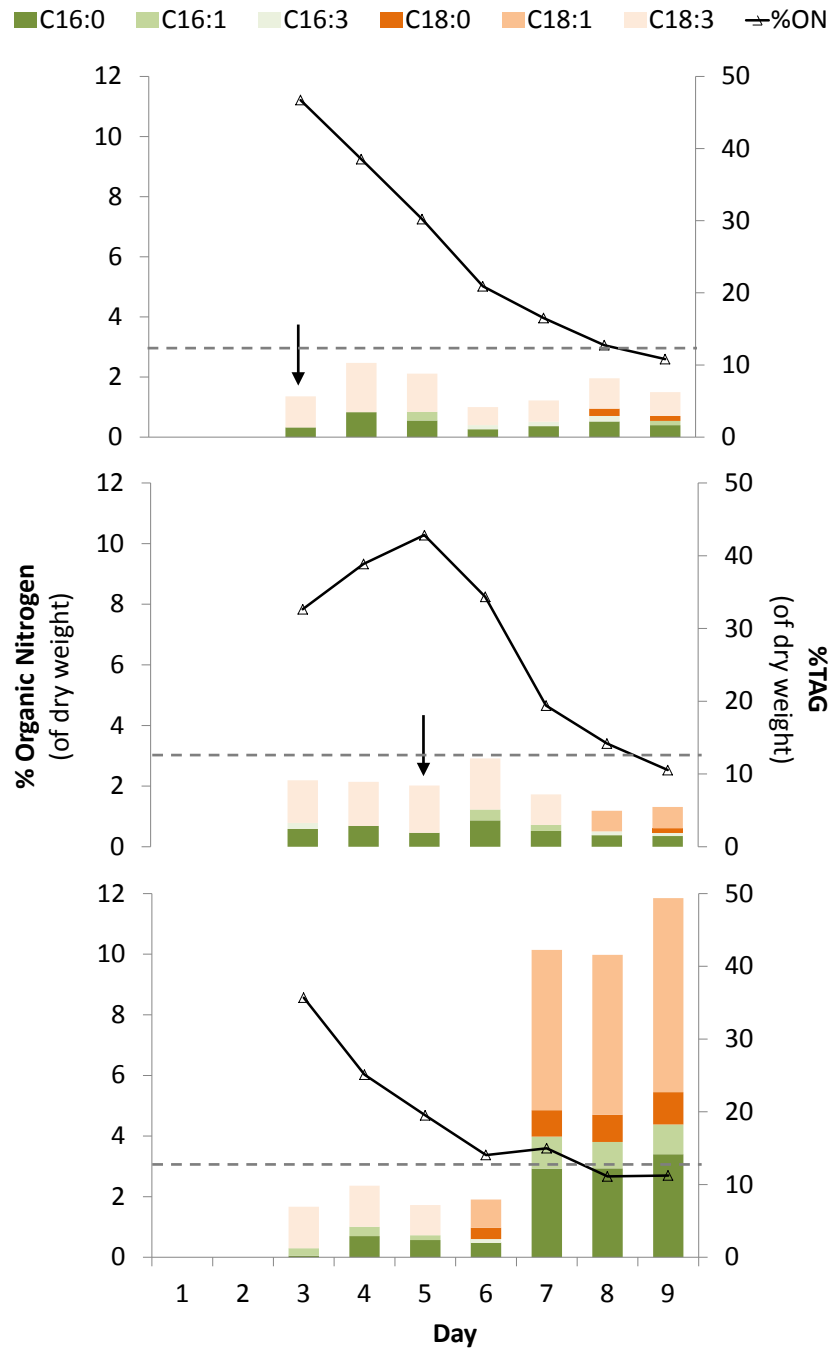


Figure 27. Daily total TAG content with respective fatty acid profiles for three treatments: (a) light shifted on day 3, (b) light shifted on day 6, and (c) double-side illumination. Cellular starvation occurs when the %ON (\triangle) reaches below 3-5% (dashed horizontal line).

4.3.6 Light-shift Experiment Discussion

The antagonistic relationship between biomass productivity and triglyceride production was manifested differently in all cultures throughout the experiment. This experiment displayed the various avenues in which to separately increase biomass or TAG content in microalgae grown in wastewater.

The amount of light intensity and when it is available is critical for the robustness of a microalgae population. Single-sided illumination did produce higher concentrations of chlorophyll-a, but these pigments did not appear to have an effect on TAG concentrations after the change to high light intensity through double-sided illumination (Figure 26, Figure 27). Light-shift 1 demonstrated the mechanism in which to increase biomass production and cell density within a culture by increasing light intensity available to cells in media with ample ammonia concentration. The light-shift before N-depletion created a large microalgae population of many lean algae cells (Figure 24). The Light-shift 1 method would be desirable for increasing biomass productivity, but does not increase TAG production.

Light-shift 2 had the longest period with single-sided illumination and achieved the highest concentration of chlorophyll-a (Figure 26). However, the increase in light intensity at the time when ammonia concentrations were nearly exhausted appeared to stunt the growth of the microalgae population (Figure 24). From this experiment it does not appear that chlorophyll-a concentrations assisted in increasing TAG content in the cells (Figure 27). The discrepancy between our results and Benemann (1987) could be a result of the wastewater media, the microalgae species, or the timing of increased light intensity and N-depletion. The literature is vague on when a culture reaches N-depletion. Investigation into the approximate concentration of nitrogen at a depletion status would benefit further studies on the matter.

High levels of TAG content were observed in the Double Illumination treatment via the combination of high light intensity (via double-sided illumination) throughout nitrogen depletion within 7 days of the experiment (Figure 27). An acute rise in TAG content was evident through a spike in TAG concentrations on day 7 which is similar to findings on microalgae grown in artificial wastewater (Feng, Li, & Zhang, 2011). The high light intensity contributed to the rapid depletion of ammonia in the media and the culture reached starvation (<3% ON) by day 8. Interestingly, the TAG spike was observed one day prior to surpassing the starvation threshold which suggests that the physiological stress was achieved sooner. The consistent high light environment along with depleting nitrogen resources may have played a part in the increase in TAG content rather than relying on a light shift to increase the TAG content.

The composition of the fatty acids in this experiment are also the same ones commonly found in biodiesel produced from plant oils as well as from other N-depletion microalgae triglyceride research (Grittiths, 2012). If saturated and monosaturated fatty acids can be targeted for production by microalgae, it would greatly aid in the quality of biodiesel derived from these sources.

Chapter 5: Conclusion

The results from this project describes potential TAG productivities from open raceway ponds in San Luis Obispo, California and showcases the ability to improve triglyceride content in wastewater microalgae through nitrogen depletion and high light intensity. In order for the production of biofuels to become a viable product of microalgae wastewater bioremediation, biomass productivity and lipid content must be increased. These goals are difficult to achieve simultaneously in outdoor cultivation and therefore the best alternative would be to de-couple both high biomass productivity and lipid induction through subsequent processing steps.

Results from the pond study show that:

- Periods of high insolation in San Luis Obispo, California and high nitrogen concentrations in the pond influent produced maximum biomass productivities of 24 g/m²-day with a TAG content of 10% dry weight.
- Because the ponds are a continuous culture, ammonia concentrations were a poor indicator of possible TAG content increases or disappearances because it never fell below 17.2 mg/L or breached a stressful limit for the microalgae.
- Optimization of biomass intended for biofuel use would be best harvested during April and September when biomass productivity is 13g/m²-day and TAG content is 13%.
- Calculated TAG productivity during April and September were calculated at 1.7g/m²-day and would produce 754 gal/acre-year of biodiesel. This is a conservative estimate considering the observed values in April and September were 2.6 and 2.2 g/m²-day; respectively.

In order to improve TAG concentrations in the cells, a second step involving the initiation of TAG production in harvested microalgae biomass would be necessary. This process would involve transferring the culture of microalgae into structures with increased light penetration and allowing the microalgae to deplete the available nitrogen.

Results from the project suggest that:

- Single sided illumination, or low light intensity increases chlorophyll-a concentrations in the microalgae, however:
 - A change to high light intensity before N-depletion increases cell numbers and biomass.
 - A change to high light intensity one day prior to N-depletion can stunt the growth of the culture.
 - Both light shift treatments did not appear to increase TAG content in nitrogen depleted microalgae cultures.
- The combination of high light intensity during nitrogen depletion stimulates TAG accumulation in wastewater microalgae (predominately *Scenedesmus sp.*) to between 43-49% TAG of dry weight biomass.
- Chlorophyll-a can be used a proxy to determine the status of organic nitrogen content—and therefore starvation—in nitrogen depleted microalgae cultures.
- Using the maximum TAG productivity from the experiment (Double Illumination, 15.7 mg/L-day) it would be possible to produce 2,088 gal/acre-year of biodiesel.

Much research is still needed before algae biodiesel can make a significant impact in energy market. Future works should investigate the potential of operating an open raceway pond as one large batch culture. Literature on nitrogen depletion in the raceway ponds is lacking and could provide promising data on increased triglyceride improvement in the field. The batch can

easily be exposed to higher light intensities through water dilutions or increasing the surface area of the culture—both of which would require extra resources. Explorations into the organic nitrogen content threshold for increased lipid production should also be explored below levels of 3% organic nitrogen. Percent chlorophyll-a could be used as a quick and faster proxy of in situ nitrogen starvation. The relationship between % chlorophyll-a and % organic nitrogen would require a standardization method as well. Light-shift experiments could be performed for a longer time frame with larger culture volumes in order to ensure enough samples for a protracted study period. Investigation of using other waste streams, such as agriculture or ranching, should also be explored.

BIBLIOGRAPHY

- Ahmad, I., & Hellebust, J. A. (1990). Regulation of chloroplast development by nitrogen source and growth conditions in a *Chlorella protothecoides* strain. *Plant physiology*, 94(3), 944-949.
- Balat, M., & Balat, H. (2010). Progress in biodiesel processing. *Applied energy*, 87(6), 1815-1835.
- Becker, E. W. (1994). *Microalgae: biotechnology and microbiology* (Vol. 10). Cambridge University Press.
- Benemann, J. R., Goebel, R. P., Weissman, J. C., & Augenstein, D. C. (1982, December). Microalgae as a source of liquid fuels. In *Proceedings of the June 1982 SERI Biomass Program Principal Investigators' Review Meeting, Aquatic Species Program Reports* (pp. 1-16).
- Benemann, J. R., & Tillett, D. M. (1987). *Effects of fluctuating environments on the selection of high yielding microalgae* (No. SERI/SR-232-14380). National Renewable Energy Laboratory (NREL), Golden, CO.. United States Department of Energy. (2010). National Algal Biofuels Technology Roadmap, (May).
- Benemann, J. R., & Oswald, W. J. (1996). *Systems and economic analysis of microalgae ponds for conversion of CO₂ to biomass. Final report* (No. DOE/PC/93204--T5). California Univ., Berkeley, CA (United States). Dept. of Civil Engineering.
- Bligh, E., & Dyer, W. J. (1959). A rapid method of total lipid extraction and purification. *Canadian journal of biochemistry and physiology*, 37(8), 911-917.
- Brennan, L., & Owende, P. (2010). Biofuels from microalgae—a review of technologies for production, processing, and extractions of biofuels and co-products. *Renewable and Sustainable Energy Reviews*, 14(2), 557-577. Chisti, Y. (2007). Biodiesel from microalgae. *Biotechnology advances*, 25(3), 294–306. doi:10.1016/j.biotechadv.2007.02.001
- Christie, W. 2003. *Lipid Analysis: Isolation, Separation, Identification and Structural Analysis of Lipids*. Third Ed. Bridgwater, England: The Oily Press.
- Dismukes, G. C., Carrieri, D., Bennette, N., Ananyev, G. M., & Posewitz, M. C. (2008). Aquatic phototrophs: efficient alternatives to land-based crops for biofuels. *Current Opinion in Biotechnology*, 19(3), 235-240.
- Dortch, Q. (1990). The interaction between ammonium and nitrate uptake in phytoplankton. *Marine ecology progress series. Oldendorf*, 61(1), 183-201.
- Durrett, T. P., Benning, C., & Ohlrogge, J. (2008). Plant triacylglycerols as feedstocks for the production of biofuels. *The Plant Journal*, 54(4), 593-607.

- Eaton, A. D., Clesceri, L. S., & Greenberg, A. E. (1995). Standard methods for the examination of water and wastewater, 19th edition. Washington: APHA American Public Health Association.
- Enssani, E. (1989, August). Liquid hydrocarbons from biomass grown on waste. In *Energy Conversion Engineering Conference, 1989. IECEC-89., Proceedings of the 24th Intersociety* (pp. 1953-1958). IEEE.
- Falkowski, P. G. (1994). The role of phytoplankton photosynthesis in global biogeochemical cycles. *Photosynthesis Research*, 39(3), 235-258.
- Fargione, J., Hill, J., Tilman, D., Polasky, S., & Hawthorne, P. (2008). Land clearing and the biofuel carbon debt. *Science*, 319(5867), 1235-1238.
- Feng, Y., Li, C., & Zhang, D. (2011). Lipid production of *Chlorella vulgaris* cultured in artificial wastewater medium. *Bioresource technology*, 102(1), 101-105.
- Fulton, L. M. (2009). Nutrient Removal by Algae Grown in CO₂-Enriched Wastewater over a Range of Nitrogen-to-Phosphorus Ratios. *Master's Theses and Project Reports*, 194.
- Geider, R. J. (1987). Light and temperature dependence of the carbon to chlorophyll a ratio in microalgae and cyanobacteria: implications for physiology and growth of phytoplankton. *New Phytologist*, 1-34.
- Golueke, C. G., & Oswald, W. J. (1959). Biological conversion of light energy to the chemical energy of methane. *Applied microbiology*, 7(4), 219-227.
- Griffiths, M. J., Dicks, R. G., Richardson, C., Harrison, S. T. L., (2011) Advantages and Challenges of Microalgae as a Source of Oil for Biodiesel - Feedstocks and Processing Technologies, Dr. Margarita Stoytcheva (Ed.), ISBN:978-953-307-713-0, In Tech, Available from: <http://www.intechopen.com/biodiesel-feedstocks-and-processing-technologies/advantages-and-challenges-of-microalgae-as-a-source-of-oil-for-biodiesel>
- Griffiths, M. J., van Hille, R. P., & Harrison, S. T. (2012). Lipid productivity, settling potential and fatty acid profile of 11 microalgal species grown under nitrogen replete and limited conditions. *Journal of Applied Phycology*, 24(5), 989-1001.
- Guckert, J. B., & Cooksey, K. E. (1990). TRIGLYCERIDE ACCUMULATION AND FATTY ACID PROFILE CHANGES IN CHLORELLA (CHLOROPHYTA) DURING HIGH pH-INDUCED CELL CYCLE INHIBITION1. *Journal of Phycology*, 26(1), 72-79.
- Hill, J., Nelson, E., Tilman, D., Polasky, S., & Tiffany, D. (2006). Environmental, economic, and energetic costs and benefits of biodiesel and ethanol biofuels. *Proceedings of the National Academy of Sciences*, 103(30), 11206-11210.
- Hutton, M.W. (2009). *Extraction and Characterization of Lipids from Microalgae Grown in Municipal Wastewater*. San Luis Obispo: Cal Poly.

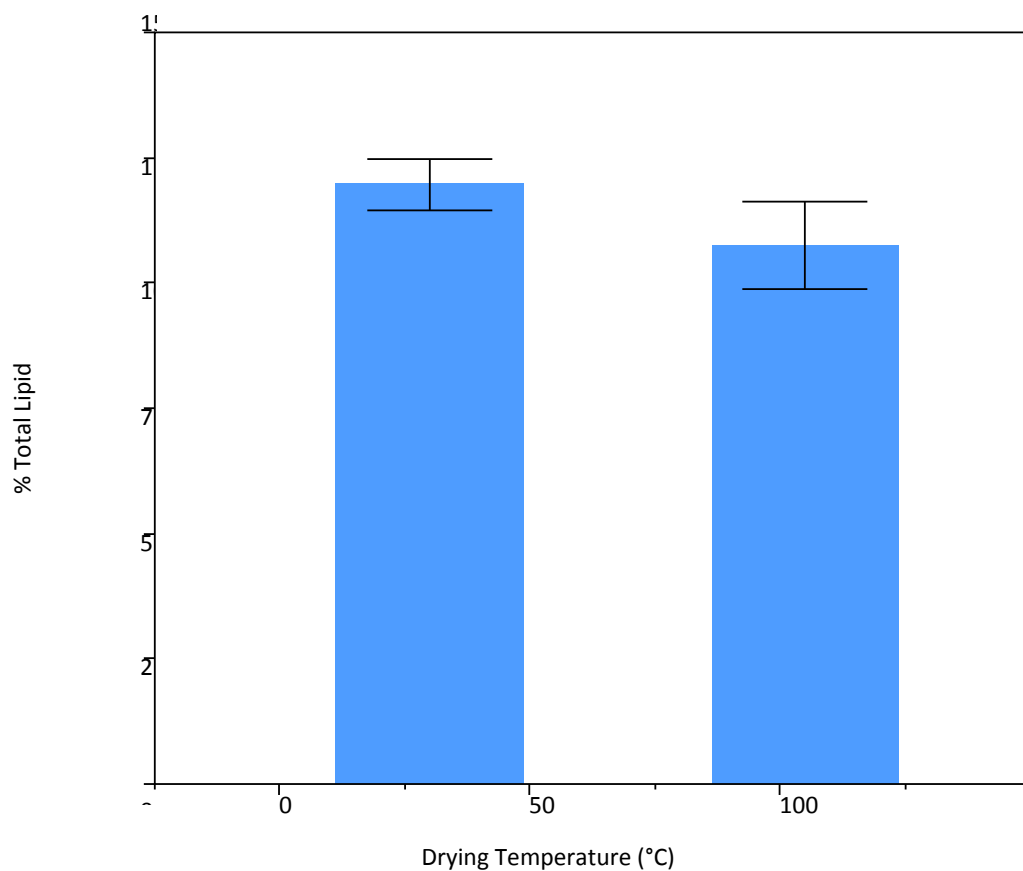
- Intergovernmental Panel on Climate Change. (2012). Managing the Risks of Extreme Events and Disasters to Advance Climate Change Adaptation. A Special Report of Working Groups I and II of the Intergovernmental Panel on Climate Change [Field, C.B., V. Barros, T.F. Stocker, D. Qin, D.J. Dokken, K.L. Ebi, M.D. Mastrandrea, K.J. Mach, G.-K. Plattner, S.K. Allen, M. Tignor, and P.M. Midgley (eds.)]. Cambridge University Press, Cambridge, UK, and New York, NY, USA, 582 pp.
- Lewis, L. A., & McCourt, R. M. (2004). Green algae and the origin of land plants. *American Journal of Botany*, 91(10), 1535-1556.
- Lien, S., & Spencer, K. G. (1983). Microalgal production of oils and lipids. In *Energy from biomass and wastes 7. Symposium* (pp. 1107-1122).
- Lundquist, T. J., Woertz, I. C., Quinn, N. W. T., & Benemann, J. R. (2010). A realistic technology and engineering assessment of algae biofuel production. *Energy Biosciences Institute*, 1.
- Mandal, S., & Mallick, N. (2009). Microalga *Scenedesmus obliquus* as a potential source for biodiesel production. *Applied microbiology and biotechnology*, 84(2), 281-291.
- National Institute of Standards and Technology. (2006). National Institute of Standards and Technology. Retrieved October 14, 2009, from The NIST Reference on Constants, Units and Uncertainty: <http://physics.nist.gov/cgi-bin/cuu/Value?auedm>
- Nigam, P. S., & Singh, A. (2011). Production of liquid biofuels from renewable resources. *Progress in Energy and Combustion Science*, 37(1), 52-68.
- Oehrl, L. L., Hansen, A. P., Rohrer, C. A., Fenner, G. P., & Boyd, L. C. (2001). Oxidation of phytosterols in a test food system. *Journal of the American Oil Chemists' Society*, 78(11), 1073-1078.
- Ohlrogge, J. B., & Jaworski, J. G. (1997). Regulation of fatty acid synthesis. *Annual review of plant biology*, 48(1), 109-136.
- Orr, J. C., Fabry, V. J., Aumont, O., Bopp, L., Doney, S. C., Feely, R. A., ... & Yool, A. (2005). Anthropogenic ocean acidification over the twenty-first century and its impact on calcifying organisms. *Nature*, 437(7059), 681-686.
- Oswald, W. J., Gotaas, H. B., Ludwig, H. F., & Lynch, V. (1953). Algae symbiosis in oxidation ponds: III. Photosynthetic oxygenation. *Sewage and Industrial Wastes*, 25(6), 692-705.
- Park, J., & Craggs, R. (2010). Wastewater treatment and algal production in high rate algal ponds with carbon dioxide addition.
- Park, J. B. K., Craggs, R. J., & Shilton, A. N. (2011). Wastewater treatment high rate algal ponds for biofuel production. *Bioresource technology*, 102(1), 35-42.

- Ratledge, C. (2002). Regulation of lipid accumulation in oleaginous microorganisms. *Biochemical Society Transactions*, 30(6), 1047-1049.
- Richardson, B., Orcutt, D. M., Schwertner, H. A., Martinez, C. L., & Wickline, H. E. (1969). Effects of nitrogen limitation on the growth and composition of unicellular algae in continuous culture. *Applied microbiology*, 18(2), 245-250.
- Richardson, K., Beardall, J., & Raven, J. A. (1983). Adaptation of unicellular algae to irradiance: an analysis of strategies. *New Phytologist*, 93(2), 157-191.
- Rodolfi, L., Chini Zittelli, G., Bassi, N., Padovani, G., Biondi, N., Bonini, G., & Tredici, M. R. (2009). Microalgae for oil: Strain selection, induction of lipid synthesis and outdoor mass cultivation in a low-cost photobioreactor. *Biotechnology and bioengineering*, 102(1), 100-112.
- Roessler, P. G. (1990). Environmental control of glycerolipid metabolism in microalgae: commercial implications and future research directions. *Journal of Phycology*, 26(3), 393-399.
- Schenk, P. M., Thomas-Hall, S. R., Stephens, E., Marx, U. C., Mussnug, J. H., Posten, C., Kruse, O., et al. (2008). Second Generation Biofuels: High-Efficiency Microalgae for Biodiesel Production. *BioEnergy Research*, 1(1), 20-43. doi:10.1007/s12155-008-9008-8
- Schlyter, P. (2010, April 13). How bright are natural light source? *Radiometry and photometry in astronomy*. Retrieved Feb 6, 2013, from <http://stjarnhimlen.se/comp/radfaq.html#10>.
- Scott, S. A., Davey, M. P., Dennis, J. S., Horst, I., Howe, C. J., Lea-Smith, D. J., & Smith, A. G. (2010). Biodiesel from algae: challenges and prospects. *Current Opinion in Biotechnology*, 21(3), 277-286.
- Sheehan, J., Camobreco, V., Duffield, J., Shapouri, H., Graboski, M., & Tyson, K. S. (2000). *An overview of biodiesel and petroleum diesel life cycles* (No. NREL/TP-580-24772). National Renewable Energy Lab., Golden, CO (US).
- Sheehan, J., Dunahay, T., Benemann, J., & Roessler, P. (1998). *A look back at the US Department of Energy's Aquatic Species Program: Biodiesel from algae* (Vol. 328). Golden: National Renewable Energy Laboratory.
- Shifrin, N. S., & Chisholm, S. W. (1981). PHYTOPLANKTON LIPIDS: INTERSPECIFIC DIFFERENCES AND EFFECTS OF NITRATE, SILICATE AND LIGHT-DARK CYCLES1. *Journal of phycology*, 17(4), 374-384.
- Sims, R. E., Mabee, W., Saddler, J. N., & Taylor, M. (2010). An overview of second generation biofuel technologies. *Bioresource Technology*, 101(6), 1570-1580.
- Singh, A., Nigam, P. S., & Murphy, J. D. (2011). Renewable fuels from algae: an answer to debatable land based fuels. *Bioresource technology*, 102(1), 10-16.

- Singh, Y., & Kumar, H. D. (1992). Lipid and hydrocarbon production by *Botryococcus* spp. under nitrogen limitation and anaerobiosis. *World Journal of Microbiology and Biotechnology*, 8(2), 121-124.
- Solovchenko, A. E., Khozin-Goldberg, I., Didi-Cohen, S., Cohen, Z., & Merzlyak, M. N. (2008). Effects of light intensity and nitrogen starvation on growth, total fatty acids and arachidonic acid in the green microalga *Parietochloris incisa*. *Journal of applied Phycology*, 20(3), 245-251.
- Spoehr, H. A., & Milner, H. W. (1949). The chemical composition of *Chlorella*; effect of environmental conditions. *Plant physiology*, 24(1), 120.
- Suen, Y., Hubbard, J. S., Holzer, G., & Tornabene, T. G. (1987). TOTAL LIPID PRODUCTION OF THE GREEN ALGA *NANNOCHLOROPSIS* SP. QII UNDER DIFFERENT NITROGEN REGIMES1. *Journal of Phycology*, 23(s2), 289-296.
- Sukenik, A., Carmeli, Y., & Berner, T. (1989). Regulation of fatty acid composition by irradiance level in the eustigmatophyte *Nannochloropsis* sp. 1. *Journal of Phycology*, 25(4), 686-692.
- Tedesco, M. A., & Duerr, E. O. (1989). Light, temperature and nitrogen starvation effects on the total lipid and fatty acid content and composition of *Spirulina platensis* UTEX 1928. *Journal of Applied Phycology*, 1(3), 201-209.
- Thompson Jr, G. A. (1996). Lipids and membrane function in green algae. *Biochimica et Biophysica Acta (BBA)-Lipids and Lipid Metabolism*, 1302(1), 17-45.
- United States Energy Information Administration. (2012a). *Annual Energy Review 2011*. Washington, D.C.: United States Department of Energy.
- United States Energy Information Administration. (2012b). *International Energy Statistics*. Washington, D.C.: United States Department of Energy.
<http://www.eia.gov/cfapps/ipdbproject/IEDIndex3.cfm?tid=44&pid=44&aid=2>
- United States Environmental Protection Agency. (2013). *Draft Inventory of U.S. Greenhouse Gas Emissions and Sinks: 1990-2011* (p. 470). Washington, DC.
- Valero, M.A. Camargo; Mara, D. D. (2007). Nitrogen removal via ammonia volatilization in maturation ponds. *Water Science & Technology*, 55(11), 87. doi:10.2166/wst.2007.349
- Wahal, S., & Viamajala, S. (2010). Maximizing algal growth in batch reactors using sequential change in light intensity. *Applied biochemistry and biotechnology*, 161(1-8), 511-22. doi:10.1007/s12010-009-8891-6
- Wang, B., Li, Y., Wu, N., & Lan, C. Q. (2008). CO₂ bio-mitigation using microalgae. *Applied microbiology and biotechnology*, 79(5), 707-18. doi:10.1007/s00253-008-1518-y

- Ward, P.E. (2011). *Bioflocculation and CO₂ Supplementation in Wastewater Treatment by Algal High-Rate Ponds*. San Luis Obispo: Cal Poly.
- Weyer, K. M., Bush, D. R., Darzins, A., & Willson, B. D. (2009). Theoretical Maximum Algal Oil Production. *BioEnergy Research*, 3(2), 204–213. doi:10.1007/s12155-009-9046-x
- Widjaja, A., Chien, C.-C., & Ju, Y.-H. (2009). Study of increasing lipid production from fresh water microalgae *Chlorella vulgaris*. *Journal of the Taiwan Institute of Chemical Engineers*, 40(1), 13–20. doi:10.1016/j.jtice.2008.07.007
- Wigley, T.M.L., Raper, S.C.B. (1987). Thermal expansion of sea water associated with global warming. *Nature*, 330, 127-131. doi:10.1038/330127a0
- Woertz, I. (2007). *Lipid Productivity of Algae Grown on Dairy Wastewater as a Possible Feedstock for Biodiesel*. San Luis Obispo: Cal Poly.

Appendix A



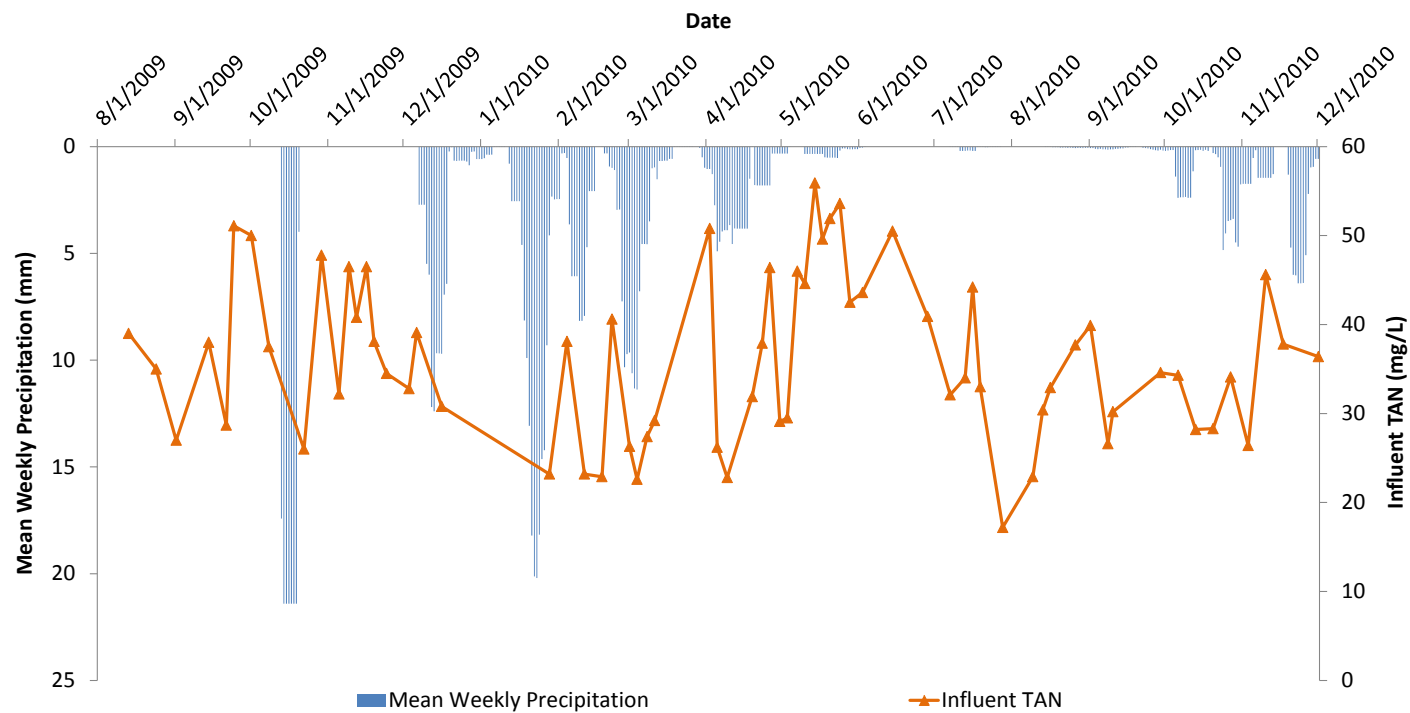
Appendix A. Mean % Total Lipids with standard error for drying temperatures 30°C and 105°C. Samples were analyzed via gravimetric method and in triplicate. Although the mean %Total Lipids for the elevated temperature (105°C) was lower, a comparison of the mean % Total Lipids for the two drying temperatures was not significantly different ($p= 0.298$).

Appendix B

Appendix B. Influent water quality data compiled from Ward (2011) includes solids, nitrogen analyses, alkalinity, soluble carbonaceous biological oxygen demand (scBOD), and DRP (dissolved reactive phosphorous). Constituent data for each time period are displayed in means with standard deviation of time series data ($\bar{x} \pm \text{SD}$). TN analysis was switched to TKN methods on 6/24/2010.

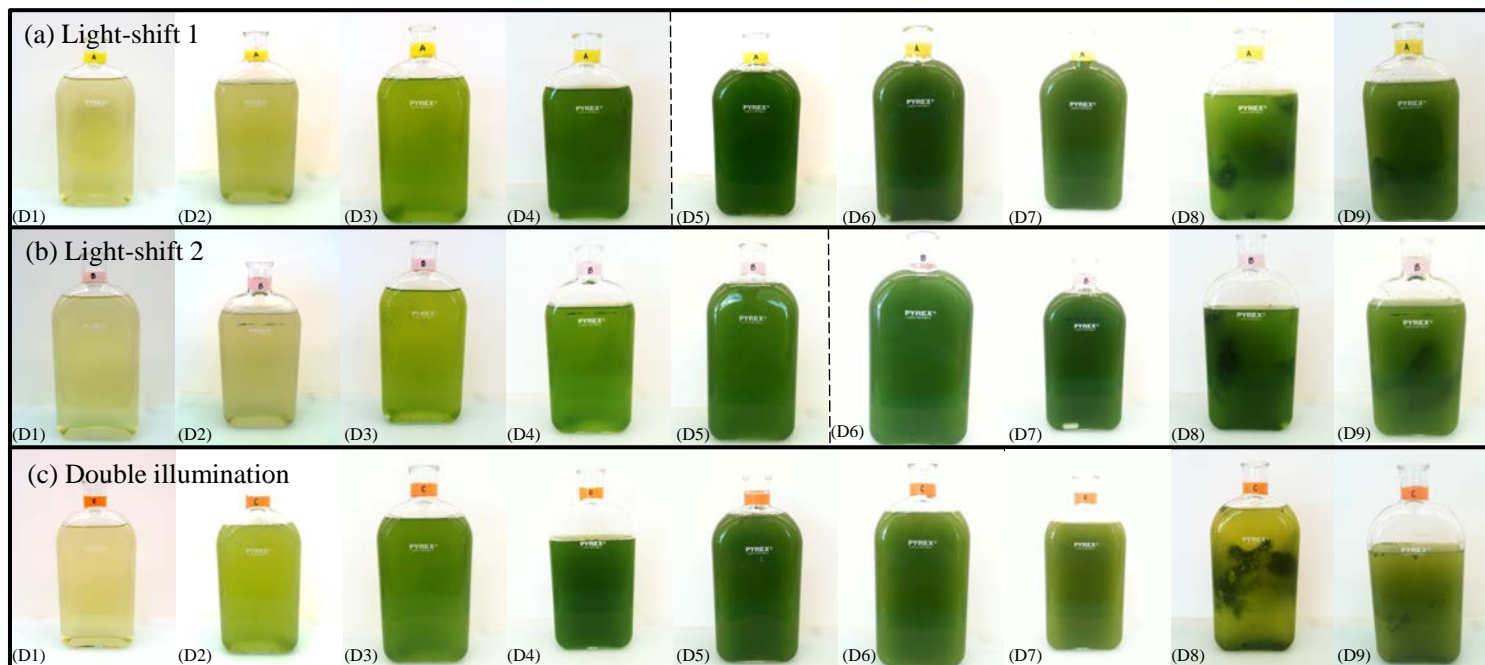
Influent Water Quality					
Constituent	2009 Autumn 9/22-12/21	Winter 12/21/09-3/20/10	2010 Spring 3/20-6/21	Summer 6/21-9/22	Autumn 9/22-12-21
TSS (mg/L)	78±21.6 (n=15)	53.5±25.8 (n=12)	64.9±16.4 (n=17)	69.7±17.0 (n=10)	61.6±13.4 (n=10)
VSS (mg/L)	70.3±19.2 (n=13)	45.5±15.1 (n=11)	61.2±16.0 (n=17)	59.1±16.7 (n=10)	60.3±13.6 (n=9)
NH _x -N (mg/L)	39.6±7.85 (n=3)	28.2±6.76 (n=9)	41.9±10.4 (n=17)	32.5±7.43 (n=13)	32.0±5.91 (n=9)
TN* (mg/L)	77.5±12.1 (n=9)	--	40.3±7.50 (n=5)	38.9±2.35 (n=4)	37.8±5.66 (n=7)
NO ₃ -N (mg/L)	--	1.18±1.10 (n=5)	1.65±0.00 (n=3)	0.006±0.012 (n=5)	--
NO ₂ -N (mg/L)	--	0.456±0.213 (n=4)	0.575±0.855 (n=1)	--	--
scBOD (mg/L)	66.2±20.9 (n=15)	23.6±9.21 (n=6)	40.6±13.3 (n=10)	30.48±8.57 (n=8)	--
Alkalinity (4.5) (mg/L)	358.5±35.3 (n=10)	614±194 (n=6)	379±44.5 (n=9)	369±6.03 (n=8)	--
DRP (mg/L)	--	--	5.58±1.09 (n=8)	--	--

Appendix C



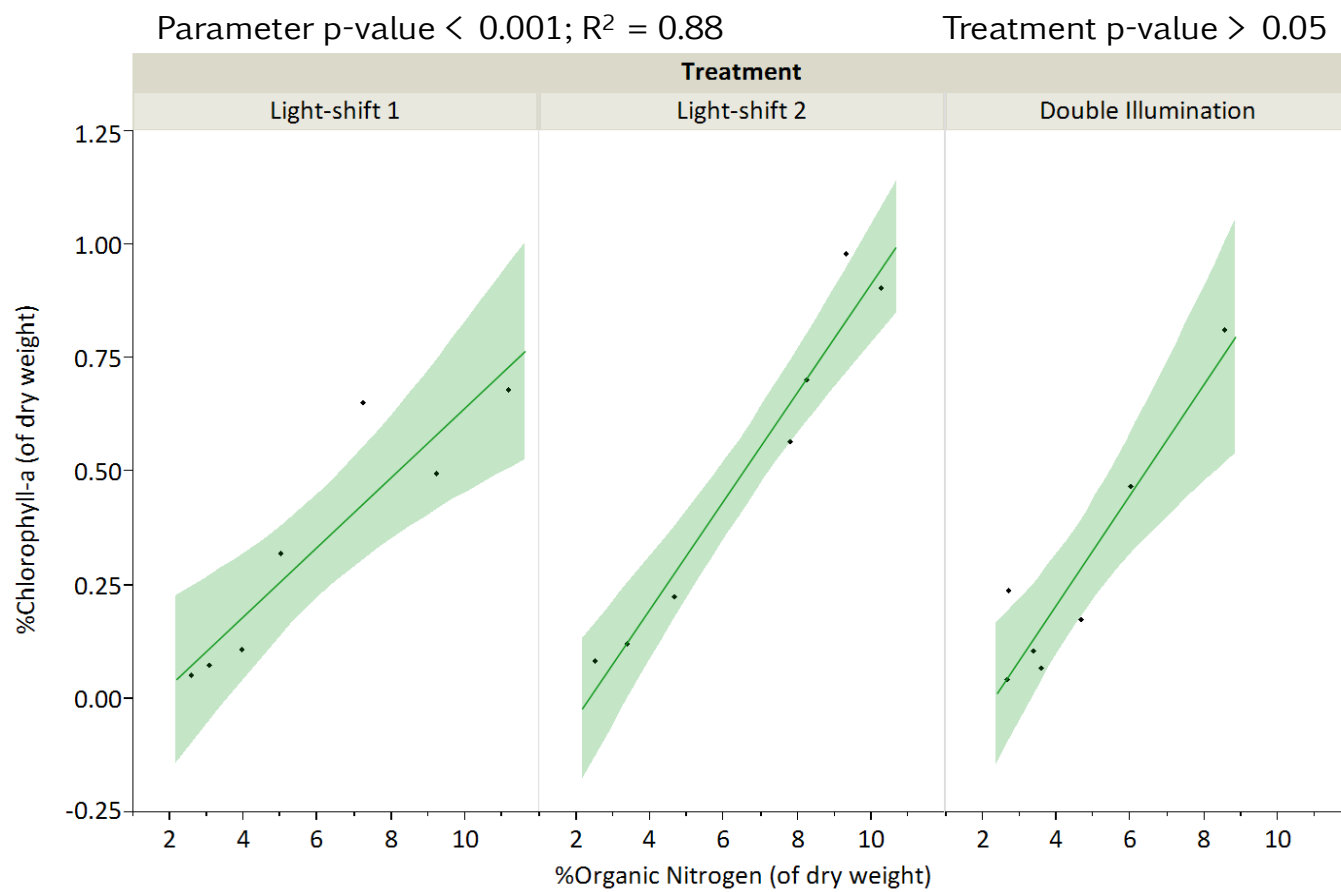
Appendix C. Influent TAN (mg/L) plotted along with mean weekly precipitation from Cal Poly, San Luis Obispo CIMIS station. Mean weekly precipitation axis is reversed and simulates the dilution effect of rain events.

Appendix D



Appendix D. Time-series photographs of all culture bottles from the three treatments for the 9 day experiment. (a) Light was shifted on day 4 and reached depleted ammonia ($<1\text{mg/L TAN}$) on day 5. (b) Light was shifted on day 5 and reached depleted nitrogen by day 6. (c) Double illumination was constant for 9 days and reached nitrogen depletion by day 4. Cultures became chlorotic (yellowing) indicating nitrogen depletion and the potential for TAG accumulation in the Double Illumination culture. Each culture was completely mixed before refilling the Roux Bottles and as so the conspicuous wall growth observed on Day-8 and Day-9 in all three treatments formed over the period of one day.

Appendix E



Appendix E. The direct relationship between organic nitrogen content and chlorophyll-a content as a percentage of microalgae biomass.

Appendix F

Culture composition

Light Shift-1																		
Day	Biomass				Cell			Light Lux	Temp °C	pH	NH ₄ mg/L	TKN mg/L	NOx mg/L	%ON	%ON Rate	ON mg/L	Chlorophyll-a mg/L	% Chl-a
	TSS	VSS	Mean VSS	SE	#	#/ ml	Mean cell/mL											
1	40	33.3																
	46.7	33.3	35.53333333	2.233333	n/a	n/a	n/a	7000	n/a	n/a	37.12							
	46.37	40																
2	100	93.3			124	1.24E+06												
	106.67	93.3	88.86666667	4.433333	164	1.64E+06	1.44E+06	14000	26	7.4	31.09						0.297	0.334208552
	100	80			144	1.44E+06												
3	160	160			201	2.01E+06												
	193.3	193.3	177.7666667	9.677523	124	1.24E+06	1.63E+06	14000	28	7.47	22.35	42.3	1.59	11.21133		18.3	1.208	0.679542471
	180	180			162.5	1.63E+06												
4	340	333.3			288	2.88E+06												
	1320	320	331.1	5.877358	299	2.99E+06	2.94E+06	14000	28	7.33	9.43	40.0	1.6	9.244941	-1.966384602	29.0	1.638	0.494714588
	-	340			293.5	2.94E+06												
5	566.7	533.3			n/a	n/a												
	586.7	546.7	540	3.868247	834	8.34E+06	8.34E+06	14000	21	7.29	0.04	39.2	0.86	7.251852	-1.993089254	38.3	3.506	0.649259259
	633.3	540			834	8.34E+06												
6	833.3	826.7			1028	1.03E+07												
	813.3	786.7	808.9	11.75472	1147	1.15E+07	1.09E+07	14000	26	7.42	0.02	40.6	0.96	5.016689	-2.235162521	39.6	2.569	0.317591791
	840	813.3			1087.5	1.09E+07												
7	123.3	1186.7			1330	1.33E+07												
	1240	1173.3	1180	3.868247	1297	1.30E+07	1.31E+07	14000	24	7.33	0.07	46.8	0.89	3.960169	-1.05651984	45.8	1.252	0.106101695
	1226.7	1180			1313.5	1.31E+07												
8	1493.3	1453.3			1128	1.13E+07												
	1506.7	1466.7	1453.333333	7.707644	1096	1.10E+07	1.11E+07	14000	23.5	7.43	0.05	44.5	1.23	3.058486	-0.901683253	43.2	1.039	0.071490826
	1486.7	1440			1112	1.11E+07												
9	1733.3	1693.3			1155	1.16E+07												
	1733.3	1686.7	1693.333333	3.839415	1071	1.07E+07	1.11E+07	14000	25	7.71	0.05	44	0.87	2.595472	-0.463013798	43.1	0.865	0.051082677
	1746.7	1700			1113	1.11E+07												

Appendix F1. Daily sampling components of Light-shift 1 including VSS, cell counts, light intensity, temperature, pH, and nitrogen tests.

Triglyceride Table

Light Shift-1															
Day	Pellet Biomass				Percent FAME						TOTAL % TAG	P _{VOL} mg/L	P _{VOL} max mg/L	Q _P mg/L-day	Q _P max mg/L-day
	Sample Volume (L)	SUP TSS	SUP VSS	VSS (mg)	C16:0	C16:1	C16:3	C18:0	C18:1	C18:3					
1															
2															
3	0.575	33.3	33.3	83.06833333	1.35448257	0	0	0	0	4.3057596	5.6602422	10.062024	22.07471893	-3.50638615	10.259502
4	0.28	40	40	81.508	3.45679109	0	0	0	0	6.8384109	10.295202	34.087414	30.55870588	24.02539005	11.3194232
5	0.22	36.7	36.7	110.726	2.31054323	1.1881746	0	0	0	5.3025192	8.801237	47.52668	38.44972711	13.43926582	7.89102122
6	0.3	33.3	30	233.67	1.09486545	0	0.5629917	0	0	2.5126321	4.1704893	33.735088	47.09296452	-13.7915922	8.64323742
7	0.3	50	86.7	327.99	1.5282833	0	0.6000961	0	0	2.9578177	5.0861971	60.017126	70.72656333	26.28203863	23.6335988
8	0.3	40	40	424	2.17920984	0	0.7572306	1.0179496	0	4.1942895	8.1486796	118.42748	94.67386956	58.41035	23.9473062
9	0.3	26.7	26.7	499.99	1.66018127	0.5871395	0	0.6958436	0	3.2916983	6.2348626	105.57701	112.0022412	-12.85046993	22.77994

Appendix F2. Algae pellet mass, individual FAME constituents and total TAG content for Light-shift on day 3.

Culture composition

Light-shift 2

Day	Biomass				Cell			Light Lux	Temp °C	pH	NH ₄ mg/L	TKN mg/L	NOx mg/L	%ON	%ON Rate	ON mg/L	Chlorophyll-a mg/L	% Chl-a
	TSS	VSS	Mean VSS	SE	#	#/ ml	Mean cell/mL											
1	40	33.3																
	46.7	33.3	35.53333333	2.233333	n/a	n/a	n/a	7000	n/a	n/a	37.12							
	463.7	40																
2	80	66.7			114	1.14E+06												
	86.7	73.3	73.33333333	3.839415	105	1.05E+06	1.10E+06	7000	22	7.3	34.34						0.125	0.170454545
	86.7	80			109.5	1.10E+06												
3	140	140			100	1.00E+06												
	146.7	146.7	151.1333333	8.020044	76	7.60E+05	8.80E+05	7000	23	7.48	25.68	37.52	1.3	7.834142		10.5	0.855	0.565725629
	166.7	166.7			88	8.80E+05												
4	260	260			146	1.46E+06												
	260	260	266.6666667	6.666667	246	2.46E+06	1.96E+06	7000	24.5	7.57	13.76	38.64	1.22	9.33	1.495857962	23.7	2.607	0.977625
	280	280			196	1.96E+06												
5	360	326.7			361	3.61E+06												
	406.7	366.7	348.9	11.75472	422	4.22E+06	3.92E+06	14000	22.5	7.18	2.21	38.08	1.2	10.28088	0.950882774	34.7	3.152	0.903410719
	380	353.3			391.5	3.92E+06												
6	513.3	486.7			639	6.39E+06												
	553.3	520	502.2333333	9.677523	685	6.85E+06	8.04E+06	14000	23	7.34	0.02	41.44	0.82	8.247163	-2.033720101	40.6	3.517	0.700272118
	533.3	500			1087.5	1.09E+07												
7	933.3	886.7			922	9.22E+06												
	926.7	886.7	888.9	2.2	899	8.99E+06	9.11E+06	14000	25	7.47	0.04	41.44	0.76	4.657442	-3.589720891	40.6	1.992	0.224097199
	926.7	893.3			910.5	9.11E+06												
8	1306.7	1273.3			923	9.23E+06												
	1306.7	1273.3	1273.3	0	651	6.51E+06	7.87E+06	14000	25.5	7.39	0.04	43.4	0.79	3.405325	-1.252117035	42.6	1.524	0.119688997
	1300	1273.3			787	7.87E+06												
9	1560	1513.3			808	8.08E+06												
	1526.7	1493.3	1502.2	5.877358	963	9.63E+06	8.86E+06	14000	25	7.4	0.05	38.08	0.72	2.53162	-0.873704456	37.3	1.225	0.081547064
	1526.73	1500			885.5	8.86E+06												

Appendix F3. Daily sampling components of Light-shift 2 including VSS, cell counts, light intensity, temperature, pH, and nitrogen tests.

Triglyceride Table

Light-shift 2															
Day	Pellet Biomass				Percent FAME						TOTAL % TAG	P _{VOL} mg/L	P _{VOL} max mg/L	Q _P mg/L-day	Q _P max mg/L-day
	Sample Volume (L)	SUP TSS	SUP VSS	VSS (mg)	C16:0	C16:1	C16:3	C18:0	C18:1	C18:3					
1															
2															
3	0.69	30	30	83.582	2.43877924	0	0.842914	0	0	5.85773	9.1394232	13.812715	18.79831728	-2.256155794	3.85752441
4	0.33	33.3	33.3	77.011	2.87493069	0	0	0	0	6.0440392	8.9189698	23.78392	22.3081754	9.971204617	4.41967363
5	0.22	23.3	23.3	71.632	1.91171205	0	0	0	0	6.4941038	8.4058159	29.327892	38.02039631	5.543972053	15.7122209
6	0.3	40	36.7	139.66	3.62019399	1.4930157	0	0	0	7.0224599	12.13567	60.949378	51.41171026	31.62148607	13.3913139
7	0.3	90	76.7	243.66	2.16556667	0.8394385	0	0	0	4.1901643	7.1951695	63.957861	62.63534961	3.008483724	11.2236393
8	0.3	70	70	360.99	1.59082548	0	0.5263718		2.8304828	0	4.94768	62.99881	69.66586654	-0.959051746	7.03051693
9	0.3	26.7	26.7	442.65	1.4643086	0	0.4866667	0.5761077	2.9343022	0	5.4613852	82.040929	72.51986909	19.04211882	9.04153354

Appendix F4. Algae pellet mass, individual FAME constituents and total TAG content for Light-shift on day 5.

Culture composition

Double Illumination																		
Day	Biomass				Cell			Light Lux	Temp °C	pH	NH ₄ mg/L	TKN mg/L	NOx mg/L	%ON	%ON Rate	ON mg/L	Chlorophyll-a mg/L	% Chl-a
	TSS	VSS	Mean VSS	SE	#	#/ ml	Mean cell/mL											
1	40	33.3																
	46.7	33.3	35.5333333	2.233333	n/a	n/a	n/a	14000			37.12							
	463.7	40																
2	153.3	133.3			144	1.44E+06												
	173.3	146.7	142.2333333	4.466667	143	1.43E+06	1.44E+06	14000	35	7.8	27.81						0.403	0.283337239
	146.7	146.7			143.5	1.44E+06												
3	340	340			439	4.39E+06												
	340	340	335.5666667	4.433333	428	4.28E+06	4.34E+06	14000	28	8.24	8.78	37.52	1.23	8.564617		27.5	2.722	0.811165193
	340	326.7			433.5	4.34E+06												
4	633.3	600			741	7.41E+06												
	626.7	600	620	20	618	6.18E+06	6.80E+06	14000	28.5	7.68	0.04	37.4	0.66	6.025806	-2.538810614	36.7	2.9	0.467741935
	673.3	660			679.5	6.80E+06												
5	820	780			897	8.97E+06												
	820	786.7	802.2333333	18.98213	888	8.88E+06	8.93E+06	14000	25.5	8.06	0.03	37.6	0.71	4.683176	-1.342630318	36.9	1.388	0.173016994
	873.3	840			892.5	8.93E+06												
6	1166.6	1133.3			771	7.71E+06												
	1146.6	1100	1111.1	11.1	808	8.08E+06	7.90E+06	14000	29.5	7.25	0.03	37.52	0.75	3.374134	-1.309042392	36.7	1.143	0.102871029
	1133.3	1100			789.5	7.90E+06												
7	1313.3	1273.3			872	8.72E+06												
	1193.3	1186.7	1244.433333	28.86667	917	9.17E+06	8.95E+06	14000	31	7.25	0.05	44.8	0.71	3.596014	0.221880509	44.0	0.822	0.066054161
	1320	1273.3			894.5	8.95E+06												
8	1506.7	1466.7			1063	1.06E+07												
	1486.7	1466.7	1466.7	0	991	9.91E+06	1.03E+07	14000	28	7.28	0.05	39.2	0.73	2.669258	-0.926756733	38.4	0.582	0.039680916
	1506.7	1466.7			1027	1.03E+07												
9	1580	1546.7			914	9.14E+06												
	1666.7	1613.3	1595.566667	24.73765	886	8.86E+06	9.00E+06	14000	25	7.2	0.05	43.12	0.77	2.699354	0.030096944	42.3	3.75	0.235026218
	1660	1626.7			900	9.00E+06												

Appendix F5. Daily sampling components of Double Illumination including VSS, cell counts, light intensity, temperature, pH, and nitrogen tests.

Triglyceride Table

Double Illumination															
Day	Pellet Biomass				Percent FAME						TOTAL % TAG	P _{VOL} mg/L	P _{VOL} max mg/L	Q _p mg/L-day	Q _p max mg/L-day
	Sample Volume (L)	SUP TSS	SUP VSS	VSS (mg)	C16:0	C16:1	C16:3	C18:0	C18:1	C18:3					
1															
2															
3	0.37	26.7	26.7	114.2806667	0.2179357	1.0396569	0	0	0	5.6887398	9.2074153	30.897017	45.95498044	3.438611433	16.7772695
4	0.15	80	80	81	2.92254106	1.2781284	0	0	0	5.640128	9.8407975	61.012944	49.84039067	30.11592758	10.0509353
5	0.22	93.3	43.3	166.9653333	2.37286804	0.6598024	0	0	0	4.148683	7.1813534	57.611211	68.93195703	-3.401733111	19.0915664
6	0.3	40	36.7	322.32	2.02015813	0	0.4924373	1.5487342	3.8742041	0	7.9355338	88.171716	223.8700649	30.5605046	154.938108
7	0.3	36.7	73.3	351.34	12.1859146	4.4138719	0	3.625677	22.028891	0	42.254354	525.82727	407.947341	437.6555522	184.077276
8	0.3	46.7	43.3	427.02	12.2198168	3.6323012	0	3.7439472	21.983197	0	41.579262	609.84304	641.1614021	84.01577143	233.214061
9	0.3	46.7	46.7	464.66	14.1587553	4.0950214	0	4.4561926	26.66521	0	49.375179	787.8139	698.8284692	177.9708597	130.993316

Appendix F6. Algae pellet mass, individual FAME constituents and total TAG content for Double Illumination.